UNITED NATIONS EDUCATIONAL, SCIENTIFIC AND CULTURAL ORGANIZATION
INTERNATIONAL ATOMIC ENERGY AGENCY
INTERNATIONAL CENTRE FOR THEORETICAL PHYSICS
I.C.T.P., P.O. BOX 586, 34100 TRIESTE, ITALY, CABLE: CENTRATOM TRIESTE

SMR.1065 - 6

COLLEGE ON SOIL PHYSICS
14 - 30 APRIL 1998

"Soil Structural Properties"
"Measurement of Soil Water - Part I & II"
"Soil Water Potential"
"Soil Water Retention Curve"
"Water Balance"

Roger H. HARTMANN
University of Ghent
Laboratory of Soil Physics
Department of Soil Management & Soil Care
Faculty of Agriculture & Applied Biological Sciences
Coupure Links 653, B-9000 Ghent
BELGIUM

These are preliminary lecture notes, intended only for distribution to participants

LECTURE NOTES

by

R. HARTMANN[1]

1 *Laboratory of Soil Physics*
Department of Soil Management and Soil Care
Faculty of Agricultural and Applied Biological Sciences
University Gent - Belgium

TEXTBOOKS

Rose, C.W., 1956.
Agricultural physics.

Slayter, R.O., 1967.
Plant-water relationships.
New York: Academic.

Childs, E.C., 1969.
An introduction to the physical basis of soil water phenomena.
New York: Intersciences.

Hillel, D., 1971.
Soil and water: Physical properties and processes.
New York: Academic.

Nielsen, D.R., Jackson, R.D., Corry, J.W. and Evans, D.D., 1972.
Soil water.
Madison, Wisconsin, Am. Soc. of Agronomy.

Baver, L.D., Gardner, W.H. and Gardner, W.R., 1972.
Soil Physics.
New York: Wiley.

Kirkham, D. and Powers, W.C., 1972.
Advanced soil physics.
New York: Interscience.

Taylor, S.A. and Ashcroft, G.L., 1972.
Physical edaphology.
San Francisco: W.H. Freeman and Company.

Drainage Principles and Applications, 1973.

I. Introductory subjects.
II. Theories of field drainage and watershed runoff.
III. Surveys and investigations.
IV. Design and management of drainage systems.

International Institute for Land Reclamation and Improvement, Wageningen, The Netherlands.

Hillel, D., 1974.

L'eau et sol.
Principes et processus physiques.
Louvain: Vander.

Yong, R.N. and Warketin, B.P., 1975.

Soil properties and behaviour.
Amsterdam: Elsevier.

Henin, S., 1977.

Cours de physique du sol, I et II.
Paris: Orstom.

Marshall, T.J. and Holmes, J.W., 1979.

Soil physics.
Cambridge: Cambridge University Press.

Hanks, R.J. and Ashcroft, G.L., 1980.

Applied soil physics.
Berlin: Springer-Verlag.

Hillel, D., 1980.

Fundamentals of soil physics.
New York: Academic.

Hillel, D., 1980.

Applications of soil physics.
New York: Academic.

Koorevaar, P., Menelik, G. and Dirksen, C., 1983.
Elements of Soil Physics.
Elsevier, Amsterdam.

Campbell, G., 1985.
Soil physics with basic.
Elsevier, Amsterdam.

Iwata, S., Tabuchi, T. and Warketin, 1988.
Soil-water interactions. Mechanisms and applications.
New-York and Basel: Marcel Dekker, Inc.

Ghildyal, B.P. and Tripathi, R.D., 1987.
Soil Physics.
John Wiley and Sons, New-York.

Jury, W.A., Gardner, W.R. and Gardner, W.H., 1991.
Soil Physics.
Fifth Edition: John Wiley & Sons, Inc.

Smith, K.A. and Mullins, C.E., 1991.
Soil Analysis (Physical Methods).
Marcel Dekker Inc., New York, Bazel, Hong Kong.

Topp, G.C., Reynolds, W.D. and Gran, R.E., 1992.
Advances in measurement of soil physical properties:
Bringing theory into practice.
SSSA Special Publication n° 30.

Hanks, R.J., 1992.
Applied Soil Physics.
Soil Water and Temperature Application, 2th edition, Springer-Verlag.

Kutilek, M. and Nielsen, D.R., 1994.
Soil Hydrology
Geo-ecology textbook, Catena Verlag.

TABLE OF CONTENTS

1. SOIL WATER CONTENT 1

1.1 THERMOGRAVIMETRIC METHOD 5
1.2 NEUTRON SCATTERING TECHNIQUE 5
1.2.1 Principle (figure 3) 6
1.2.2 Neutron moisture gauge 8
1.2.3 Neutron sources 9
1.2.4 Neutron detectors 9
1.2.5 Probe housing 11
1.2.6 Radiation shield 11
1.2.7 Standard 11
1.2.8 Depth indication 12
1.2.9 Access tubes 12
1.2.10 Calibration 12
1.2.10.1 Drum calibration in the laboratory 14
1.2.10.2 Field calibration 15
1.2.10.3 Calibration according to the chemical soil analysis 15
1.2.11 The sphere of influence concept 17
1.2.12 Measuring a soil water profile in the field 18
1.2.13 Some applications for the neutron probe 19
1.3 TIME DOMAIN REFLECTOMETRY 20
1.3.1 Permittivity 21
1.3.2 Operating principle 22
1.3.3 Wave form analysis 25
1.3.4 Calibration 27
1.3.5 Strengths and weaknesses of the TDR technique 29

2. SOIL WATER POTENTIAL 32

2.1 INTRODUCTION 32
2.2 ENERGY STATE OF SOIL WATER 32
2.3 QUANTITATIVE EXPRESSION OF SOIL WATER POTENTIAL 35
2.4 GRAVITATIONAL POTENTIAL 35
2.5 OSMOTIC POTENTIAL 37
2.6 MATRIC POTENTIAL 38
2.7 EXTERNAL GAS PRESSURE POTENTIAL 41
2.8 HYDRAULIC HEAD 42

3. TENSIOMETER 45

3.1 HYDROSTATIC PRESSURE POTENTIAL - PIEZOMETER 45
3.2 MATRIC POTENTIAL - TENSIOMETER 46
3.3 PRINCIPLE OF THE TENSIOMETER 47
3.4 HOW TO CALCULATE THE SOIL WATER PRESSURE HEAD h AND THE HYDRAULIC HEAD H 49
3.5 SOME CHARACTERISTICS OF THE TENSIOMETER 55
3.5.1 Cup conductance "C" 55

3.5.2 Sensitivity of the manometer "S" 55
3.6 PRACTICES AND LIMITATIONS OF TENSIOMETERS 57
3.7 APPLICATIONS OF MEASUREMENTS 59
3.7.1 Determination of the direction of water flow at different levels in the soil profile (figure 32) 59
3.7.2 Flux control at a certain depth 60
3.7.3 Determination of the soil water characteristic curve (or retentivity curve) 60
3.7.4 Scheduling irrigation 63

4. SOIL WATER CHARACTERISTIC CURVE 66

4.1 MEASUREMENT 66
4.1.1 Hanging Water Column (Range -100 cm < h < 0) 66
4.1.2 Pressure Plate (Range - 15000 cm ≤ h ≤ - 300 cm) 67
4.1.3 Equilibration over Salt Solutions (h < - 15000 cm) 68
4.2 HYSTERESIS IN WATER CONTENT-ENERGY RELATIONSHIPS 69

5. HOW TO EVALUATE THE FIELD WATER BALANCE 73

5.1 INTRODUCTION 73
5.2 ITEMIZATION OF THE WATER BALANCE IN THE ROOT ZONE 73
5.3 TIME-PERIOD CONSIDERATIONS 75
5.4 EVALUATION OF THE WATER BALANCE 75
5.5 SOIL WATER CONTENT PROFILE - SOIL WATER STORAGE 77
5.6 HYDRAULIC HEAD PROFILE 78
5.7 ESTIMATION OF EVAPORATION OR EVAPOTRANSPIRATION UNDER DIFFERENT SITUATIONS 80
5.7.1 Absence of a zero flux plane 80
5.7.1.1 Downward flow 80
5.7.1.2 Upward flow 82
5.7.2 Presence of a zero flux plane 82
5.7.2.1 Bare soil 83
5.7.2.2 Cropped soil 84
5.8 CONCLUSIONS 86
5.9 REFERENCES 86

1. SOIL WATER CONTENT

Soil water is important in itself as a feature of the physical environment but especially prominent in its relationships with climatology and with the surface and the subsurface hydrologic regimes as a component in the terrestrial water balance. To understand the behaviour of soil water one must measure it. This have long proved a difficult task both from the instrumental aspect as because of the complexity of the soil body surpasses that of the vegetated layer and the atmosphere above.

There are numerous procedures and types for the determination of the soil water content. Since each method has its advantages and limitations it is well to consider both the purpose for which determinations are to be made and the features of each possible method including the cost of buying equipment and operating and maintenance costs.

Eight of these are listed in table 1. Only the most frequently applied methods will be discussed.

Table 1. Methods of measuring soil water content

1. Thermogravimetric method
2. Neutron scattering technique
3. Gamma-ray attenuation technique
4. Gamma-ray backscattering technique
5. Electrical resistance
6. Thermal conductivity
7. Time Domain Reflectometry
8. Capacitance method

The soil water content (wetness) can be expressed in terms of either mass or volume ratios or fractions.

- *Mass wetness or dry mass fraction of water (w).*

$$w = \frac{M_w}{M_s} \tag{1}$$

This is the mass of water relative to the mass of dry (105°C) soil particles where w is the mass wetness, M_w water mass and M_s dry (105°C) soil mass.

- *Volume wetness or volume fraction of water (θ).*

$$\theta = \frac{V_w}{V_s + V_w + V_a} \tag{2}$$

It is the dimensionless ratio of the water volume (V_w) relative to total bulk soil volume V_t. The latter is the sum of the volume of solids (V_s), water (V_w) and air (V_a) (figure 1).

The two expressions can be related to each other as follows:

$$\frac{\theta}{w} = \frac{V_w \; M_s}{V_t \; M_w} \tag{3}$$

with : $M_s/V_t = \rho_b$ (mass of dry soil per unit bulk volume and usually lies in the range of 1.3 and 1.7 g cm^{-3})

$M_w/V_w = \rho_w$ (mass of water per unit volume of water and is approximately equal to 1 g cm^{-3})

Equation (3) becomes

$$\theta = \frac{w \rho_b}{\rho_w} \quad (4)$$

So in order to obtain the soil water content on a volume basis the mass wetness is multiplied with the dry bulk density. Both w and θ are usually multiplied by 100 and reported as percentages by mass or volume.

The usefulness of the soil water content by volume lies in the fact that it can be converted easily into head units of water therefore being compatible with quantities of rainfall or irrigation water applied. All calculations involving the water balance of the soil, including calculation of irrigation deficits, water application efficiency and recharge of the soil moisture reservoir by rainfall, involve the use of the volumetric soil water percentage (vol.% of water = mm of water per 10 cm soil depth).

If the soil water content is measured at different depths of the profile than the depth-interval dz_i for which θ_i is valid, is taken as the vertical distance between the measuring point and the points located half-way respectively the above and underlying measuring point (figure 2).

The soil water storage "S" is than equal to the equivalent waterhead (mm or cm) present in the profile until a depth z and is obtained through the summation of the moisture contents over each depth interval:

$$S = \sum_{i=1}^{i=n} \theta_i \, dz_i \quad (5)$$

with the same unit as that of z which is compatible with the amount of precipitation or evaporation.

Two moisture content profiles, measured at respectively time t_1 and t_2, allows us to calculate the change in water storage $\Delta S(z_1, z_2)$ during the period Δt.

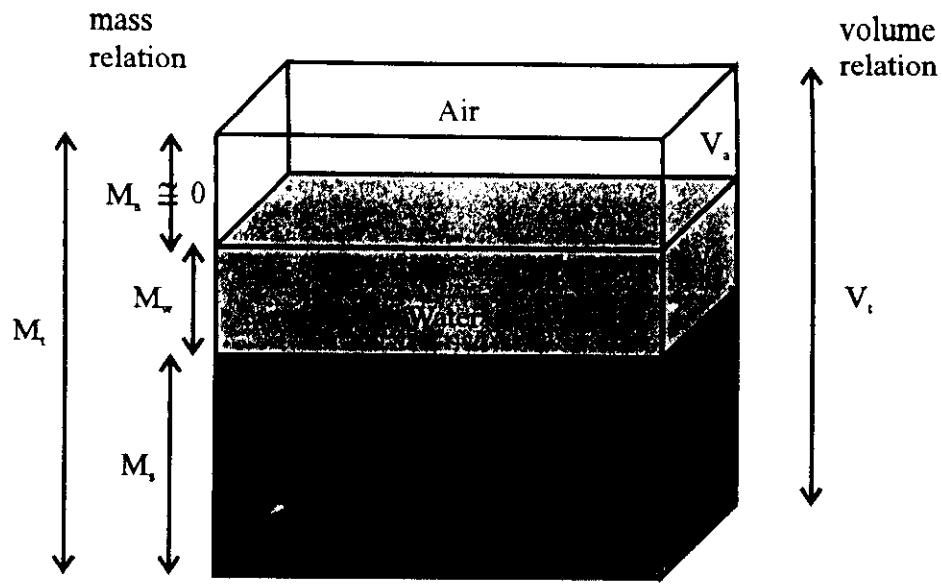

Figure 1. Schematic diagram of the soil as a three-phase system.

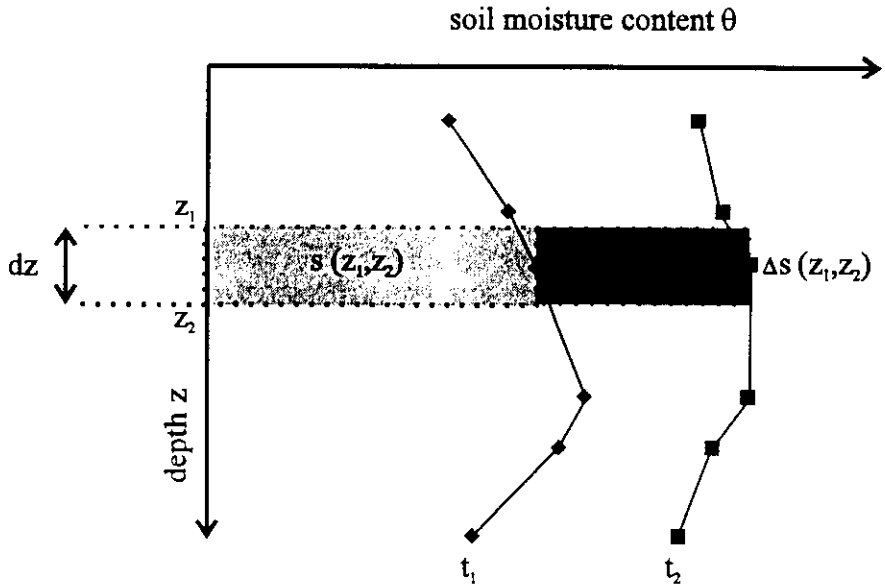

Figure 2. Soil moisture content profiles.

1.1 Thermogravimetric method

The thermogravimetric method of measuring soil water content consists of removing a sample by augering into the soil and then determining its moist and dry weight. The moist weight is determined by weighing the sample as it is at the time of sampling and the dry weight is obtained after drying the sample to a constant weight in an oven. The standard method of drying is to place the sample in an oven at 105°C for 24 hours.

The mass wetness is the ratio of the weight loss in drying to the dry weight of the sample:

$$w = \frac{wet\ weight\ -\ dry\ weight}{dry\ weight} = \frac{weight\ loss\ by\ drying}{weight\ of\ dried\ sample}$$

The method depending at it does on sampling, transporting and repeated weighings entails practically inevitable errors. It is also laborious and time consuming, since a period of at least 24 hours is usually considered necessary for complete oven drying. The standard method of oven drying is itself arbitrary. Some clays may still contain appreciable amounts of adsorbed water even at 105°C. On the other hand, some organic matter may oxidize and decompose at this temperature so that the weight loss may not be due entirely to the vaporization of water.

The errors of the gravimetric method can be reduced by increasing the sizes and the number of samples. However the sampling method is destructive and may disturb an observation or experimental plot sufficiently to distort the results. For these reasons many prefer indirect methods, which permit making frequent or continuous measurements at the same point and once the equipment is installed and calibrated with much less time, labor and soil disturbance.

Although the gravimetric determination of soil moisture content is rather laborious it is, because of its simplicity and reliability, the most extensively applied technique and is used as calibration standard for other methods.

1.2 Neutron scattering technique

The neutron scattering technique is one of the two radiological methods available for the measurement of the soil moisture content. It is based on the interaction between high energy neutrons (fast neutrons) and the nuclei of hydrogen atoms in the soil. The other method is based on the attenuation or backscattering of gamma rays as they pass through the soil. Both methods use portable equipment for taking measurements at permanent observation sites. These methods

are therefore non-destructive and have the additional advantage of yielding data from the same location at each observation. Both methods require careful calibration with the soil in which the equipment is to be used.

However the radiological methods have common drawbacks. The equipment is expensive and requires considerable maintenance. It is necessary to train the operator not only to produce satisfatory results but also to observe necessary safety precautions. Indeed improper use in handling the equipment might involve radiation hazards.

1.2.1 Principle (figure 3)

If a radioactive source, emitting high energy neutrons (fast neutrons), is placed in the soil, the fast neutrons are emitted radially into the soil from the source at high speed, colliding on their way with nuclei of various elements found in the soil. When a fast neutron collides with a heavy nucleus, its direction will be changed but its kinetic energy will be relatively unaffected. However, when the fast neutron collides with a light nucleus (especially H), an appreciable part of its energy will be transmitted to this nucleus. The neutrons of high energy (fast neutrons) gradually lose their energy by this interaction until they have been moderated to "slow" or "thermal" neutrons.

In the soil, hydrogen is the most common atom with a light nucleus and which has the same mass as the neutron. Most of the hydrogen found in the soil is a component of water. So the majority of neutron-moderating collisions that take place occur between the fast neutrons and hydrogen atoms associated with water.

After a fast neutron has been converted to a slow or thermal neutron it will continue to travel through the soil colliding with additional atoms and having a generally random path. Some of the thermal neutrons produced in the surrounding soil will diffuse back to the source so that, if a detector for thermal neutrons is placed close to the source and both source and detector are small enough, the number detected per unit time is directly proportional to the water content of the medium.

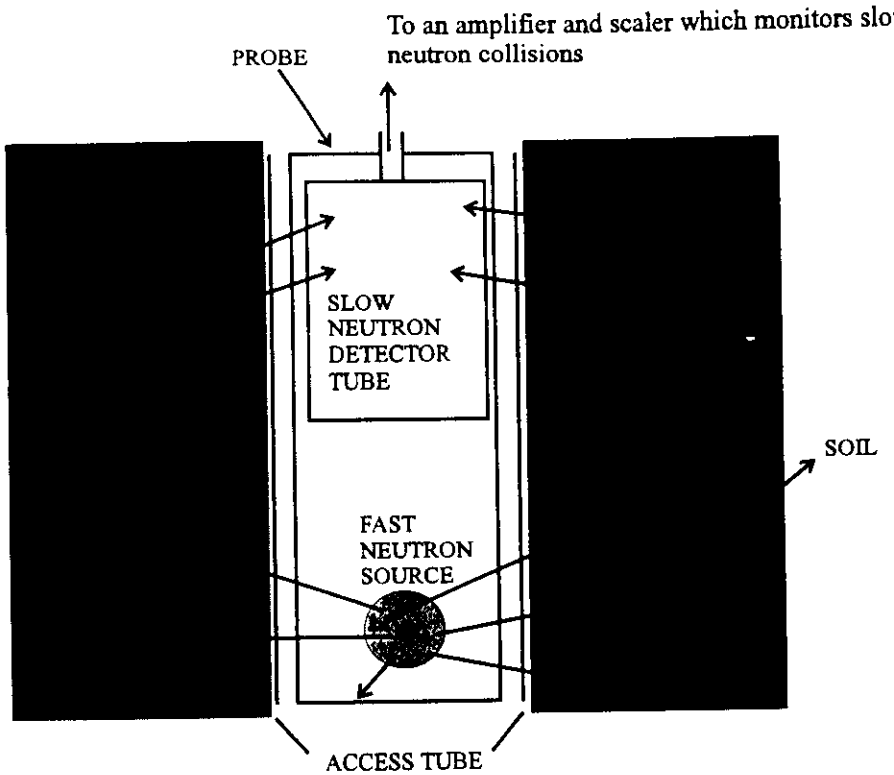

Figure 3.How a neutron moisture meter operates.

Excluding the presence in the soil of hydrogen atoms not due to water and of other atoms with light nuclei which may also participate in fast neutron moderation, it can be concluded that the higher the volumetric moisture content of the soil the greater the likelihood that any single fast neutron will collide with the hydrogen atom and become moderated within a given distance from the source.

Conversely the lower the soil water content the greater the likelihood that a fast neutron will traverse a certain distance without colliding with a hydrogen atom. At a given uniform soil moisture content the number of unmoderated or fast neutrons per unit volume of soil decreases with distance from the source.

From this it is seen that the radius of the volume of soil which effectively participates in neutron moderation is itself a function of soil moisture content.

1.2.2 Neutron moisture gauge

The basic parts of a neutron moisture gauge are the neutron source, the neutron detector and the electronic supply and indicating unit. Source and detector are contained in a probe housing. For safety reasons the source is shielded by a neutron and gamma radiation shield. To check instrument stability a standard is used. In subsurface measurements there must be some means of depth indication. In most cases subsurface probes are lowered into the ground through an access tube. In some cases surface and subsurface probes are combined neutron moisture and gamma (backscatter or transmission) density probes. These probes also contain a gamma source and a gamma radiation detector. A typical design of a subsurface probe is illustrated schematically in figure 4.

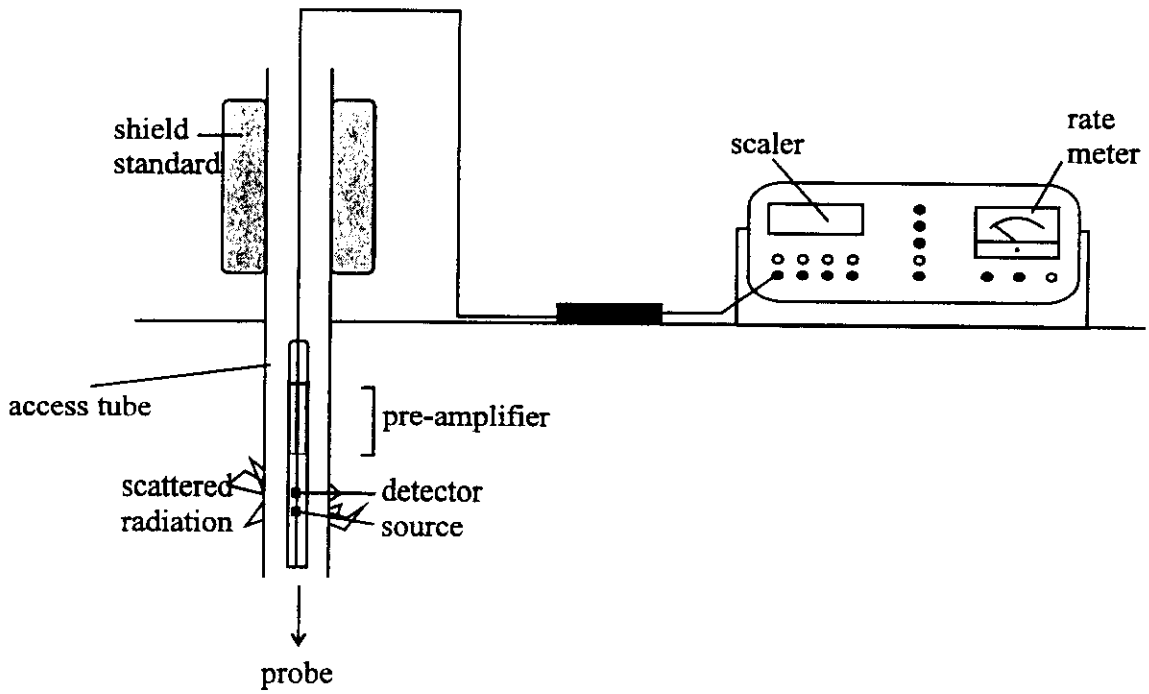

Figure 4. Schematic drawing of a depth probe installation

1.2.3 Neutron sources

The most common radio-isotope neutron sources used in moisture gauges are ^{226}Ra-Be and ^{241}Am-Be viz. an α-source mixed with beryllium. In these sources, alpha particles emitted by radium or americium are adsorbed by the nucleus of ^{9}Be with the subsequent emission of a neutron, the final product nucleus being ^{12}C. The process may be described symbolically as follows:

$$Be_9^4 + \alpha_2^4 \rightarrow n_0^1 + C_{12}^6 + 5.74\ MeV$$

The 5.74 MeV is surplus energy of the nuclear reaction and is known as the reaction energy. Most neutron sources emit also gamma radiation.

Radium-beryllium sources have a much higher output of gamma-rays than americium-beryllium sources. Most of the gamma radiation from americium-beryllium is of low energy and thus needs very little shielding. Sources are usually encapsulated in cylindrical double-walled stainless steel containers with welded or silverbrazed seals. Table 2 gives some useful data for these sources.

Table 2. Basic data for some neutron sources

Source	Half-life	Emission ($n\ s^{-1}\ mCi^{-1}$)	Gamma dose rate per 10^6 $n\ s^{-1}$ (mrem/h at 1m)
Ra-Be	1620 yr	1.3×10^4	60
Am-Be	458 yr	2.5×10^3	1

1.2.4 Neutron detectors

The detection of nuclear particles requires some type of interaction of the radiation with the detector. Slow neutrons are mainly detected by means of neutron-induced transmutations in which the product particles make possible the detection.

Reactions used in neutron detectors for moisture gauges are :

$$^{10}B\ (n, \alpha)^{7}\ Li$$

$$^{3}He\ (n, p)^{3}\ H$$

$$^{6}Li\ (n, \alpha)^{3}\ H$$

$$^{113}Cd\ (n, \gamma)^{114}Cd$$

The first two reactions are used in gas-filled proportional counters. The third reaction is used in scintillation detectors and the last one in cadmium-covered Geiger-Müller tubes.

At presence the most widely used detector is the *$^{10}BF_3$-filled proportional counter*. The very low sensitivity to gamma radiation makes it possible to have very compact source-detector geometry's without shielding between source and detector. On the other hand, this fact makes it difficult to use the BF_3-tube as the detector in a gauge for simultaneous moisture and density measurement. The BF_3-tube is not sensitive to epithermal or fast neutrons. The main disadvantage of the BF_3-tube is its comparatively low slow-neutron detection efficiency which is to some extent overcome by the use of large tubes.

^{3}He-filled proportional counters have come into use comparatively recently. Their efficiency for slow neutron detection is higher than the BF_3-tubes. They have some efficiency for epithermal and fast neutron detection and a low gamma-detection efficiency. In some countries *Geiger-Müller counters* covered with cadmium foil are used.They have the advantage that the associated electronic equipment is simple, but the disadvantage of a low efficiency for slow neutron detection.

Scintillation detectors for neutron moisture probes make use of europium-activated lithium iodide crystals or lithium-containing glass scintillators. In both cases the lithium used is highly enriched in ^{6}Li. The main advantage of the lithium-containing scintillators compared to gas-filled detectors is their very high neutron detection efficiency. As they are solids, a large amount of the element necessary for the detection of neutrons can be present in a small volume. They also have a high efficiency for gamma-radiation detection and, therefore, a few centimetres of lead shielding between source and detector are necessary. Their sensitivity to gamma radiation makes scintillation detectors useful in gauges for combined moisture and density determination. In this case both neutrons and gamma rays are detected by the same detector and the pulses separated by means of electronic pulse height discrimination in the indicating instrument.

1.2.5 Probe housing

A housing is placed around the source and detector to make a robust, watertight measuring probe. For subsurface probes, cylindrical tubing of aluminium or stainless steel and of minimum diameter is used. The wall thickness particularly for steel is small to minimize absorption of thermal neutrons. Usually the probe housing also contains an electronic preamplifier or impedance converter to permit the use of a long cable without distortion of the pulse signal from the detector.

1.2.6 Radiation shield

Users of neutron moisture gauges have to be shielded against the neutron and gamma radiation emitted by the source. As neutron shields, hydrogen-containing material such as paraffin or plastics are used. When Am-Be source is used the neutron shield will also shield against the low-energy gamma radiation emitted by the source. When Ra-Be sources are applied it is necessary to use lead to shield against the high-energy gamma radiation emitted.

With subsurface probes the shield is a separate unit, usually a cylinder into which the probe fits when not in use. Generally, the shield has a hole running along its axis through which the probe can be lowered into the ground. The shield acts as a transport and storage container for the probe. It should be fitted with a lock so that the probe cannot be removed from the shield by unauthorized persons. It should have a proper handle for convenient carrying and placing the probe on top of the access tubes.

1.2.7 Standard

The stability of the gauge has to be checked at regular intervals by carrying out measurements in or on a standard made from a non-hygroscopic, mechanically-stable, hydrogen-containing material. For subsurface probes the shield container is used as standard. To avoid errors due to instrumental instabilities it is often suggested that the probe is calibrated in terms of N/N_s against volumetric soil water content θ, where N is the count rate in the soil and N_s the count rate in the standard being the shield container or a water standard.

1.2.8 Depth indication

For subsurface probes used to determine moisture profiles it is necessary to know the depth at which the measurement is being made and marks on the cable are commonly used for this purpose. Alternatively, mechanical registers driven by a wheel held against the cable can be used. Subsurface probes should be supplied with a cable clamp to hold the probe at the required depth.

1.2.9 Access tubes

Subsurface probes for soil moisture measurements are mostly introduced into the ground through access tubes which are left in position as long as measurements are required. Access tubes are usually made from aluminium or steel (ordinary or stainless). Aluminium tubes have the advantage that aluminium is not a strong slow neutron absorber. In stony ground or for deep holes aluminium may not be strong enough and steel tubes may have to be used. If the soil has corrosive properties, stainless steel tubes will have to be used.

Access tubes should be closed at the bottom to avoid the ingress of water into the tube. When not in use, they should be covered with a stopper to prevent the ingress of rain and dirt.

Installation of the access tube must ensure as tight a fit as possible between the tube and the soil without causing unnecessary soil disturbance.

1.2.10 Calibration

The calibration of a neutron moisture probe is usually presented as a curve relating the count ratio CR (N/N_s) to the volumetric water content of the soil dried at 105°C. Although manufacturers of probes supply a generalized calibration with each unit, it is generally considered necessary to recalibrate the probe for each soil type since different soil parameters influence the neutron moisture gauge readings.

Those soil parameters are:

- dry bulk density : As the neutron flux depends on the dry bulk density of the soil, variations in density cause a change in the apparent water content. More exactly, a small variation of dry density will involve a displacement of the calibration curve, but when this curve is a straight line, the slope will not be changed very much. Figure 5 illustrates the influence of soil dry bulk density on moisture gauge readings. The curves are practically parallel above 25% moisture. They converge slightly towards lower moisture values.

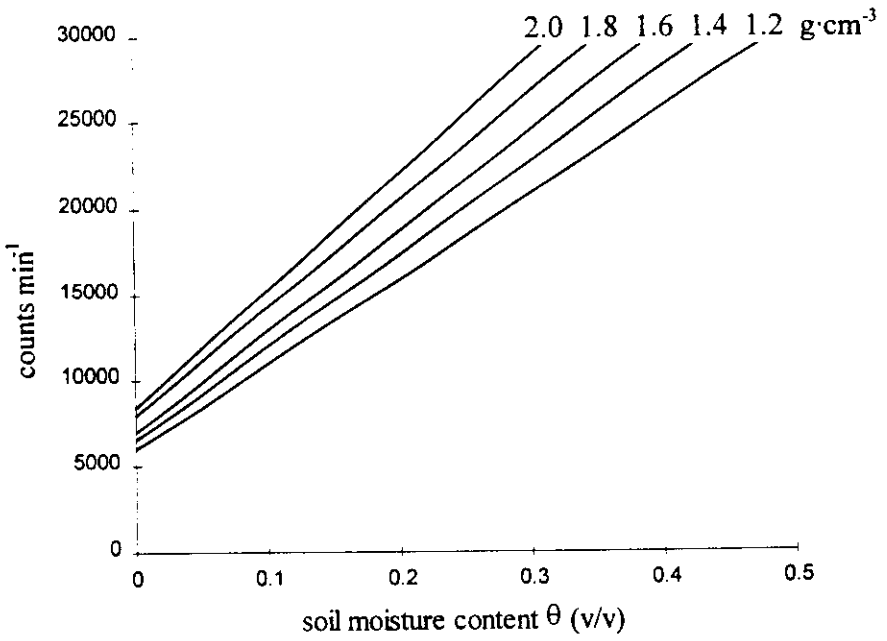

Figure 5. Calibration curves of a soil at different dry bulk densities.

- soil composition : Not all water is expelled at 105°C, some remaining as water of crystallisation or hydration of various minerals, nor is all the hydrogen present as water. Hydrogen in organic compounds is not expelled at 105°C but affects the count rate exactly as if it were the equivalent amount of water.

The presence of neutron absorbing elements in the soil leads to lower thermal neutron flux and gauge readings. Particularly important elements are B, Cl, Mn, Fe, K which have high absorption probabilities.

One may note that all materials in the soil will, to some extent, thermalize and absorb neutrons. Hence the final flux of slow neutrons at the detector depends on the scattering and absorbing properties of all the atomic nuclei in the soil.

Besides soil parameters the calibration curve is also influenced by measurements parameters such as:

- diameter and thickness of the access tube : As the calibration curve is also a function of the diameter of the access tube, variations in the diameter will affect the gauge readings. Similarly, variations in the thickness of the access tube change not only the amount of absorption of the thermal neutrons (particularly if an iron tube is used), but the average distance from the probe to the measured medium. To obtain high efficiency and calibration curve gradient, the access tube should have a diameter of a few centimeters.

- the distortion caused by drilling and insertion of the access tube.

- the fall in neutron flux for near surface measurements : When the probe is near the surface, the loss of neutrons leads to a decrease in count rate and the apparent moisture content given by the neutron moisture gauge is too low (see sphere of influence).

Consequently it might be necessary to calibrate a neutron probe at various levels within a soil profile and one can state "Until the effects of non-water hydrogen, bulk density, soil constituents etc... are resolved, it would be desirable to carefully obtain calibrations for the different soils being studied".

There are three basic ways for calibrating soil moisture against count rate "N" or the count ratio "CR = N/Ns".

1.2.10.1 Drum calibration in the laboratory

A laboratory calibration is performed on a large sample of the soil which is dried, mixed and packed into a large drum to its original bulk density. However, only soils which are homogeneous in chemistry and texture, which can be repacked uniformly in the laboratory to something like their field conditions and which do not change their dry bulk density with water content are suitable. According to these criteria only gravel, sand and silt soils are suitable for drum calibration. The drum must be at least 1.5 m deep and 1 m in diameter to give a valid result (if a smaller drum is used, the results can only be regarded with suspicion due to the escape of neutrons, particularly at the dry end of the moisture range). An access tube is installed in the centre of the drum and a count rate profile plotted to confirm that the packing is uniform; this should be demonstrated by a uniform plateau in the count rate profile through the central part of the drum. The probe is set in the centre of this plateau and a large number of counts are taken and meaned. The mean count ratio is plotted against the measured moisture content of the drum, giving the first calibration point. The volumetric moisture content is obtained through undisturbed soil samples taken at the measuring depths.

The soil should now be removed and wetted to a certain moisture content and leave for equilibrium. Afterwards the drum should be refilled to the same bulk density and the measuring procedure repeated. This procedure should continue over a large moisture content range. Finally a calibration curve can be obtained using the count ratio values and the corresponding moisture contents (figure 6a).

1.2.10.2 Field calibration

This is the common way for calibration but due to soil heterogeneity and various sampling errors there is often a fairly wide scatter in the calibration points. Many points are required from each site, therefore to perform a linear regression it usually takes a year to finalise the calibration. Since the count ratio is usually interpreted as volumetric soil water content a knowledge of the soil bulk density is required for calibration. This is probably the largest single source of error in the calibration procedure. Precise count ratio are obtained from the appropriate depth or depths and at the end of the calibration year at least six know-volume soil cores are taken to estimate the bulk density. Figure 6b gives an example of a field calibration curve.

1.2.10.3 Calibration according to the chemical soil analysis

A mathematical model based on the probability for a neutron to be captured by the soil-water system has been elaborated by Couchat (France):

$$N = f(\theta_p, \rho_b, \alpha, \beta, \gamma, \delta)$$

where : N = is the count rate of slow neutrons
θ_p = volumetric moisture content
ρ_b = bulk density
α, ß, γ and δ are constants obtained through chemical analysis and by direct use of a soil sample as a target in a high flux reactor

The equation can be written as follows:

$$N = (\alpha \rho_b + \beta)\theta_p + \gamma \rho_b + \delta$$

or

$$N = a\theta_p + b$$

the calibration curve for each specific horizon.

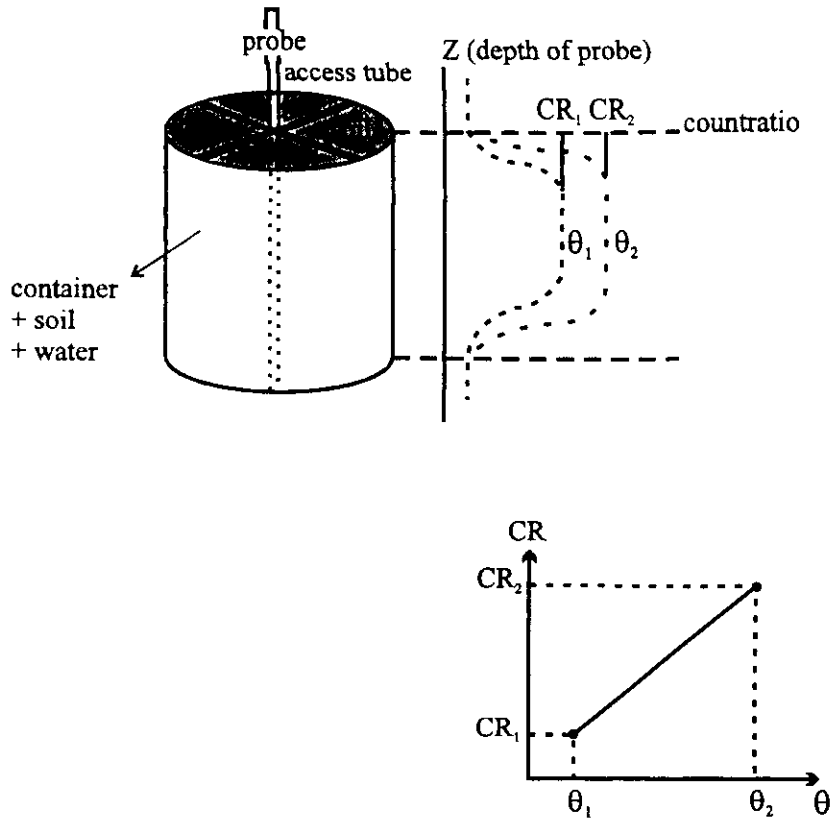

Figure 6a. Laboratory calibration of neutron moisture meter.

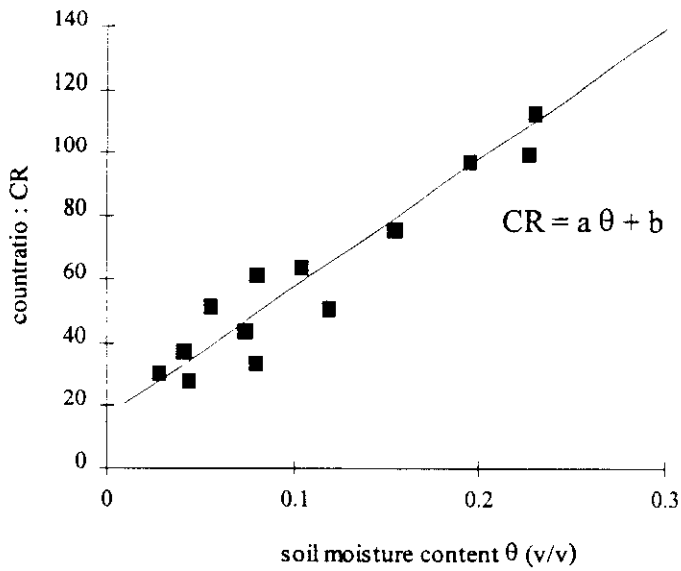

Figure 6b. Field calibration of neutron moisture meter.

1.2.11 The sphere of influence concept

Some knowledge of the volume measured by neutron moisture gauges is of importance for several reasons. First, if laboratory calibration or any other laboratory experiment is planned, samples of proper dimensions must be used. Secondly, in field measurements the volume actually measured should be known to estimate the optimum measurement intervals in subsurface measurements.

The problem is difficult to deal with and several different simplified approaches have been used. One of these is the concept of the "sphere of influence". It was defined as the sphere around the neutron source which contains 95% of all thermal neutrons. The concept of the sphere of influence has a number of shortcomings. One important shortcoming is that the neutrons in the outer part of the sphere will, for hydrogenous media, have little chance to get to the counter in case the latter is situated near or at the source. A different concept viz. the "sphere of importance" was introduced and it was defined as the sphere around the source, situated in a moderating medium, which if all soil and water outside the sphere was removed, will yield a neutron flux at the source which is 95% of the flux obtained if the medium is infinite. If the medium is smaller than the sphere of importance, the neutron leakage becomes significant and the count rate will therefore decrease. Figure 7 gives the relation between the radius of the measured sphere and the soil moisture content.

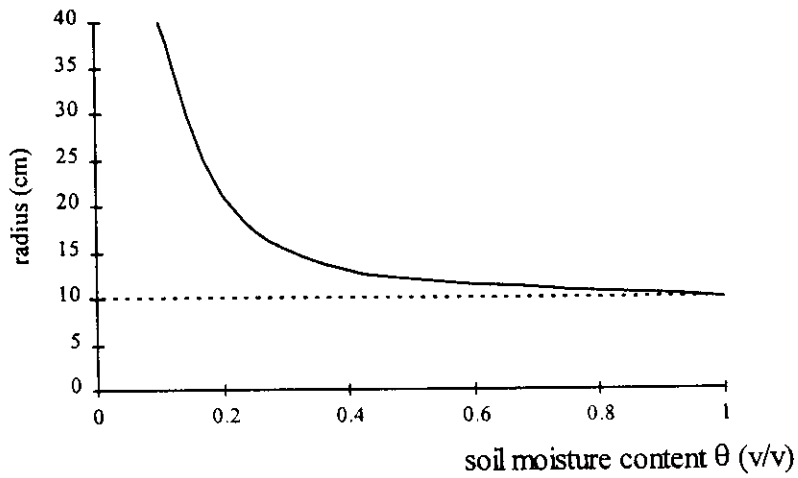

Figure 7. Relation between the radius of the measured sphere and the soil moisture content for a neutron moisture meter.

1.2.12 Measuring a soil water profile in the field

The count rate of slow neutrons depends upon the probability of any fast neutron emitted eventually being scattered back to the detector. Neutrons which become thermalised farthest away from the detector have very little chance of getting back to it since thermal neutrons are easily absorbed. It is thus very difficult to define a distance at which a certain change in moisture will affect the count rate significantly.

In practice, for soil in the field it is reasonable to assume that unless there is a marked interface involved, the effective radius is about 15 cm in wet soil and up to something like 30 cm in very dry soil. Expressed in another way, this may be taken to mean that the indicated soil moisture content value is the mean for a sphere of that radius, centred at the measuring point. The optimum spacing of readings is therefore 10 - 15 cm and no greater resolution can be gained by decreasing this figure. Readings spaced at depth intervals of 10 cm tend to form a smoothed version of the true soil water content profile.

The area beneath the profile curve so defined represents the total water in the profile between the surface and the depth of the lowest measurement (figure 8). Where a sharp interface occurs, as between soil layers of different moisture contents, the introduction of small errors is unavoidable. The worst case is the soil/air interface at the soil surface, which greatly affects readings taken in the surface layer. Neutrons are lost from the soil when the probe is within some 25 cm of the surface and the normal calibration curve no longer applies. Various ways round this problem have been used, including the use of "reflectors", "surface extension trays" and special calibration curves. None of these are entirely satisfactory and this is a major limitation of the neutron probe principle. Probably the best solution is the use of a specially derived calibration curve for a specific depth below the surface, for example 10 cm (and perhaps also 20 cm in dry sandy soils). Because the count rate gradient is so steep across the interface, small depth location errors in the surface layer create count rate errors. Further errors will arise from differences in distribution of water in this layer. For example a given amount of water in the top 20 cm immediately after rain, when most of the water will be in the top 5 cm, may give a different count rate some hours later when the same water has infiltrated to the base of the layer. Thus the data in time series will be more "noisy" for the surface layer than for deeper measurements, but if the special calibration is correct there should be no bias in the surface layer readings.

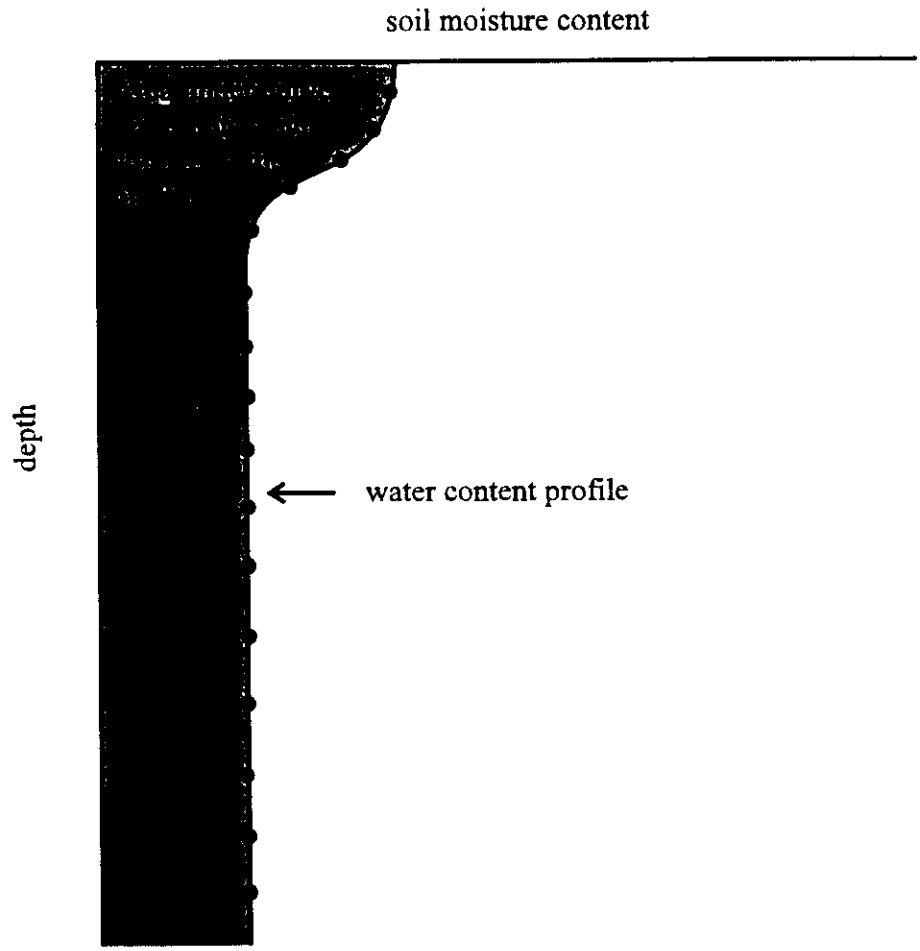

Figure 8. Typical soil water content profile.

For most soils the use of a single calibration curve for all depths below 20 cm is justifiable but in strongly layered soils as such, for example, a podzol or a clay overlying a gravel, the use of different calibration curves for each principal soil layer may be necessary.

1.2.13 Some applications for the neutron probe

The labour involved in setting up an access tube network and performing the necessary calibrations restricts the use of the neutron probe to medium or long term experiments requiring repeated determinations from the same sites and depths. While the main applications of the neutron probe tend at present to be in hydrological and agricultural research, the possibilities of extending its use into applied studies and routine management should be seriously considered, particularly in the context of irrigation and water resource studies. The main uses of the neutron probe may be summarised as follows:

APPLICATIONS	CONTEXT
1. Determination of soil water reservoir characteristics	- process studies - land use capability - agricultural research - planning irrigation regimes
2. Measurements of crop water use	- feasibility studies for irrigation schemes - optimisation of irrigation water use - soil salinity control - groundwater recharge measurements - infiltration and drainage studies - studies of chemical pollution in the unsaturated zone
3. Measurement of soil water storage for water balances	- catchment and plot studies for various hydrological purposes

1.3 Time Domain Reflectometry

The recently developed method for the determination of soil moisture content by means of Time Domain Reflectometry (TDR) has many attractive features and is already being used world-wide. The method involves measuring the propagation velocity (travel time) of an electromagnetic pulse launched along parallel metallic probes (a sensor) embedded in the soil. Theoretical analysis and experimental correlations show that the pulse travel time is proportional to the dielectric constant of the soil (soil permittivity), which in turn is a sensitive measure of the volumetric fraction of soil water. For the latter relationship a widely used empirical calibration equation is available. If this is not accurate enough a soil specific calibration can be obtained easily. The method is non-destructive, yield results immediately and can be fully automated.

1.3.1 Permittivity

With TDR the soil water content measurement is ultimately a correlation between an instrument response (i.e. pulse transit time over the path lenght of the TDR probe) and an independent measure of soil water content (i.e. gravimetric measurements). The fundamental physical property that affects the pulse transit time is the dielectric property of the medium. The dielectric behaviour of a medium is characterized by its relative permittivity (relative dielectric constant). One speaks of relative permittivity of a medium as it is expressed versus that of vacuum. Although the relative permittivity is a complex quantity, for soil water content measurements the imaginary part can be neglected so that the relative permittivity is equal to the real part and one speaks of "*apparent*" relative permittivity "ε_a". Further discussion on this matter falls outside the scope of this paper. As commonly found in literature the term dielectric constant will be further used for referring to the relative apparent permittivity.

The electrodynamic expression for pulse velocity "v" of an electromagnetic (E.M.) wave along a transmission line, consisting of two parallel conductors, is given in terms of the propagation velocity of light in vacuum c, which is equal to 3 10^8 m s^{-1} and the dielectric constant ε_a of the medium :

$$v = \frac{c}{\sqrt{\varepsilon_a}} \tag{6}$$

For vacuum or air $\varepsilon_a = 1$, for water $\varepsilon_a = 81$ while for most mineral soil components $\varepsilon_a = 3$ to 7. As a result the dielectric constant of moist soil varies strongly with the water content and can be used to determine soil moisture content indirectly. With TDR, the dielectric constant is determined by measuring the propagation velocity of an electromagnetic pulse. The latter is obtained knowing the travelling time t of an E.M. wave along a transmission line of known length L embedded in the soil. Since the wave travels forth and back along the transmission line (rods) of length L embedded in the soil, the mechanical propagation velocity is given by following equation :

$$v = \frac{2L}{t} \tag{7}$$

By equating this mechanical pulse velocity with the electrodynamic pulse velocity of Eq.(6) the dielectric constant can be calculated as follows :

$$\varepsilon = \left[\frac{ct}{2L}\right]^2 \tag{8}$$

When a calibration relationship is available for the particular combination of soil, TDR apparatus, and sensor, the obtained e value can be converted into volumetric water content θ.

1.3.2 Operating principle

The main components of a typical TDR instrumentation are schematically drawn in figure 9. The electronic apparatus includes a control unit needed for synchronisation of the pulse generator, the sampling receiver and the output device or display.

The operating principle of indirect water content measurements by TDR is illustrated in figure 10. A TDR unit, for instance, the widely used Tektronix cable tester , generates a step voltage pulse with a very fast rise time (usually less than 0,1 ns). This electromagnetic wave travels along a coaxial cable to a sensor embedded in the soil. A TDR sensor usually consist of two or three parallel, rod-shaped, metallic electrodes, diameter of ± 5 mm and spacing of 3 - 5 cm, mounted in a handle (figure 11). The sensor rods form a transmission line or wave guide and the soil acts as a dielectric medium. When the step pulse encounters an impedance change, part of the pulse is reflected to the input source and the rest continues. Such reflections occur in particular at the beginning and the end of the sensor rods. Reflected signals on the way back to the apparatus are in turn partially reflected by impedance changes etc... until the pulse is dissipated. Also it shows clearly the effects of the impedance variations on the TDR outputs (figure 12).

A sampling receiver and timing device in the TDR unit measure the sum of the step voltage input and all the reflected voltages arriving back at the instrument as a function of time elapsed since the initiation of the pulse (figure 13). More often the reflection coefficient ρ is represented on the TDR output instead of voltage V. The reflection coefficient being the ratio of the voltage of the returning signal to that of the incident voltage wave. A variable number of samplings can be averaged for each wave form to increase the accuracy of the measurements.

The propagation velocity of the electromagnetic pulse in the soil can be derived from the time t between points A and B in the wave form and the length of the sensor rods L (figure 10). Point A corresponds with the first reflection due to the impedance change at the entrance of the sensor rods into the soil. For a given sensor and cable length, point A is always the same. Point B corresponds with the first reflection at the end of the sensor rods and varies with water content. The net travel time t in the soil, t, is the difference between point A and point B. Since the wave travels forth and back along the rods of length L embedded in the soil, the dielectric constant ε_a can be calculated using Eq. (8).

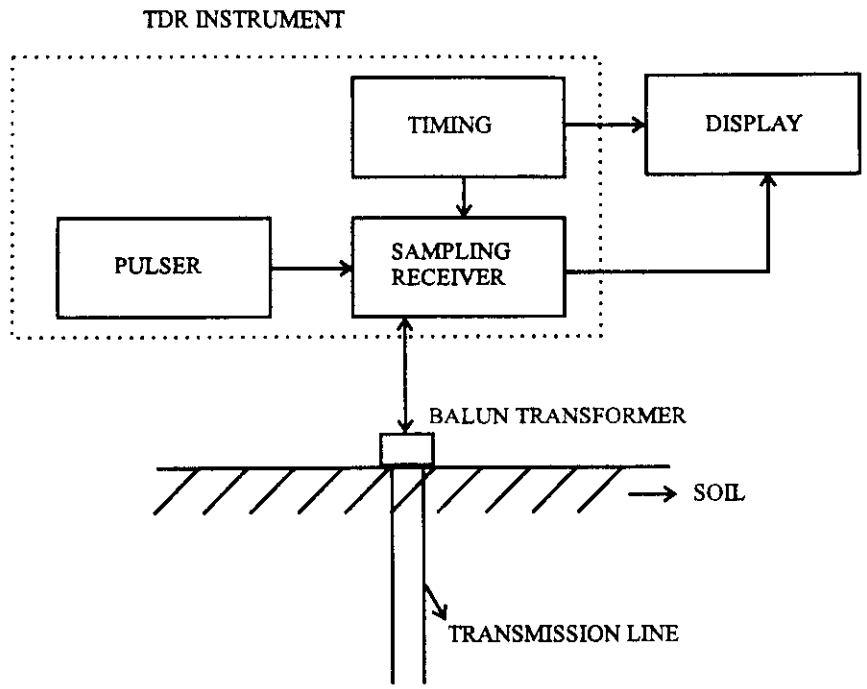

Figure 9. A block diagram of a TDR instrument and its display unit.

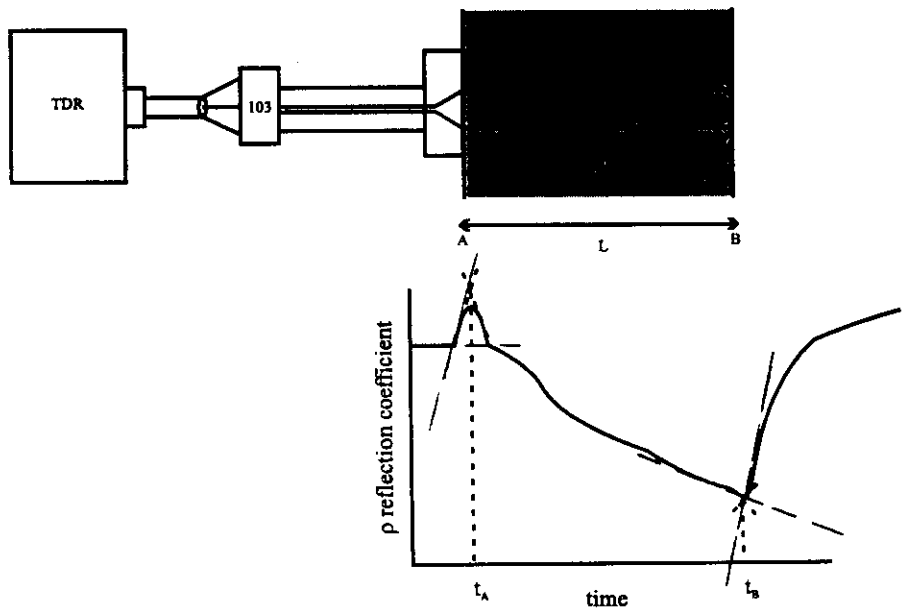

Figure 10. A typical TDR trace from a two-rod probe as portrayed at the top. The time interval t_B - t_A represents the time of travel of the signal for one return trip from A to B and back to A. This time is used in Eq [8] to calculate ε.

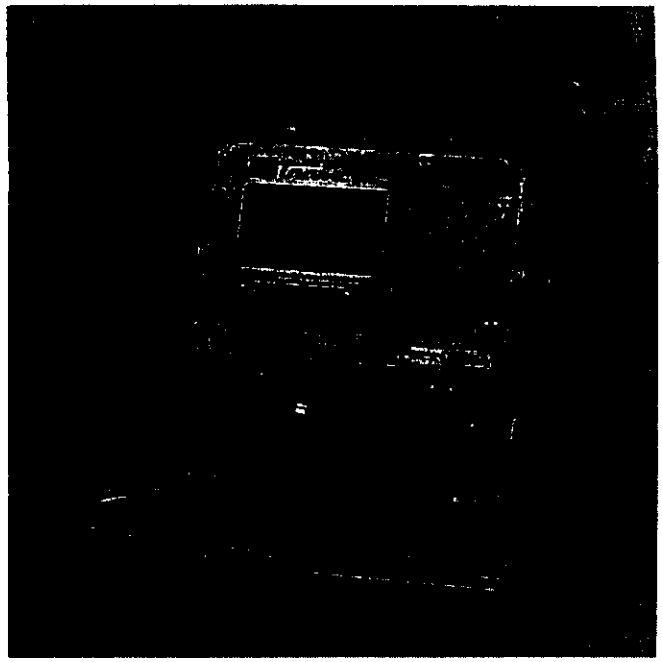

Figure 11. Three-rod probe with coaxial cable and cable tester.

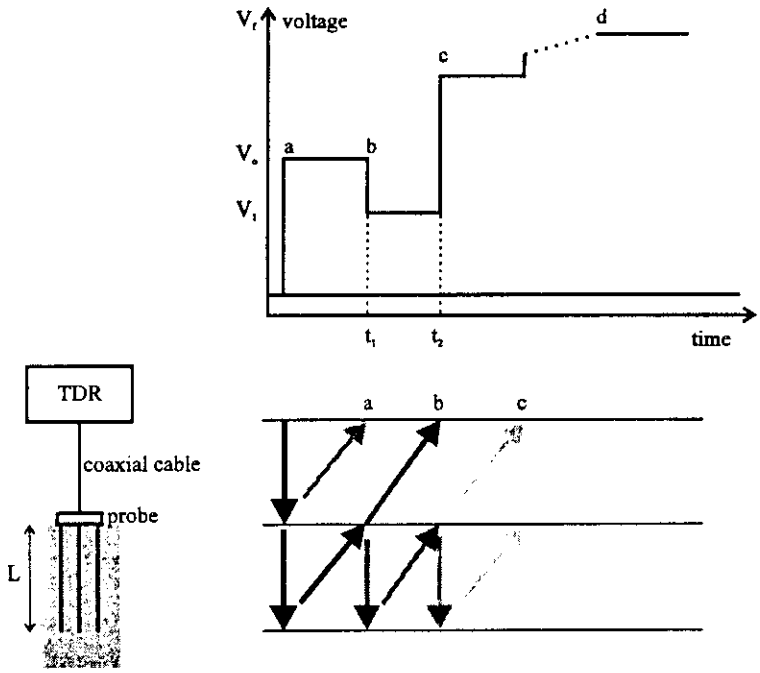

Figure 12. Idealized TDR voltage vs. time trace and 3-wire TDR probe with wire length L. Travel time is $t = t_2 - t_1$ in uniform material with a dielectric constant ε_a. Positions a, b, c and d correspond to signal production, reflection from start of probe, reflection from end of probe, and final asymptotic voltage after all reflections, respectively. Voltage levels V_0, V_1 and V_f are output voltage level, voltage level after reflection from probe start, and final asymptotic voltage level respectively.

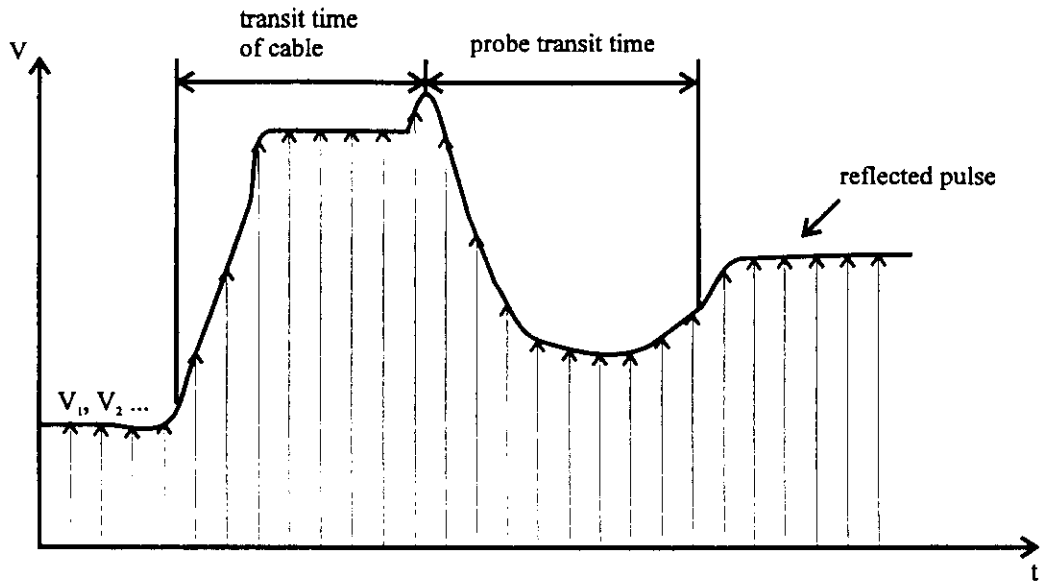

Figure 13. TDR-pulse measurement by sampling technique

1.3.3 Wave form analysis

The wave form shown in figure 14 is only the part corresponding with the first reflections by the beginning and end of the sensor. Reflections are actually registered by the TDR cable tester during a much longer time interval. The flat part before point A is proportional to the length of the coaxial cable and is of no interest. The multiple reflections following point C are complex and hard to analyse, but they are not needed for water content measurements.

The epoxy resin in the handle of the sensor created a distinct reflection at point A which can be determined accurately by the intersection of the tangents to the wave form. In some sensors an electronic element has been implanted at a fixed distance from the beginning of the rods to create an easily detectable reflection in the wave form. The peak starting in A is given by minor reflections due to the connection between the cable and the probe head. The graph between B and C is referred to the portion of the transmission line in the soil. The abrupt change in dielectric properties determines a strong reflection of energy. Therefore the registered voltage drops rapidly. The remaining signal propagates itself along the probe wires until it reaches their end. At this point all the energy is reflected back toward the source.

After new reflections (encountered along the opposite direction) the pulse reaches the emitter and a voltage increase is registered as shown by point C in the graph. The abscissa difference of points B and C is the time interval needed for the pulse to travel along the line and to be reflected back. While the point B can always be clearly distinguished, the location of point C on TDR graphs may present some troubles. In first instance, the voltage rise is not very fast due to

effects at the end of the probe. Furthermore, the extent of attenuation of energy reflected at the probe end when measuring in clay or saline soils or when long probes are used may be so relevant that only small voltage increase is detected. In the worst case the point C can not be individuated at all. A commonly used procedure for reducing this uncertainty is the identification of the position of point C from the intersection of tangent lines to the ascending portion of the graph and the previous sub-horizontal section as shown in figure 14.

The analysis of wave forms as illustrated in figure 14 can be performed visually and manually on the cable tester screen or on an analogue recording of the wave form. For large numbers of measurements this is tiring and time-consuming. Software is now available by which the needed part of the wave forms is first stored digitally and analysed later automatically by determining the intersections of the tangents to the wave form as shown in figure 14. Completely automated multiplexing of sensors, data acquisition and analysis is also possible. The nearly constant voltage (or reflection coefficient) at large time is also stored and used to calculate the bulk electrical conductivity of the soil and therefore the soil water salinity.

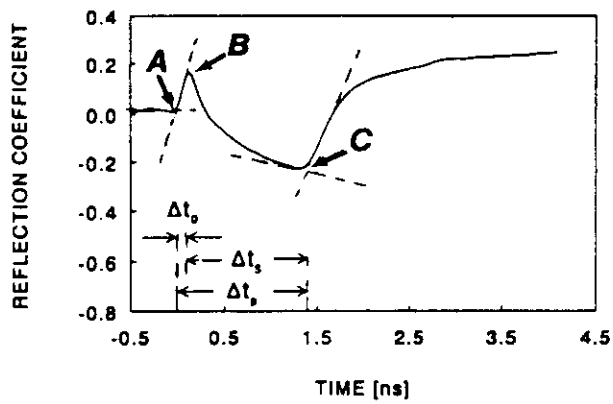

Figure 14. TDR wave form measured in a loamy sand with a triple-wire probe. The points A and C are the two reflection points that are obtained with the double-reflection analysis procedure. Δt_p is the travel time of the voltage signal in the probe, Δt_s the travel time in the soil and Δt_o the travel time in the epoxy resin.

1.3.4 Calibration

Several approaches have been tried out for relating the volumetric soil water content θ to the dielectric constant ε_a determined by means of TDR. In many cases, empirical relationships have been defined by simply interpolating observed data without paying too much attention to their physical interpretation. A commonly used "*universal calibration formula*" in the form of a third degree polynomial function has been proposed by Topp et al., (1980) :

$$\varepsilon = 3.03 + 9.3\theta + 146\theta^2 - 76.7\theta^3 \qquad (9)$$

The inversion of this equation is more convenient for converting measured permittivities to volumetric water content :

$$\theta = -5.3*10^{-2} + 2.92*10^{-2}\,\varepsilon - 5.5*10^{-4}\,\varepsilon^2 + 4.3*10^{-6}\,\varepsilon^3 \qquad (10)$$

This equation, often referred as the Topp equation, has given satisfactory results for many soils all over the world and has contributed greatly to the rapid introduction and development of TDR for indirect water content measurements. The water content determination is reduced to the measurement of the transit time of a voltage pulse over a know path length. However it has been found that this equation was not quite as "universal". Indeed for low bulk densities, specific mineralogical properties, clays, organic soils, etc..soil specific calibration is necessary.

Different researchers used the direct relation between measured transit time and volumetric water content. A physically based approach has been tried out by relating the dielectric constant of a multiple-phases mixture to the values of ε_a for each component and to their corresponding volumetric fraction (Dobson et al, 1985). Considering the wet soil as a three-phases mixture of air, water and mineral particles, its dielectric constant ε_a may be found by means of the following equation :

$$\varepsilon = \left[\theta\varepsilon_w^\alpha + (1 - n)\varepsilon_s^\alpha + (n - \theta)\varepsilon_a^\alpha\right]^{\frac{1}{\alpha}} \qquad (11)$$

where n is the soil porosity, 1-n, θ, and n-θ are volume fractions and ε_s, ε_w and ε_a are dielectric numbers of solid, liquid and gaseous phases respectively and α a parameter representing the geometry of the medium in relation to the applied electrical field. If the assumption of medium homogeneity and isotropy is assumed the value of 0.5 can be assigned to α.

Using this dielectric mixing model and making the summation for the travel time through each fraction and for $\alpha = 0.5$, following linear relation is obtained (figure 15) :

$$t = t_0 + A\theta \tag{12}$$

where : t = transit time
t_0 = running time through dry soil and constant for each soil
A = regression coefficient and probe dependent
θ = volumetric water content

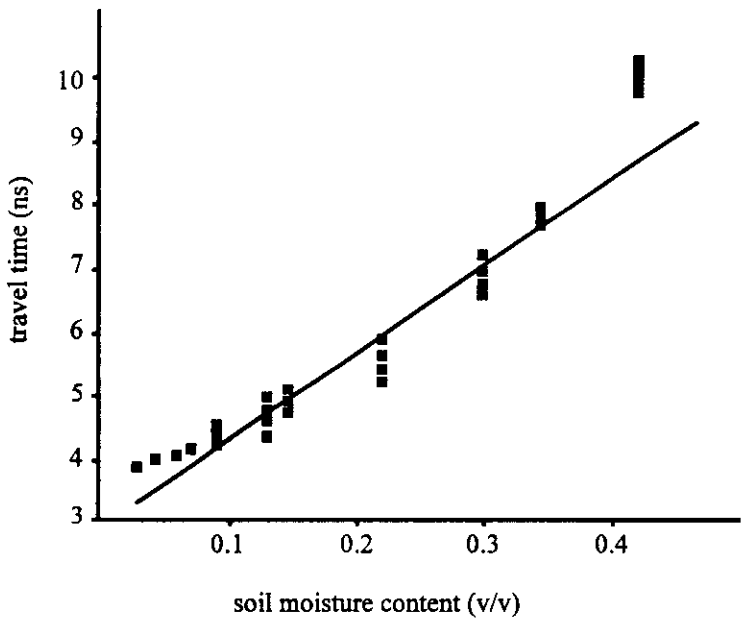

Figure 15. Transit time measured by TDR directly correlated to the volumetric soil moisture content.

This linear relation between transit time and volumetric water content was adapted to obtain a better curve fitting to a quadratic relation (figure 16):

$$t = a_0 + a_1\theta + a_2\theta^2 \tag{13}$$

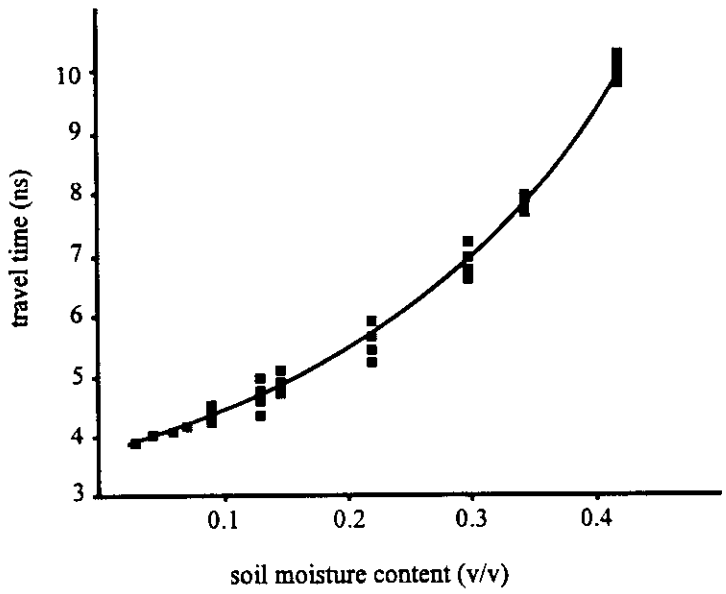

Figure 16. A quadratic calibration relation between transit time and volumetric soil water content.

1.3.5 Strengths and weaknesses of the TDR technique

The main attractiveness in estimating the soil water content from measurements of the propagation speed of a E.M. wave lies on the minimal influence of soil salinity, temperature and probe geometry. Variations of dimensions and parallelism imperfections of the conductors do not hamper the accuracy of determinations in most practical applications. The use of TDR is particularly advantageous when measurements are taken near the surface, where large and fast variations of water content are possible. In this case vertically inserted probes provide quick and reliable measurements of average water content.

The measuring volume does not extend much beyond the end of the sensor rods, but the cross-section of the measuring volume is approximately a cylinder with twice the distance between the rods as diameter. To measure the travel time with sufficient accuracy the sensor should obviously not to be too short (approximately 30 cm). Generally 10 cm is considered a practical limit, 5 cm an absolute minimum and it is advisable to restrict the maximum length to 50 cm. Hard or compacted clay soils further limits the probe length to 15 - 20 cm.

Repetitive and automatic measurements can be more easily performed with respect to other techniques and several equipment's have been designed for this purpose. Within the limitations described the TDR technique is largely flexible, and the inserted probes can be easily installed either for permanent continuous monitoring or for temporary measurements in laboratory and

either for permanent continuous monitoring or for temporary measurements in laboratory and field conditions. The use of datalogging devices allows a continuous monitoring in several locations within the same plot. The TDR technique is particularly suitable in mineral soils with low values of clay contents and electrical conductivity. In such soils "universal" calibration formulae can be used for accurate predictions of θ. This approach leads to accurate estimation of the total water storage in a profile with an error less than 10%. In clay and/or organic soils the use of TDR is certainly more difficult since site-specific calibrations are suggested.

However a non uniform distribution of water content along the vertical inserted probe due to steep wetting front or to the presence of soil layers with different hydraulic characteristics causes a dielectric discontinuity and therefore an impedance mismatching. The consequent additional reflections may increase the difficulties when interpreting TDR registrations.

Also the presence of soil heterogeneity within the volume investigated by the TDR probe, results in multiple reflections causing troubles in the analysis of TDR wave-form and so large errors in the determinations of the propagation time are possible. Air gaps and soil cracking near the conductors should also be avoided. So the installation of TDR probes should be made for minimising soil disturbance and for avoiding the formation of air gaps around the probes, where there is the maximum sensitivity. The presence of gravel and stones may obstacle a correct insertion of TDR probes. Some difficulties arise if measurements are required at large depths and digging is required.

Another source of inaccuracy is the increase in attenuation of the TDR signal with increasing electrical conductivity, although the entity of signal attenuation is often used for soil electrical conductivity estimates. It is difficult to use the TDR technique in field soils with bulk electrical conductivity greater than 600 mS m^{-1}. Other weaknesses are the current price of measurement equipment and the fact that TDR provides measurements over a relatively small soil sample.

REFERENCES

- Dobson, M.C.,Ulaby F.T., Hallikainen M.T. and El-Rayes M.A., 1985. Microwave dielectric behaviour of wet soil : part II. Dielectric mixing models. IEEE Trans. Geosci. Remote Sens., GE-23, pp 35-46.

- Topp G.C., Davis J.L. and Annan A.P., 1980. Electromagnetic determination of soil water content : Measurements in coaxial transmission lines. Water Resources. Res. 16 (3), pp. 574 -582

2. SOIL WATER POTENTIAL

2.1 Introduction

Soil water content is not sufficient to specify the entire status of water in soil. For example, if soils with a same water content but with different particle size distribution are placed in contact with each other, water will flow from a coarse textured soil to a fine textured soil. One needs to define a property that will help to explain this observation.

Perhaps the following analogy will help. Heat content (analogous to soil water content) is a property of a material that is useful for many purposes. It will not, however, tell us directly whether heat will flow. Therefore a heat intensity term, temperature, has been defined which permits to determine the direction of heat flow. The soil water term that is analogous to temperature (i.e. the intensity with which the water is in the soil) is called the soil water potential. Water potential is a much more complicated property than temperature.

2.2 Energy state of soil water

Soil water, like other bodies in nature, can contain energy in different quantities and forms. Classical physics recognizes two principal forms of energy, kinetic and potential. Since the movement of water in the soil is quite slow, its kinetic energy, which is proportional to the velocity squared, is generally considered to be negligible. On the other hand, the potential energy, which is due to position or internal condition, is of primary importance in determining the state and movement of water in the soil.

The potential energy of soil water varies over a very wide range. Differences in potential energy of water between one point and another give rise to the tendency of water to flow within the soil. The spontaneous and universal tendency of all matter in nature is to move from where the potential energy is higher to where it is lower and to equilibrate with its surroundings. In the soil, water moves constantly in the direction of decreasing potential energy until equilibrium, definable as a condition of uniform potential energy throughout, is reached.

The rate of decrease of potential energy with distance is in fact the moving force causing flow. A knowledge of the relative potential energy state of soil water at each point within the soil can allow us to evaluate the forces acting on soil water in all directions, and to determine how far the water in a soil system is from equilibrium. This is analogous to the well-known fact that an object will tend to fall spontaneously from a higher to a lower elevation, but that

lifting it requires work. Since potential energy is a measure to the amount of work a body can perform by virtue of the energy stored in it, knowing the potential energy state of water in the soil and in the plant growing in that soil can help us to estimate how much work the plant must expend to extract a unit amount of water.

Clearly, it is not the absolute amount of potential energy "contained" in the water which is important in itself, but rather the relative level of that energy in different regions within the soil. The concept of soil water potential is a criterion, for this energy. It expresses the specific potential energy (= per unit mass) of soil water relative to that of water in a standard reference state. The standard state generally used is that of a hypothetical reservoir of pure free water (i.e. water not influenced by the solid phase), at atmospheric pressure, at the same temperature as that of soil water (or at any other specified temperature) and at a given and constant elevation.

It is the convention to assign to free and pure liquid water a potential value of zero.

Since the elevation of this hypothetical reservoir can be set at will, it follows that the potential which is determined by comparison with this standard is not absolute, but by employing even so arbitrary a criterion we can determine the relative magnitude of the specific potential energy of water at different locations or times within the soil.

The concept of soil water potential is of great fundamental importance. This concept replaces the arbitrary categorizations which prevailed in the early stages of the development of soil physics and which purported to recognize and classify different forms of soil water : e.g. gravitational water, capillary water, hygroscope water.

New definition by the soil physics terminology committee of the International Soil Science Society provided more clarity in what used to be a rather complicated theoretical set of criteria. The total potential of soil water was defined as follows : " the amount of work that must be done per unit quantity (mass, volume or weight) of pure free water in order to transport reversibly and isothermally an infinitesimal quantity of water from a pool of pure water at a specified elevation at atmospheric pressure (standard reference state) to the soil water at the point under consideration in the soil-plant-atmosphere-system" (figure 17).

If work is required the potential is positive, but if water in the reference state can accomplish work in moving into the soil the potential is negative.

Soil water is subjected to a number of force field which cause its potential to differ from that of pure free water. Such forces result from the attraction of the solid matrix for water, as well as from the presence of dissolved salts and the action of the local pressure in the soil gas phase and the action of the gravitational field. Accordingly the total potential (ψ_t) of soil water relative to a chosen standard rate can be thought of as the sum of the separate contributions of the various components as follows :

$$\psi_t = \psi_g + \psi_o + \psi_m + \psi_{e.p} + \ldots$$

where : ψ_t = total soil water potential
ψ_g = gravitational potential
ψ_o = osmotic potential
ψ_m = matric potential
$\psi_{e.p}$ = external gas pressure potential
. . . = additional terms are theoretically possible

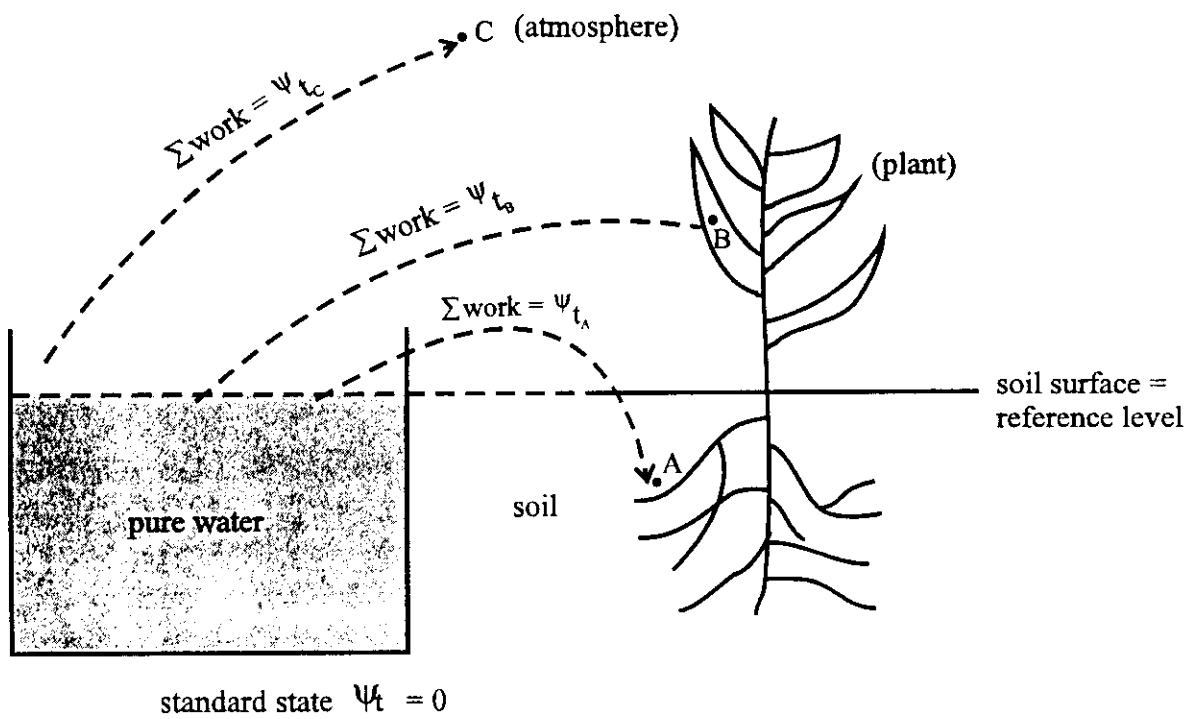

Figure 17.Potential of soil water, water in plant cell and water in the atmosphere

The main advantage of the total potential concept is that it provides a unified measure by which the state of water can be evaluated at any time and every where within the soil-plant-atmosphere system.

2.3 Quantitative expression of soil water potential

The dimensions of the soil water potential are those of energy per unit quantity of water and the units depend on the way the quantity is specified. Common alternatives used are :

a. Energy per unit mass of water (J/kg)
   This method of expression is not widely used.

b. Energy per unit volume of water (pressure) (J/m^3 or N/m^2)
   This is the most common method of expressing potential and can be written with units of either Pascal or bar or atmosphere.

c. Energy per unit weight of water (head) (J/N = Nm/N = m)
   This method of expressing potential is also common and has units of length.

For conversion from one unit to another knows that :

- 1 bar corresponds to 100 J/kg
- 1 bar = 10^5 Pa
- 1 bar corresponds to 10 m water head

2.4 Gravitational potential

Every body on the earth's surface is attracted towards the centre of the earth by a gravitational force equal to the weight of the body, that weight being the product of the body's mass by the gravitational acceleration. To rise a body against this attraction, work must be expended and this work is stored by the rised body in the form of gravitational potential energy. The amount of this energy depends on the body's position in the gravitational force field.

The gravitational potential of soil water at each point is determined by the elevation of the point relative to some arbitrary reference level. If the point in question is above the reference, ψ_g is positive. If the point in question is below the reference, ψ_g is negative. Thus the gravitational potential is independent of soil properties. It depends only on the vertical distance between the reference and the point in question.

Conversion table for units of soil water potential (*)

Specific potential units	Volumetric potential units				Weight potential units
Joule kg^{-1}	bar	millibar	Pa	atmosphere	m
0.0001	0.000001	0.001	0.1	0.000000987	0.001017×10^{-2}
1	0.01	10	10^3	0.00987	10.17×10^{-2}
100	1	1000	10^5	0.987	10.17
0.1	0.001	1	10^2	0.000987	1.017×10^{-2}
101.3	1.013	1013	1.013×10^5	1	10.30
0.09833	0.0009833	0.9833	98.33	0.0009703	10^{-2}

(*) The density of water was taken as 1.000 g cm^{-3}. This holds only at 4°C but is approximately correct at other temperatures.

At a height z below a reference level (e.g. the soil surface) the gravitational potential of a mass M of water, occupying a volume V is :

$$-Mgz = -\rho_w V g z$$

where : ρ_w = density of water
g = acceleration of gravity

Gravitational potential can be expressed :

- per unit mass : $\psi_g = -gz$ (J/kg)

- per unit volume : $\psi_{gv} = \psi_g \rho_w = -\rho_w g z$ (Pa)

- per unit weight : $\psi_{gw} = \frac{\psi_g}{g} = -z$ (m)

2.5 Osmotic potential

The osmotic potential is attributable to the presence of solutes in the soil water. The solutes lower the potential energy of the soil water. Indeed, the fact that water molecules move through a semi-permeable membrane from the pure free water into a solution (osmosis) indicates that the presence of solutes reduces the potential energy of the water on the solution side (figure 18). At equilibrium sufficient water has passed through the membrane to bring about significant difference in the heights of liquid. The difference (z) in the levels represents the osmotic potential.

Since the osmotic potential of pure free water is zero the osmotic potential of a solution at the same temperature of free water is negative (water flow occurs from point of high potential to one with lower potential).

Differences in osmotic potential only play a role in causing movement of water when there is an effective barrier for salt movement between the two locations at which the difference in ψ_o was observed. Otherwise, the concentration of salts will become the same throughout the profiles by the process of diffusion and the difference in ψ_o will no longer exist. Therefore osmotic potential does not act as a driving force in water flux. This potential is of importance in water movement into and through plant roots, in which there are layers of cells which exhibit different permeabilities to solvent and solute.

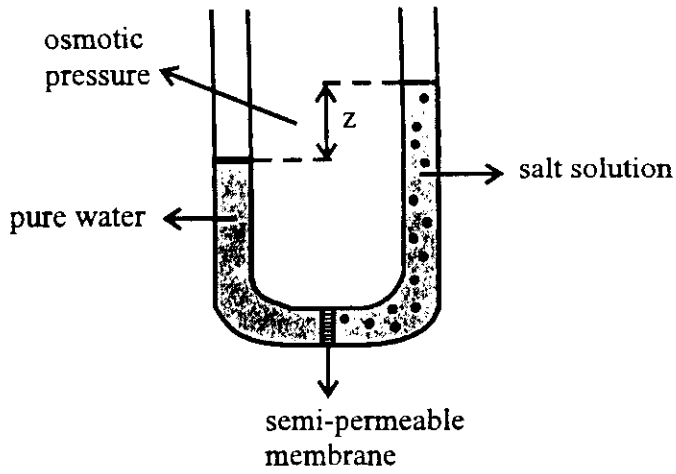

Figure 18.Schematic presentation of osmosis.

2.6 Matric potential

Matric potential results from forces associated with the colloidal matric and includes forces associated with adsorption and capillarity. These forces attract and bind water in the soil and lower its potential energy below that of bulk water. The capillarity results from the surface tension of water and its contact angle with the solid particles. In an unsaturated (three-phase) soil system, curved menisci form which obey the equation of capillarity :

$$P_i - P_a = \Delta P = \gamma(\frac{1}{R_1} + \frac{1}{R_2})$$

where : P_i = pressure of soil water, can be smaller than atmospheric
P_a = atmospheric pressure, conventionally taken as zero
ΔP = pressure deficit
γ = surface tension of water
R_1, R_2 = principal radii of curvature of a point on the meniscus, taken as negative when the meniscus is concave

As we assume the soil pores to have a cylindrical shape (figure 19) the meniscus has the same curvature in all directions and equation above becomes :

$$P_i = \Delta P = \frac{-2\gamma}{R}$$

since :

$$R = \frac{r}{\cos\alpha}$$

($\alpha = 0$: angle of contact between water and the soil particle surface)

$$P_i = \Delta P = \frac{-2\gamma}{r} \qquad \text{with } \Delta P \text{ equals - h } \rho_w \text{ g}$$

where : r = radius of the capillary tube
h = height of capillary rise
ρ_w = density of water (10^3 kg/m^3)
g = acceleration of gravity (9.81 m/s^2 ≈ 10 m/s^2 ≈ 10 N/kg)

If the soil were like a simple bundle of capillary tubes, the equations of capillarity might be themselves suffice to describe the relation of the negative pressure potential or matric potential to the radii of the soil pores in which the menisci are contained. However, in addition to the capillarity phenomenon, the soil also exhibits adsorption, which forms hydration envelopes, over the particle surfaces. These two mechanisms of soil water interaction are illustrated in figure 20.

The presence of water in films as well as under concave menisci is most important in clayey soil and at high suctions or low potential, and it is influenced by the electric double layer and the exchangeable cations present. In sandy soils adsorption is relatively unimportant and the capillary effect predominates.

In general, however, the matric potential results from the combined effect of the two mechanisms, which cannot easily be separated since the capillary "wedges" are at a state of internal equilibrium with the adsorption "films" and the ones cannot be changed without affecting the others. Hence matric potential denotes the total effect resulting from the affinity of the water of the whole matric of the soil, including its pores and particle surfaces together.

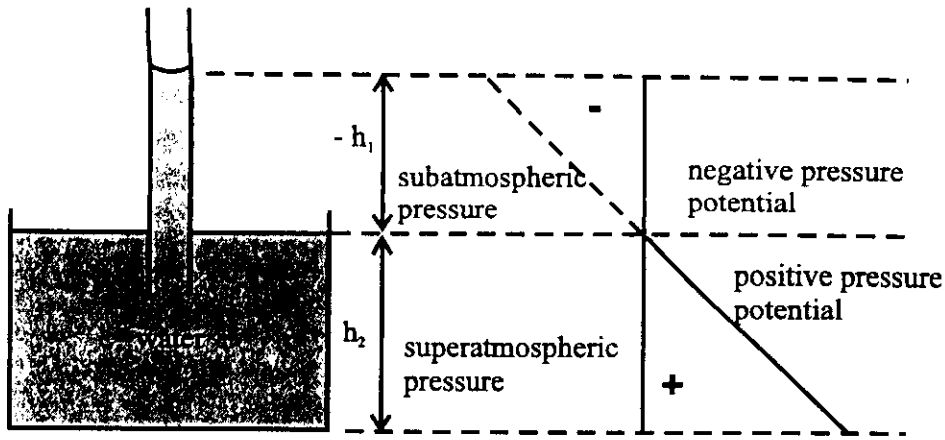

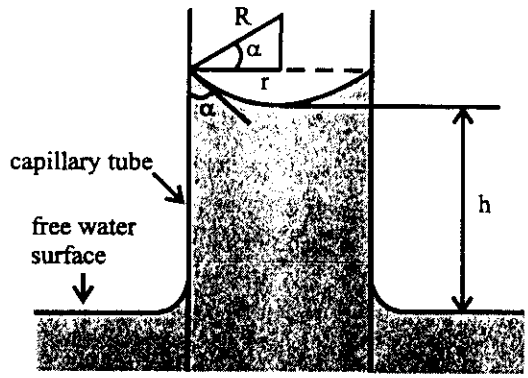

Figure 19.Capillary rise of water into a capillary tube.

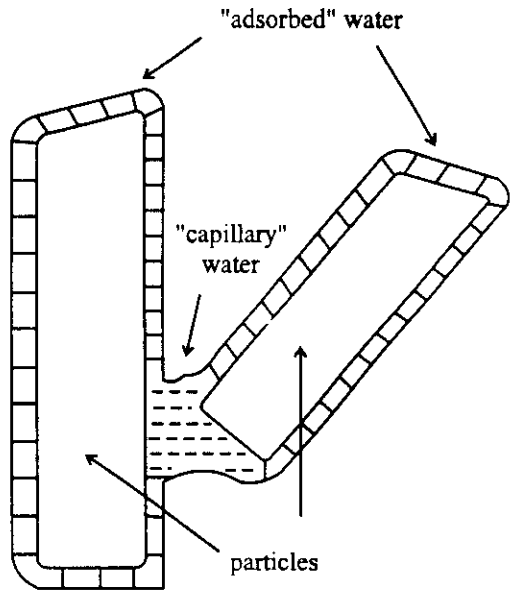

Figure 20.Water in an unsaturated soil is subject to capillarity and adsorption, which combine to produce a matric potential.

The matric potential can be expressed :

- per unit mass : $\psi_m = -gh = \frac{-2\gamma}{\rho_w r}$ (J/kg)

- per unit volume : $\psi_m \rho_w = -\rho_w g h = \frac{-2\gamma}{r}$ (Pa)

- per unit weight : $\psi_m \frac{1}{g} = -h = \frac{-2\gamma}{\rho_w g r}$ (m)

The matric potential is a dynamic property of the soil.

In saturated soil (below the ground water level) the liquid phase is at hydrostatic pressure greater than atmospheric and thus its pressure potential is considered positive (figure 19). Thus water under a free water surface is at a positive pressure potential (hydrostatic pressure potential ψ_h), while water at such a surface is at zero pressure potential (assuming atmospheric pressure in the soil) and water which has risen in a capillary tube above that surface is characterized by a negative pressure or matric potential.

Since soil water may exhibit either of the two potentials, but not both simultaneously, the matric and the hydrostatic pressure potential are referred to as the pressure potential (ψ_p).

Nevertheless it is an advantage in unifying the matric potential and hydrostatic pressure potential in that this unified concept allows one to consider the entire profile in the field in terms of a single unsaturated zone, below and above the water table.

2.7 External gas pressure potential

A factor which may affect the pressure of soil water is a possible change in the pressure of the ambient air. In general this effect is negligible in the field as the atmospheric pressure remains nearly constant small barometric pressure fluctuations notwithstanding. However, in the laboratory the application of excess air pressure to change the soil water pressure is a common practice resulting into the so called external gas pressure of pneumatic potential .

FINAL REMARKS

1. Matric potential and the former term matric suction are numerically equal - when expressed in the same units - but except for the sign.

2. The effect of an external gas pressure different from the atmospheric (reference) pressure is generally also included in the pressure potential so that :

$$\psi_p = \psi_m + \psi_h + \psi_{e.p}$$

Accordingly the total potential being :

$$\psi_t = \psi_g + \psi_o + \psi_p$$

characterizes fully the state of water in soil under the prevailing conditions ; the gradients of these three parameters are the basis for transport theory.

2.8 Hydraulic head

The total potential is obtained by combining the relevant component potentials :

$$\psi_t = \psi_g + \psi_o + \psi_p$$

Equilibrium, which is defined as the situation where mass transfer of water in the liquid phase is absent, is obtained when the value of the total potential at different points in the system in constant. Usually, sufficient condition is that the sum of the component potentials, ψ_o being ignored, is constant. The equilibrium condition states then that :

$$\psi_g + \psi_p = constant = \psi_H \qquad (14)$$

called hydraulic potential.

As already stated, the external gas pressure or pneumatic potential in the field may be assumed to be zero. Also the soil water within a profile may exhibit either matric or hydrostatic pressure potential (figure 19) but not simultaneously. Therefore it is an advantage in unifying both in a single continuous potential extending from the saturated region into the unsaturated region below and above the water table.

As it is often usual to designate the potential in terms of head, equation (14) becomes :

$$H = h + z$$

where : H = the hydraulic head (m)
h = the soil water pressure head (m)
> 0 under the water table (saturated zone)
< 0 above the water table (unsaturated zone)
z = the gravitational head (m)

The definition is very important because the hydraulic gradient between two points under consideration in a soil is the driving force for water movement.

In figure 21 the condition is applied to a vertical soil column in equilibrium with a water table. No water movement occurs in the column. The water table is taken as the reference level for the gravitational potential.

Under the water table matric potential equals zero, but a pressure potential called hydrostatic pressure potential occurs which can also be presented by a value of h but with always a positive sign.

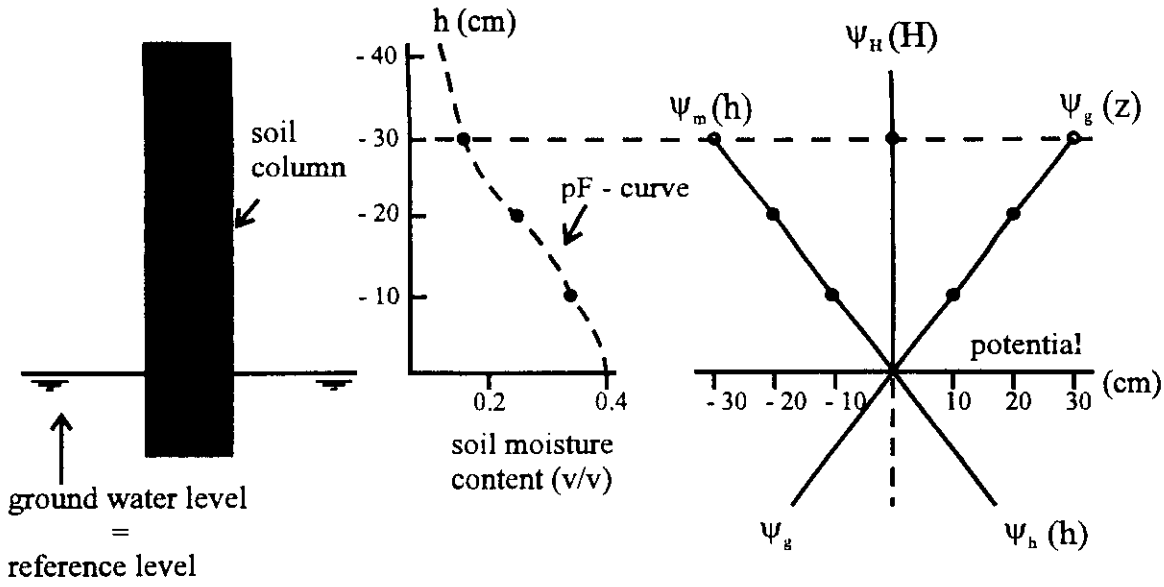

height (cm)	ψ_g (z,cm)	ψ_m (h,cm)	ψ_h (h,cm)	ψ_H (H,cm)
30	30	-30	0	0
20	20	-20	0	0
10	10	-10	0	0
0 reference level	0	0	0	0
-10	-10	0	10	0
-20	-20	0	20	0

Figure 21.Equilibrium condition in a soil column.

3. TENSIOMETER

3.1 Hydrostatic pressure potential - Piezometer

As discussed earlier the hydrostatic (positive) pressure potential ψ_h under field conditions applies to saturated soils and is measured with a piezometer (figure 22).

A piezometer is a tube of a few cm inner diameter, open at both ends, which is installed in a soil profile. If the lower end is below the groundwater table, a piezometer is partially filled with water. By determining the height of the water level in a piezometer it is possible to calculate the (positive) hydrostatic pressure potential of the soil water at the lower end of the tube. The diameter of piezometer is chosen large enough that capillary rise and resistance to water flow are negligible. As a result, any variation in hydraulic potential that may arise inside the piezometer, is instantaneously equalized. Thus, even if the hydrostatic pressure potential at the lower end is changing rapidly, the water inside a piezometer goes through a series of static equilibria and at any moment it can be assumed that the hydraulic head is uniform and equal to the hydraulic head of the soil water at the open lower end. There exchange of water takes place such that the pressure is always locally uniform. The static hydraulic head in piezometer can be determined by measuring the depth of the water level, since at the flat air-water interface the pressure potential is zero.

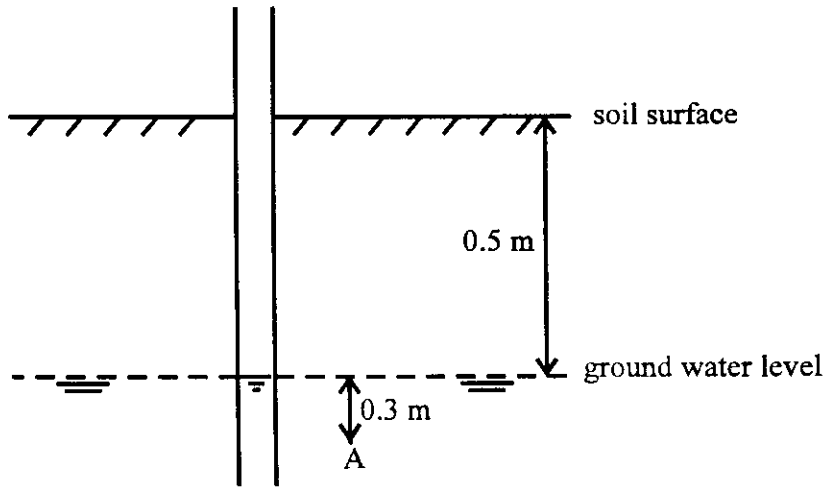

Figure 22.A piezometer in a soil profile

Figure 22 shows a piezometer in a soil profile in which the water is at static equilibrium. The reference point z = 0 is taken at the soil surface. In the piezometer at the water level H = h + z = 0 - 0.5 m = - 0.5 m. Thus at point A, H must also be - 0.5 m (H = h + z = 0.30 m - 0.80 m = - 0.50 m).

The hydrostatic pressure potential expressed per unit weight of water at any point in the soil under the water table is the distance between the point and the water level in the piezometer tube.

The water level in a piezometer tube is at the level of the groundwater table in a situation of static equilibrium, independent of the depth of the lower end.

3.2 Matric potential - Tensiometer

Piezometers cannot be used to measure negative pressure potentials because in unsaturated conditions, water flows out of the tube into the soil leaving the tube dry. The negative pressure or matric potential can be measured with the so-called tensiometer.

The tensiometer consists of a liquid filled porous cup, mostly of ceramic material and connected to a pressure measuring device such as a mercury manometer or vacuum gauge via a liquid-filled tube (figure 23).

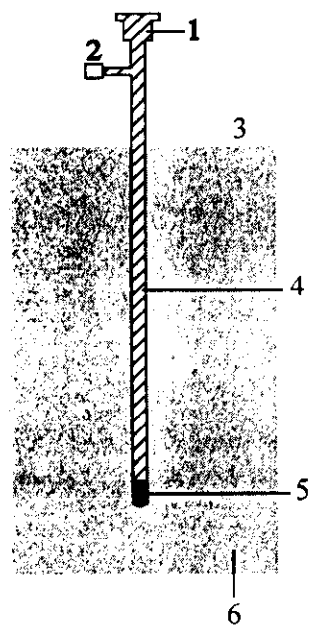

1. Flexible water reservoir
2. Gauge to measure tension
3. Soil level
4. Filled with water
5. Porous end (cup) through which water can move
6. Soil

Figure 23.Tensiometer with a vacuum gauge (jet fill tensiometer).

If the ceramic cup is embedded in soil, the soil solution can flow into or out of the tensiometer through the very small pores in the ceramic cup. Analogously to the situation discussed for piezometer, this flow continues until the (negative) pressure potential of the liquid in the cup has become equal to the (negative) pressure potential of the soil water around the cup. Thus the (negative) pressure potential called matric potential ψ_m of soil water can be measured with a tensiometer, and is therefore also often called tensiometer pressure potential.

3.3 Principle of the tensiometer

When the cup is placed in a water reservoir (figure 24), the water inside the cup comes into hydraulic contact with the water in the reservoir through the water-filled small pores in the ceramic walls. The water level in the tube will indicate the level of the water in the reservoir.

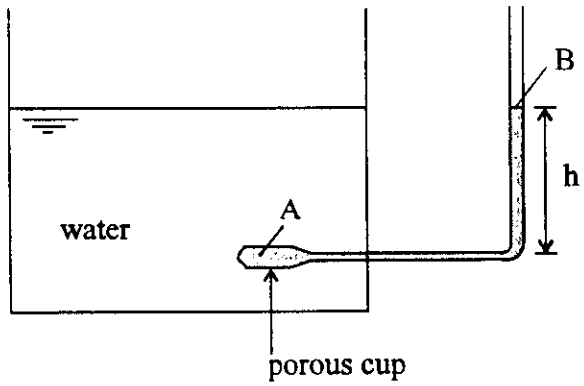

Figure 24.Porous cup connected with a piezometer tube for measuring pressure potentials under the water table

The pressure is given by the height h of the water level above the middle of the porous cup and the pressure P_A equals :

$$P_A = \rho_w g h$$

where : ρ_w = density of water
g = acceleration due to gravity

If we place now the porous cup, connected with an U-shape water filled tube in a soil than the bulk water inside the cup will come in hydraulic contact with the liquid phase in the soil. When initially placed in the soil, the water in the tensiometer is at atmospheric pressure. Soil water in unsaturated soil has a negative pressure and therefore exercises a suction which drawn out a certain amount of water from the rigid and air-tight tensiometer, causing a drop in the water level at the open end of the U-tube (figure 25).

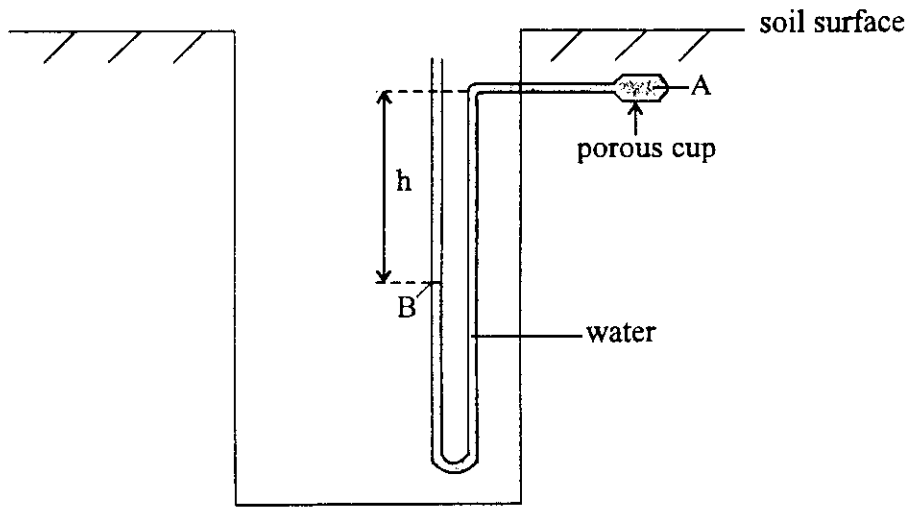

Figure 25. Tensiometer for measuring pressure potentials in soils

The drier the soil, the higher the suction and the lower the water level at equilibrium in the U-tube. The height h of the liquid column that has moved into ("sucked into") the soil in figure 25 is therefore an index of the magnitude of the potential, or :

$$P_A = -\rho_w g h$$

As h is measured downwards the minus sign is introduced so that P_A gives a negative pressure.

This type of tensiometer is very simple and useful to illustrate the basic principles involved. Practical applications often do not allow the use of the water manometer because the U-tube extends below the level of the tensiometer cup and measurements thus requires inconvenient, deep pits. Therefore open manometers, filled with immiscible liquids of different densities such as mercury are used so that these problems do not arise (figure 26).

Using mercury implies that a relatively short height indicated a relatively large pressure difference in the manometer (1 cm of mercury corresponds to 13.55 cm of water). Besides the simple water or mercury manometer a vacuum gauge or an electrical transducer is also used.

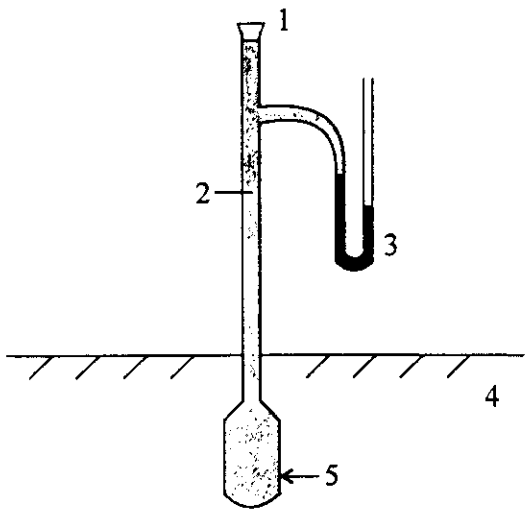

1. stop
2. water
3. mercury
4. soil
5. porous cup

Figure 26. Tensiometer with mercury manometer.

3.4 How to calculate the soil water pressure head h and the hydraulic head H

Let x be the height of the mercury in the manometer (cm) and z the vertical axis (figure 27). At the interface water-mercury in the manometer, the pressure is the same in water and in mercury (being P_B). The repartition of the pressure is hydrostatic in the water column between point B and the tensiometer cup (point A), but also between point B and the free surface of the mercury in the reservoir (point C).

Using the hydrostatic law for liquids in equilibrium one obtains per unit weight of liquid the following hydraulic head equation :

$$z + \frac{P}{\rho g} = constant$$

where : z = gravitational head
$P/\rho g$ = pressure head

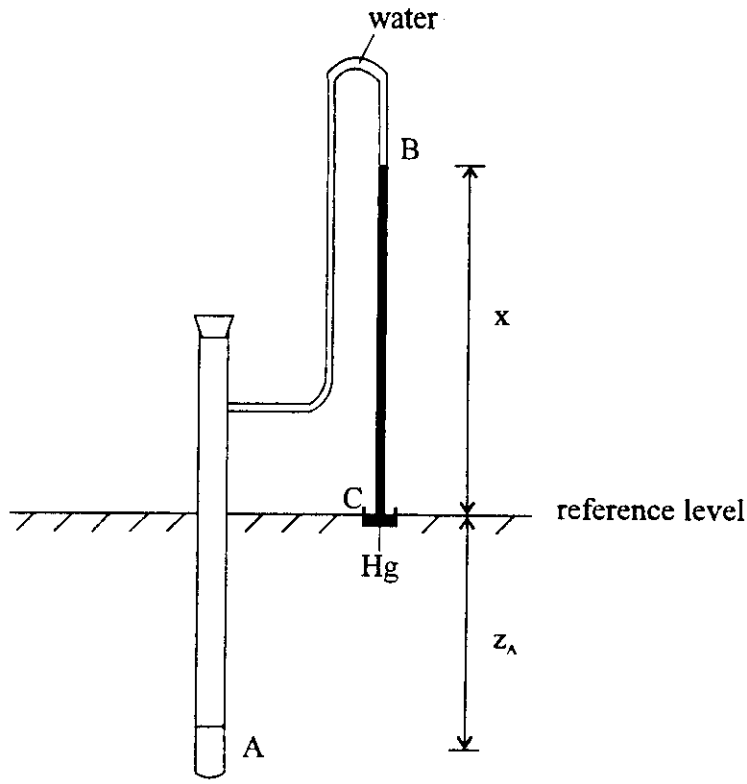

Figure 27. Tensiometer installation with the mercury level in the reservoir at the soil surface being the reference level

From figure 27 one obtains :

- in water : $$z_A + \frac{P_A}{\rho_w g} = z_B + \frac{P_B}{\rho_w g}$$

Because soil surface is taken as reference level for the gravitational potential, and point A is located below that level, the gravitational head is negative (- z_A).

$$P_A - z_A \rho_w g = P_B + z_B \rho_w g$$

$$P_A = P_B + z_B \rho_w g + z_A \rho_w g = P_B + \rho_w g (z_A + z_B) \qquad (15)$$

- in mercury : $$z_B + \frac{P_B}{\rho_{Hg}\, g} = z_C + \frac{P_C}{\rho_{Hg}\, g}$$

because : z_C = reference level = 0
P_C = atmospheric pressure = 0

the equation becomes : $$z_B + \frac{P_B}{\rho_{Hg}\, g} = 0$$

or : $$P_B = -\rho_{Hg}\, g\, z_B \qquad (16)$$

(16) in (15) gives :

$$\frac{P_A}{\rho_w\, g} = \frac{-\rho_{Hg}\, g\, z_B}{\rho_w\, g} + z_A + z_B \qquad (17)$$

since : ρ_w = 1000 kg m^{-3}
ρ_{Hg} = 13600 kg m^{-3}

(17) becomes : $$h_A = -13.6\, z_B + z_A + z_B$$

or : $$h_A = -12.6\, z_B + z_A$$

$$h_A = -12.6\, x + z_A \qquad (18)$$

Normally the free surface of the mercury in the reservoir (point C) is located y cm above the soil surface (reference level) (figure 28).

Equation (18) becomes : $$h_A = -12.6\, x + y + z_A \qquad (19)$$

The hydraulic head H, being the sum of the pressure head h and the gravitational head z, (H = h + z), becomes :

$$H = -12.6\, x + y + z_A + (-z_A)$$

$$H = -12.6\, x + y \qquad (20)$$

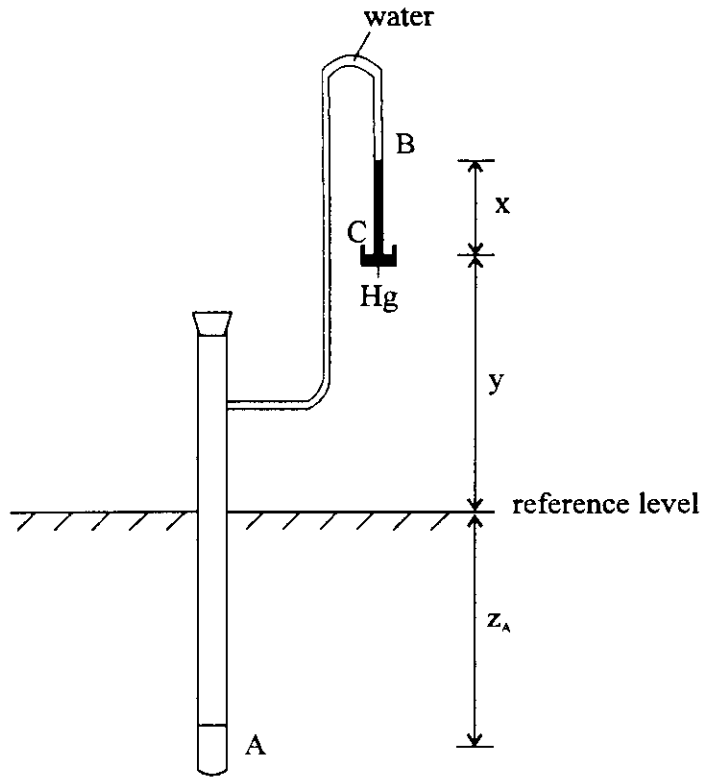

Figure 28. Tensiometer installation with the mercury reservoir y cm above soil surface.

If the soil water pressure head around the porous cup changes, the height of the mercury level will change consequently. For a situation where e.g. two tensiometers are connected to the same mercury reservoir, the value y is the same and from equation (20) it follows that :

$$H_1 - H_2 = -12.6(x_1 - x_2)$$

This means that tensiometers connected to the same mercury reservoir yield hydraulic head differences irrespective of there depths. So H_1 - H_2 = 0 where $x_1 = x_2$. Such installation provides at once the direction of the water flow: from the tensiometers with low mercury height to those with high mercury height.

The mercury manometer can be replaced by a Bourdon or dial vacuum gauge (figure 29) or by a pressure transducer (figure 30). For such manometers equation (19) and equation (20) became :

$$h = h_{man} + z_o = h_{man} + z_1 + z_2$$

$$H = h_{man} + z_1 + z_2 - z_2 = h_{man} + z_1$$

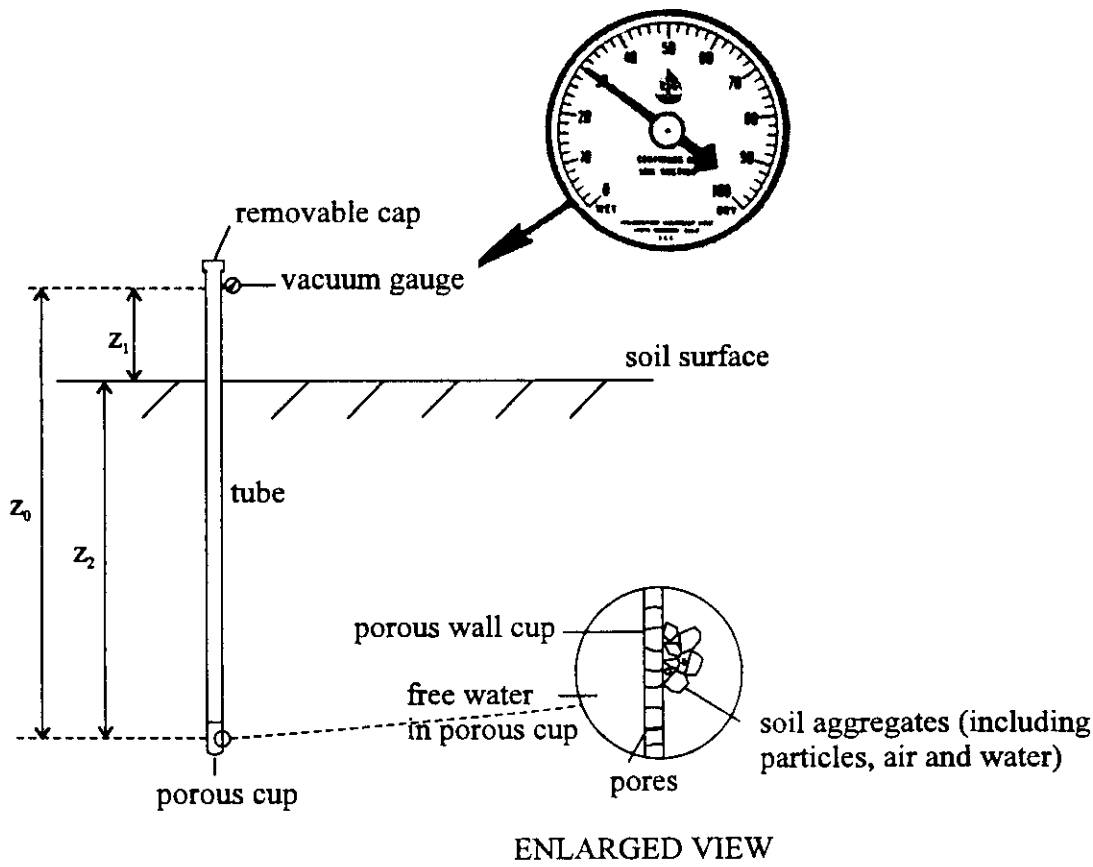

Figure 29.Principle of tensiometer with vacuum gauge

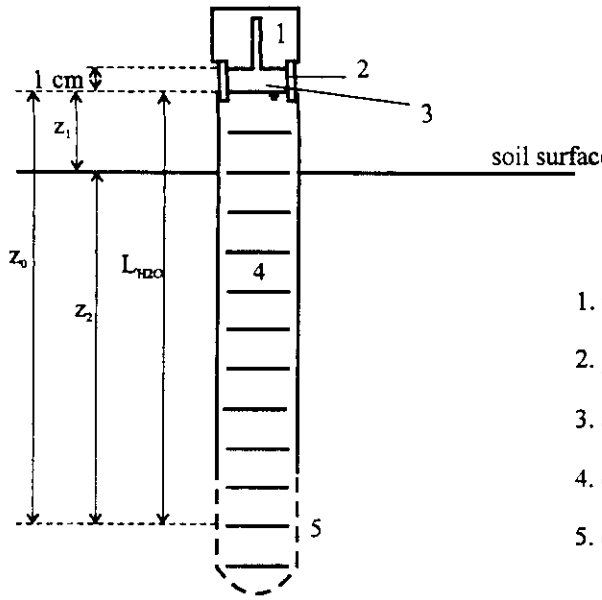

1. nitril-caoutchouc septum stopper
2. plexi-glass tube (lucid)
3. air pocket (V_l) (end of syringe needle here)
4. deaerated water
5. ceramic cup

MEASURING DEVICE

1. air vent
2. containment with p = p (atm)
3. semiconductor element
4. steel membrane (D = 13 mm)
5. guiding tube
6. guiding tube for needle
7. syringe needle (D = 0.4 mm) dead volume (V_n)
8. guiding spring
9. membrane chamber (45 mm)
10. shielded four lead wire

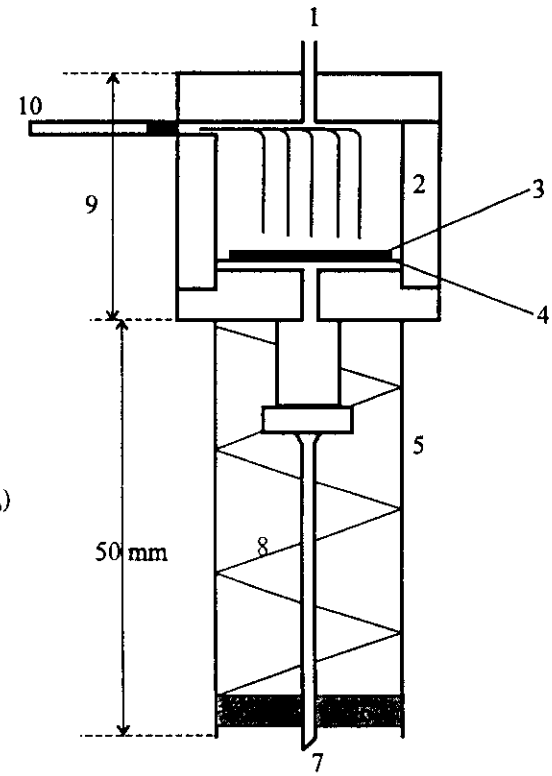

Figure 30. Diagram of tensiometer with septum stopper and pressure transducer with attached syringe needle

3.5 Some characteristics of the tensiometer

3.5.1 Cup conductance "C"

Being the volume of water dV that has to be displaced per unit time between the tensiometer and the soil through the porous cup for the measuring device to register the change in soil water pressure head dh :

$$C = \frac{dV}{dt\,dh} \qquad (m^2/s)$$

The surface area, conductivity and wall thickness of the porous cup can be varied to increase its conductance and consequently reduce the measuring time. However there are practical limits to this e.g. the air entry value of the porous cup.

3.5.2 Sensitivity of the manometer "S"

The sensitivity of the manometer determines the performance of the pressure measuring device :

$$S = \frac{dh}{dV} \qquad (m^{-2})$$

where dV is the volume of water displaced needed by the measuring device to register a pressure head change dh.

- water/mercury manometer

The water manometer has the lowest sensitivity as it requires a large volume of water to be displaced per unit soil water pressure head change. If the diameter of the manometer tube is large enough to eliminate capillary effects, soil water pressure head can be measured with a precision of ± 1 mm. Since large change in soil water pressure head requires an exchange of a large volume of water with the soil it is convenient to replace water by mercury.

The mercury manometer reduces the height of the liquid column and thus the displaced volume of water by a factor 12.6 (equation 19) and so increases the sensitivity by the same factor. The overall precision of mercury manometers is often not better than 5 cm WH. Also the size of the manometer tube influences the sensitivity. Indeed if the cross-sectional area of a manometer tube is A cm^2 the water displacement head ΔV is A Δh so that :

$$S = \frac{\Delta h}{A \Delta h} = \frac{1}{A} \qquad (m^{-2})$$

- Bourdon/dial vacuum gauges

The sensitivity are generally comparable to that of the mercury manometer.

- Pressure transducers

They have very high sensitivity since they require very small displacements of their sensing element to register a full scale pressure range. However the sensitivity of the tensiometer system is different from that of the pressure sensor. The volume of water that needs to be exchanged with the soil is generally larger because the tubing and air present in the system expand and compress with changes in pressure.

- Response time "T_r"

It is the time needed to make an accurate measurement with a particular tensiometer system and is inversely proportional to the conductance of the porous cup of the tensiometer and the sensitivity of the pressure measuring device and is characterized as follows :

$$T_r = \frac{1}{CS} \qquad (s)$$

This is for a system were the tensiometer is the limiting factor (in water or wet soil). In a soil-limited system (dry soil) the response is much slower under decreasing soil water pressure heads due to small water flow rates to the tensiometer cup as a result of low soil hydraulic conductivities. The flexibility of the tensiometer tubing and the compressibility of air bubbles inside the tubing decrease the effective sensitivity and thus increase the effective response time of a tensiometer system.

3.6 Practices and limitations of tensiometers

The purpose of the measurements with tensiometers is to characterize the existing pressure potential of the soil water.

Water within the tensiometer should be continuous throughout the system to allow a correct transfer of pressure from the soil to the mercury. Occurrence of gas bubbles disrupts this continuity and makes the system inoperative. The fine porous cup has the function of not allowing penetration of air from the unsaturated soil into the water-filled tensiometer tube, even though water can and should move through it. The fine pores inside the wall of the ceramic cup have a high air-entry value which is the pressure needed to remove the water from the pores in the cup replacing it by air. Even with a high air entry value breakdown of the system occurs due to entrapped air within the tensiometer tube or to air coming out of solution at reduced pressure.
Due to the fact that the manometer measures a partial vacuum relative to the external atmospheric pressure, measurements by tensiometry are generally limited to about - 850 cm of waterhead. Use of tensiometers in the field is therefore only possible when pressures do not fall below this value. Moreover the pressure head in the tensiometer must stay above the air-entry value of the porous material which is gives as follows :

$$h = \frac{-4\sigma \cos\theta}{\rho_w g d_{max}}$$

where : h = pressure head at which air enters the cup through the largest pore
σ = surface tension of an air-water interface (0.0073 N m^{-1} at 25°C)
θ = contact angle
d_{max} = largest pore diameter

So to cover the practical tensiometer range to h = - 850 cm for a completely wetting material ($\theta = 0$) d_{max} must be smaller than 3.6 µm. If the air-entry value is exceeded air can enter the tensiometer and the soil will drain the tensiometer.

However, the limited range of pressure measurable by the tensiometers is not as serious as it may seen at first sight. In many agricultural soils the tensiometer range accounts for more than 50% of the amount of soil water taken up by the plants. To what extend the available water range expressed e.g. as a percentage of the water between pF 2 and pF 4.2 is covered by the tensiometer depends on the shape of the moisture characteristic curve (pF-curve) as shown for three soil types in figure 31.

Thus where soil management (particularly in irrigation) is aimed at maintaining high pressure potential conditions which are mostly favourable for plant growth, tensiometers are definitely useful.

Air diffusion through the porous cup into the system requires frequent purging with deaired water. Tensiometers are also sensitive to temperature gradients between their various parts. Hence the above-ground parts should preferably be shielded from direct exposure to the sun. Therefore it is also suggested to make readings always at the same time of the day (e.g. at 08.00 a.m.).

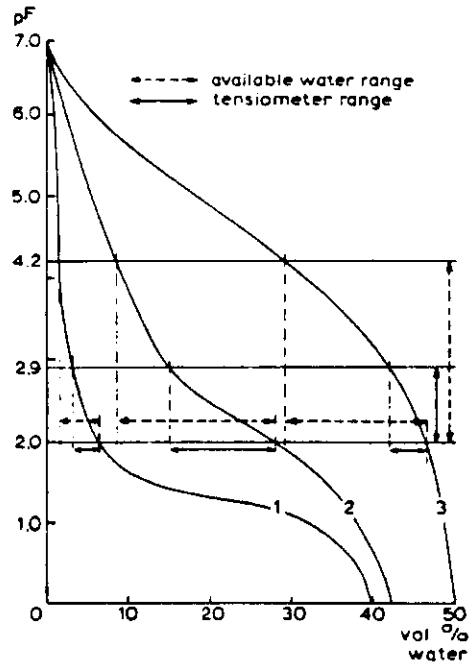

Figure 31. Part of the available moisture range covered by tensiometers, depending on soil type

1. Sand 50% of available moisture
2. Loam 75% of available moisture
3. Clay 25% of available moisture

When installing a tensiometer it is important for proper functioning that good contact be made between the porous cup and the surrounding soil. Generally the porous cup is pushed into a hole with a slightly smaller diameter to ensure good contact. If the soil is initially rather dry and hard, prewetting of the hole may be necessary. In a stony soil a small excavation should be made and filled with very fine sand into which the tensiometer can be placed.

With mercury manometers, even when small diameter nylon tubing (+/- 2 mm) is used, often a considerable volume of water must be adsorbed by the soil (during water uptake or drying process) or by the porous cup (replenishing by rainfall or irrigation) before the potential that really exists can be read off correctly. A very convenient modern device, the electronic transducer can be used which reacts to very small changes in pressure and converts these changes in a small electrical current which can be registered and amplified by a voltmeter. This system is very accurate but also very sensitive to the occurrence of small air bubbles in the tensiometer system. Moreover is it rather expensive.

Since the porous cup walls of the tensiometer are permeable to both water and solutes, the water inside the tensiometer tends to assume the same solute composition and concentration as soil water, and the instrument does not indicate the osmotic potential of soil water.

3.7 Applications of measurements

3.7.1 Determination of the direction of water flow at different levels in the soil profile (figure 32)

The concept of the water potential is well suited for the analysis of water flow in soils, since all flow is a consequence of potential gradients. Darcy's law, though originally conceived for saturated flow only, was extended to unsaturated flow, with provision that conductivity is a function of soil water content θ.

For a vertical one dimensional water flow Darcy's equation can be written as follows :

$$q = -K(\theta)\frac{dH}{dz} \qquad (21)$$

where : q = flux
$K(\theta)$ = hydraulic conductivity
H = hydraulic head
= h + z with h = soil water pressure head
z = gravitational head

The minus sign in the equation indicates that the flow is in the direction of decreasing potential. This means also that if we have two tensiometers located at depths z_1 and z_2 ($z_1 < z_2$) :

- q will be negative (upward flow - evaporation) if $H_2 > H_1$; the rise of mercury in manometer nr 2 is lower than in manometer nr 1
- q will be positive (downward flow - percolation) if $H_2 < H_1$; the opposite situation is observed
- q will be zero (plane of zero flux) at a certain depth z when the curve H(z) will show a maximum or the rise of the mercury a minimum because dH/dz = 0. A graphical example is presented in figure 32

3.7.2 Flux control at a certain depth

From agricultural point of view it could be of interest to know it there is a recharge of the water table or capillary rise. Therefore only 2 tensiometers are needed with a depth distance of say 25 cm in the control zone. A simple reading of the rise of mercury in the manometer will indicate the flow direction.

Knowing the moisture content θ at the depth between z_1 and z_2, the $K(\theta)$ relation of that soil and the hydraulic head gradient dH/dz, one can calculate the instantaneous water flow q (see equation 21).

3.7.3 Determination of the soil water characteristic curve (or retentivity curve)

The h-θ relation (retentivity curve) of a soil layer in situ can be established :

- knowing the soil water pressure head (h) using tensiometers (see equation 19)
- knowing the soil water content (θ) using the neutron moisture meter

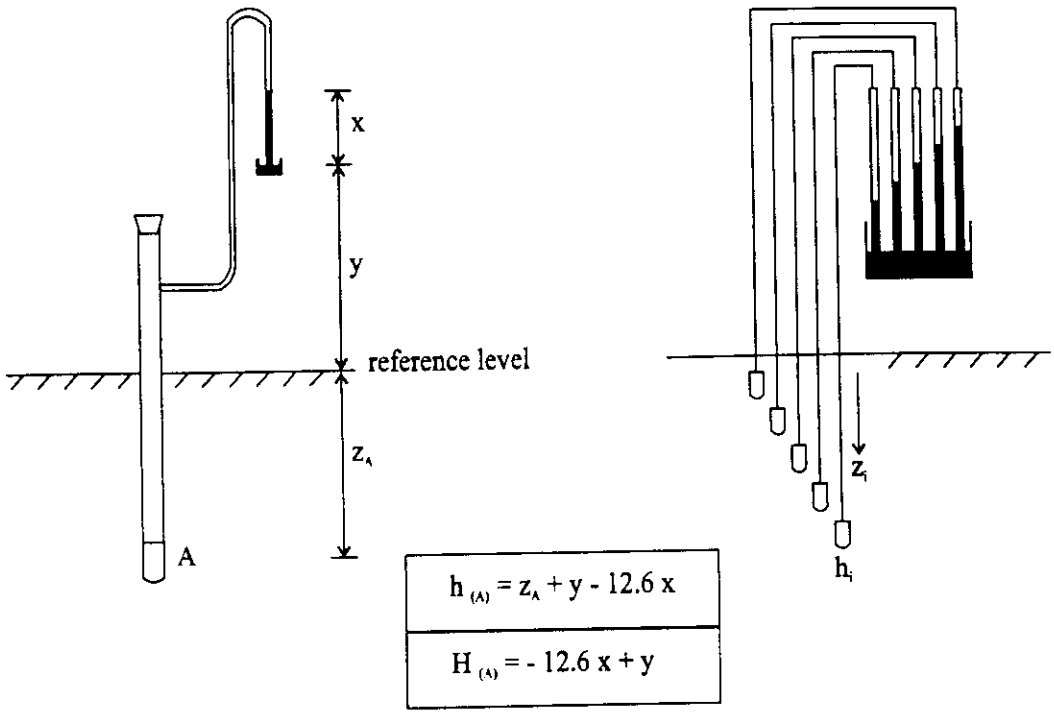

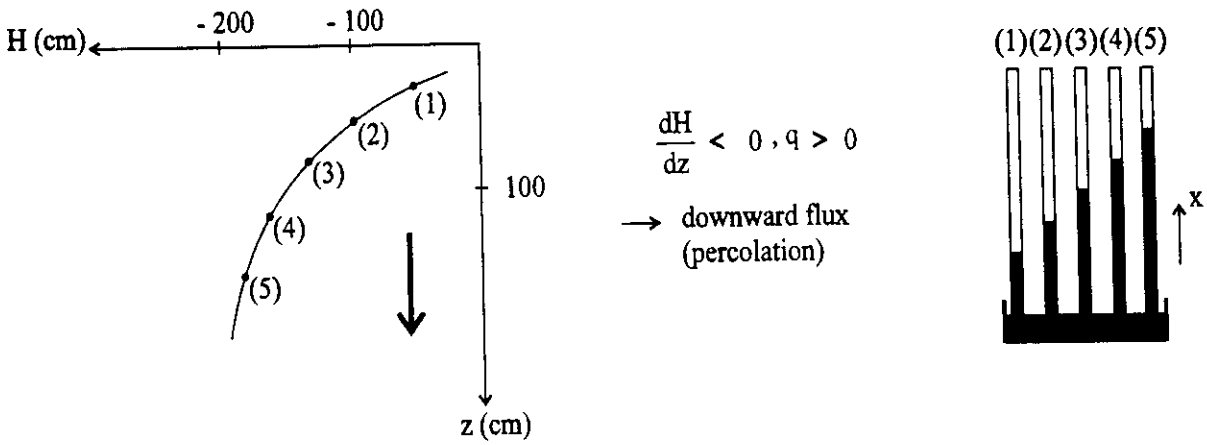

Figure 32. Hydraulic head profiles. The manometers from left to right increase with depth.

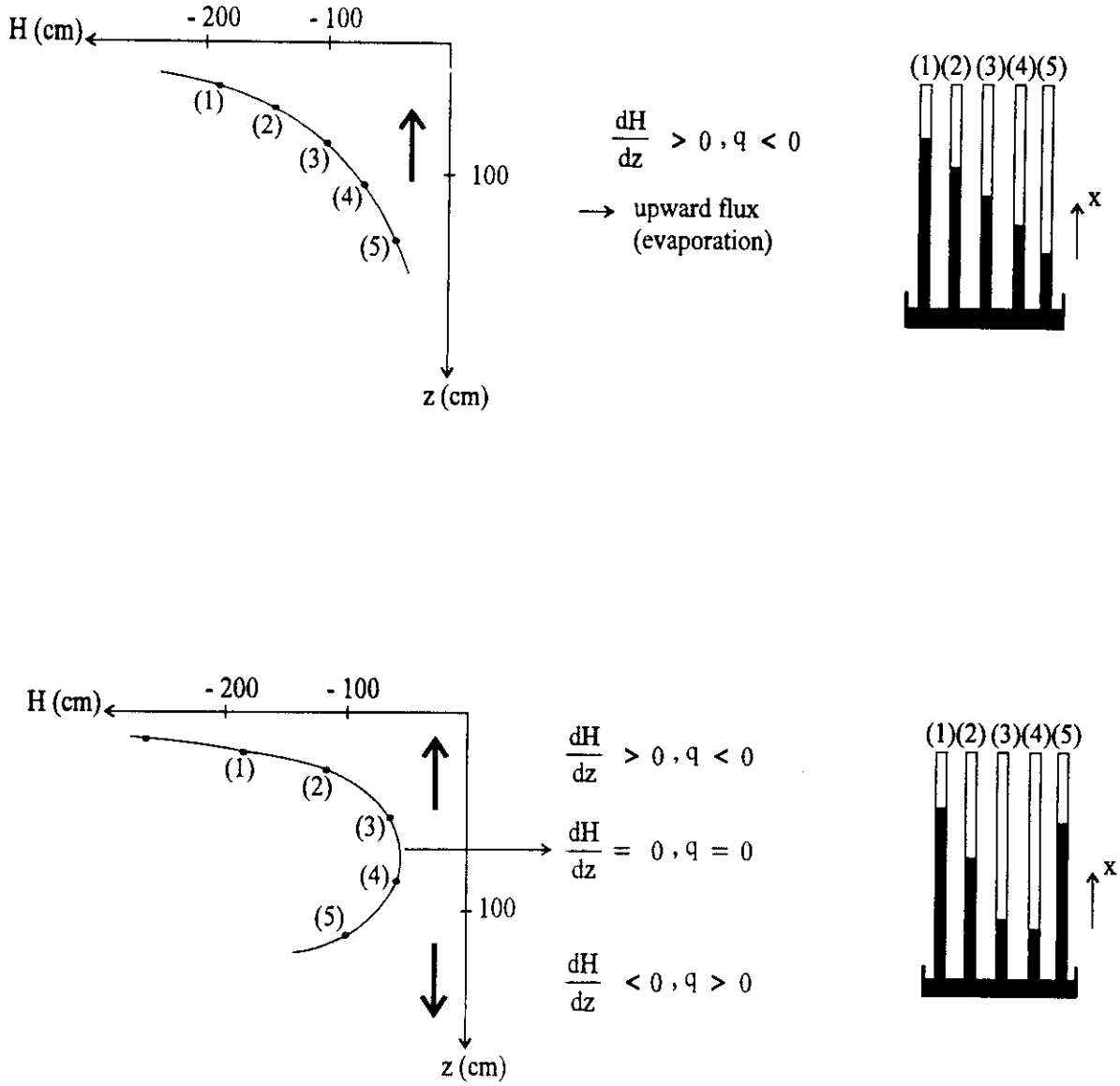

Figure 32bis. Hydraulic head profiles. The manometers from left to right increase with depth

3.7.4 Scheduling irrigation

The root zone for most agricultural plants is limited to the unsaturated part of the profile because the plant roots do not proliferate in a saturated soil where aeration is limiting. Consequently in a non-saline soil the plant behaviour is largely determined by the matric potential of the soil water. Moreover the plant does not depend as much on the quantity of water present as it does on the water potential.

Water should be applied to the soil when the matric potential is still high enough that the soil can and does supply water fast enough to meet the atmospheric demands without placing the plant under a stress that will reduce yield or quality of the harvested crop.

Although the tensiometers function over only a limited part of the available water range (0 to - 800 cm water) it is usually in this range that plants should be irrigated.

From practical point of view tensiometers are installed at minimum 2 locations. One unit should be placed in the zone of maximum root activity and another near the bottom of the active rootzone.

The time to irrigate is determined by following the matric potential readings in the zone of the greatest root activity. The exact value of the matric potential at which water should be applied is not the same for every crop. A good approximation of that matric potential is available for many common crops. For most crops it is time to irrigate when the top tensiometer reads - 300 to - 500 cm water and the bottom tensiometer begins to indicate drying (Table 1).

Table 1. Matric potential at which water should be applied for maximum yields of various crops grown in deep, well-drained soil that is fertilized and otherwise managed for maximum production. Where two values are given, the higher value is used when evaporative demand is high and the lower value when it is low; intermediate values are used when the atmospheric demand for evapotranspiration is intermediate. (The values are subject to revision as additional experimental data become available). (TAYLOR and ASHCROFT, 1972)

Crop	Matric potential (joules/kg)	Equivalent matric suction (centibars)
Vegetative crops		
Alfalfa	-150	150
Beans (snap and lima)	-75 to -200	75 to 200
Cabbage	-60 to -70	60 to 70
Canning peas	-30 to -50	30 to 50
Celery	-20 to -30	20 to 30
Grass	-30 to -100	30 to -00
Lettuce	-40 to -60	40 to 60
Tobacco	-30 to -80	30 to 80
Sugar cane		
Tensiometer	-15 to -50	15 to 50
Blocks	-100 to -200	100 to 200
Sweet corn	-50 to -100	50 to 100
Turfgrass	-24 to -36	24 to 36
Root crops		
Onions		
Early growth	-45 to -55	45 to 55
Bulbing time	-55 to -65	55 to 65
Sugar beets	-40 to -60	40 to 60
Potatoes	-30 to -50	30 to 50
Carrots	-55 to -65	55 to 65
Broccoli		
Early	-45 to -55	45 to 55
After budding	-60 to -70	60 to 70
Cauliflower	-60 to -70	60 to 70

Crop	Matric potential (joules/kg)	Equivalent matric suction (centibars)
Fruit crops		
Lemons	-40	40
Oranges	-20 to -100	20 to 100
Deciduous fruit	-50 to -80	50 to 80
Avocadoes	-50	50
Grapes		
Early season	-40 to -50	40 to 50
During maturity	< -100	> 100
Strawberries	-20 to -30	20 to 30
Cantaloupe	-35 to -40	35 to 40
Tomatoes	-80 to -150	80 to 150
Bananas	-30 to -150	30 to 150
Grain crops		
Corn		
Vegetative period	-50	50
During ripening	-800 to -1200	800 to 1200
Small grains		
Vegetative period	-40 to -50	40 to 50
During ripening	-800 to -1200	800 to 1200
Seed crops		
Alfalfa		
Prior to bloom	-200	200
During bloom	-400 to -800	400 to 800
During ripening	-800 to -1500	800 to 1500
Carrots		
During seed year at 60 cm depth	-400 to -600	400 to 600
Onions		
During seed year at 7 cm depth	-400 to -600	400 to 600
at 15 cm depth	-150	150
Lettuce		
During productive phase	-300	300
Coffee	Requires short periods of low potential to break bud dormancy, followed by high water potential	

4. SOIL WATER CHARACTERISTIC CURVE

Text from "Soil Physics" by Jury W.R., Gardner W.R. and Gardner W.H. (John Wiley & Sons, Inc., New York)

4.1 Measurement

In rigid porous media, the matric potential as defined in the preceding represents the effect of adsorptive soil solid forces and interfacial curvature on water potential energy. The functional relationship between the matric potential and the gravimetric or volumetric water content is called the water characteristic function or matric potential-water content function $\psi_m(\theta)$. This function may be evaluated by measuring matric potential and water content simultaneously with the methods already discussed during a succession of water content changes. In the laboratory, $\psi_m(\theta)$ may be measured on replicated prepared samples over a large range of water contents. Virtually the entire range from water-saturated soil to very dry soil may be covered by using a hanging water column, a pressure membrane, and equilibration over salt solutions. These devices will be illustrated using the equilibrium principle.

4.1.1 Hanging Water Column (Range -100 cm < h < 0)

A hanging water column consists of a water-saturated, highly permeable porous ceramic plate connected on its underside to a water column terminating in a reservoir open to the atmosphere. Water-saturated samples of soil held in rings are placed in contact with the flat plate when the water reservoir height is even with the top of the plate. Then the reservoir is lowered to a new height a distance z below the top of the plate (figure 33).

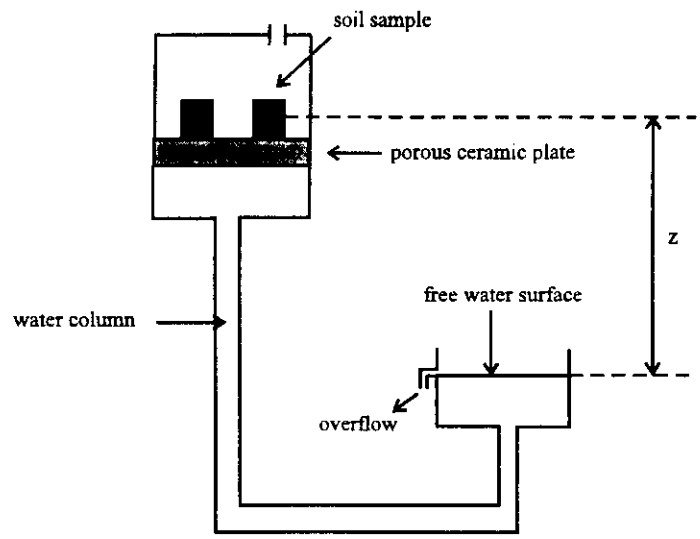

Figure 33. Desaturation of soil water samples to a desired energy state with a hanging water column.

By the equilibrium principle, water will flow from the soil samples through the ceramic to the reservoir until the total water potential of the system is constant. At this time the potential of the free reservoir may be set equal to zero, and at the soil sample height z we may write ($z = 0$; $P = P_{atm}$; neglect solutes) $\psi_m + \psi_z = 0 = \psi_m + \rho_w gz$, or $\psi_m = - \rho_w gz$. When equilibrium has been restored, some of the samples may be removed and their gravimetric or volumetric water content measured. The tube may then be lowered further and a new set of samples measured. If there is good contact between the soil and the ceramic, equilibrium will be reached rapidly (i.e. several hours) since the samples are quite moist. The range of the device is limited chiefly by the space available for lowering the water column.

4.1.2 Pressure Plate (Range - 15000 cm ≤ h ≤ - 300 cm)

The pressure plate consists of an air-tight chamber enclosing a water-saturated, porous ceramic plate connected on its underside to a tube that extends through the chamber to the open air. Saturated soil samples are enclosed in rings and placed in contact with the ceramic on the top side. The chamber is then pressurized, which squeezes water out of the soil pores, through the ceramic, and out the tube (figure 34). At equilibrium, flow through the tube will cease. We may set the total potential equal to zero at the point where the water exits the tube. Inside the plate we may write ($P = P_{atm}$; $z = 0$; neglect solutes) $\psi_{e.p.} + \psi_m = 0 = \psi_m + \Delta P$, or $\psi_m = - \Delta P$. When equilibrium is reached, the chamber may be depressurized and the water content of the samples measured. An assumption is made in this method that the matric potential of the sample does not change as the air pressure is lowered to atmospheric.

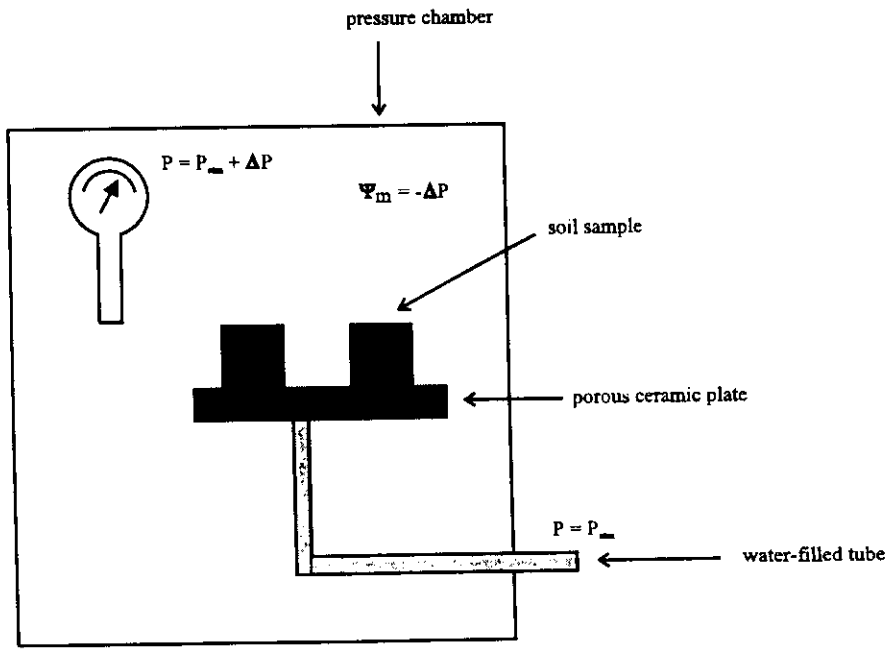

Figure 34.Desaturation of soil water samples to a desired energy state with a pressure plate.

This method may be used up to air gauge pressures of about 15 bars if special fine-pore ceramic plates are used. Since these devices have a very high flow resistance, it may require a substantial amount of time to remove the last small amount of water from the soil. Thus, the time of equilibrium is difficult to estimate.

4.1.3 Equilibration over Salt Solutions (h < - 15000 cm)

By adding precalibrated amounts of certain salts, the energy level of a reservoir of pure water may be lowered to any specified level. If this reservoir is brought into contact with a moist soil sample, water will flow from the sample to the reservoir. If the sample and the reservoir are placed adjacent to each other in a closed chamber at constant temperature, water will be exchanged through the vapor phase by evaporation from the soil sample and condensation in the reservoir until equilibrium is reached. Since the reservoir is a pool of salt solution, at equilibrium the total potential will be $\psi_t = \psi_{so}$ of the solution. In the soil $\psi_t = \psi_m + \psi_o$ since the air-water interface acts as a solute membrane. Thus $\psi_m = \psi_{so} - \psi_o$, the difference between the solute potentials of the reservoir and the soil. In practice, the soil will usually not be saline enough for its solute potential to be significant compared to ψ_o in the range where these measurements are made. The equilibration time for this method can be shortened by creating a partial vacuum in the chamber. Care should be taken that the sample and the reservoir are at the same temperature, because even small temperature differences will cause the soil and salt solution to equilibrate at very different potentials. Figure 35 shows typical matric potential-volumetric water content curves for a sandy soil and a finer textured soil high in clay measured from soil initially at water saturation. The water characteristic function for a soil desorbed from saturation may be roughly divided into three regions, as shown in the figure. The air entry region corresponds to the region at saturation where the matric potential changes but the water content does not. The minimum suction that must be applied to a saturated soil to remove water from the largest pores is called the air entry suction, which varies from about 5 to 10 cm for sands to much higher values in unaggregated, fine-textured soils. After air begins to enter the system, incremental increases in suction on the soil sample will drain progressively smaller pores, and the water content will drop. This intermediate part of the curve is called the capillary region. When essentially all of the water held in pores has been drained, only the tightly bound water adsorbed to particle surfaces remains. Large changes in matric potentials in this region, called the adsorption region, are associated with small changes in water content. The differences in the shapes of the water characteristic function for the prototype sandy and clay soils in figure 35 may be explained by considering the properties of the bulk solid phases. The clay soil generally has a lower bulk density and hence a higher water content at saturation. The clay soil has very few large pores and a broad distribution of particle sizes. Hence, it decreases gradually in water content with decreases in matric potential. The sandy soil, on the other hand, has much of its water held in large pores that drain at modest suctions. Hence it will have a very rapid decrease in water content in the

capillary region. Finally, the clay soil has a very large surface area compared to the sand and will have a large amount of water adsorbed to the surfaces.

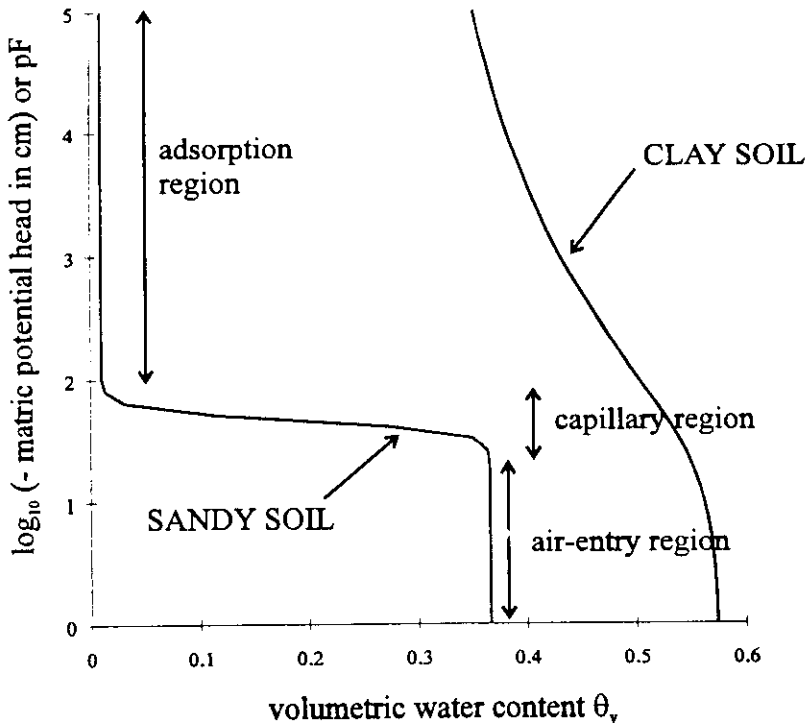

Figure 35.Matric potential-water content function (water characteristic function).

4.2 Hysteresis in Water Content-Energy Relationships

Water content and the potential energy of soil water are not uniquely related because the potential energy state is determined by conditions at the air-water interfaces and the nature of surface films rather than by the quantity of water present in pores. Soil pores are highly variable in size and shape and interconnect with each other in a variety of ways. Common to porous media are so-called bottleneck pores, which have large cavities but narrow points of connection to adjacent pores. Water is held most tenaciously in small pores, which fill first when water is admitted to a system. But they do not always empty again during drying in the same order as they were filled. The factors involved in hysteresis may be discussed most clearly by assuming that the soil is initially completely devoid of water and subsequently has no air phase (just liquid water and its vapor). If water is added at this point to the system, small pores fill first, followed by successively larger and larger pores until all pores are filled and the matric potential is zero. At intermediate values of saturation, with enough water in the system so that vapor-water interfaces can exist between particles and in small pores, the curvature of such interfaces is given by $\Delta P = - 2\gamma/R$ where the pressure difference ΔP refers to

the difference in pressure between the vapor and the liquid water. Water content and water potential in such a system will follow the wetting curve in figure 36. Some small pores could be isolated during wetting, so that they might remain dry while larger pores are filled. However, this would not be the case at equilibrium in the absence of air, in as much as vapor transfer would assure the wetting of all pores small enough to retain water at a particular matric potential.

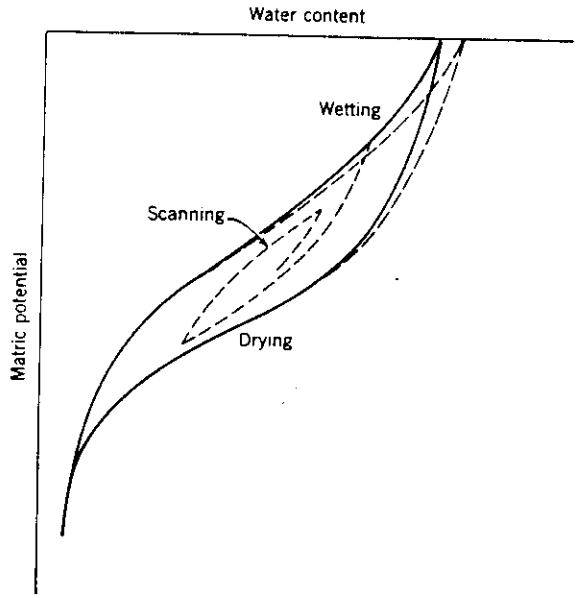

Figure 36. Wetting and drying curves and scanning curves.

If the system is dried either by evaporating water or by bringing the soil into contact with a dry, porous material that pulls water away from the system, pores will begin to empty, generally from large to small. However, liquid water may now be trapped in large pores in such a way that they will not empty in the order that they filled. Water will be held in large pores until conditions are reached where at least one interconnecting smaller pore can empty; at this time the larger pore quickly empties. The sudden release of a relatively large amount of water from a large pore floods surrounding pores and increases the matric potential in them temporarily. If matric potential were monitored in a small porous system having discrete differences in pore size, the matric potential-water content relationship for drying might be saw-toothed, as indicated by the drying curve in figure 36. In real soil systems, the pore size distribution contains many pores in all size ranges, and the water content and potential distributions tend to average out so that a smooth curve is obtained. However, the water content for a given matric potential is higher than for the wetting system, as is shown by the drying curve in figure 36. This principle is illustrated by the pore-water system in figure 37a. Here it may be observed that the curvature of the vapor-water interface in the small pores of two identical systems can be in equilibrium with each other even though their water contents

are grossly different. The matric potential is determined by the curvature of the liquid interface which at equilibrium would be precisely the same in the small pores connecting with the large pore in each case. This ideal representation commonly is called the "ink bottle principle", which refers to the fact that an ink bottle has a small opening into a large cavity. Large pores that are interconnected by smaller pores are not required for hysteresis to occur. It is possible for a single pore to contain the same amount of water at two different water potentials, as is shown in figure 37b. Water that condenses initially into such a capillary from a humid environment is shown by the diagonal cross-hatched area. However, as condensation proceeds, water at the center finally coalesces and a concave meniscus is formed as a consequence of surface tension forces (vertical cross-hatching). Whereas positive pressure existed in the system before coalescence, the system suddenly goes under negative pressure as a consequence of its new configuration. In the example in figure 37b, water in a cylindrical pore about 1 cm in length and 0.1 cm in radius would have a slight positive potential of about 0.15 mbar immediately before coalescence and a potential of - 1.5 mbars immediately afterward.

Surface wetting can also induce hysteresis. Unless particle surfaces are meticulously clean, they will form a nonzero contact angle with water when wetted (figure 37c). This results in thicker films than would be present in the drying phase where water films are drawn tightly over the surface by adsorptive forces.

Thus far the discussion of hysteresis has not involved the presence of air in the system, which can introduce additional differences between water content at a given matric potential during wetting and drying. As small pores and interstices between particles fill with water, air may become entrapped in large pores. Continued water entry into such pores will cause a buildup of air pressure. Since air is slightly soluble in water, pressures in such pores may gradually be relieved, which will sometimes allow more complete pore filling. However, the order of filling and access to pores will be influenced by entrapped air, so that water content is still permanently affected despite the fact that some air may go into solution and disappear.

In the absence of air, the water potential-water content relationship for complete wetting and complete drying will follow approximately the dashed line-solid line loop shown in figure 36. However, this loop is not exactly reproducible because of the inherent difficulty associated with repetition of the exact order of pore filling over each cycle. When air is present in the system, the curves are offset somewhat toward the dry side (solid curve, figure 36). If a soil is completely wetted so that no air is present and then is dried, it will follow the dashed-solid curve down; upon rewetting in the presence of air, it will follow the solid wetting curve and will not return to the starting point because of the presence of entrapped air. If the process is reversed at any time during wetting or drying, curves like those in the interior (dotted curves) of the hysteretic envelope are produced. These interior curves have been called scanning curves; the curves that form the hysteretic envelope have been called characteristic curves or

the soil moisture characteristic. The wetting curve of the hysteretic envelope is commonly known as a sorption curve and the drying curve a desorption curve.

Hysteretic phenomena also exist in soil materials as a consequence of shrinking and swelling, which can affect microscopic pore size geometry as well as overall bulk density. Both factors would lead to a volumetric water content for a given energy state that differs from that which would exist if the soil matrix remained fixed. Shrinking and swelling often take place slowly and usually irreversibly, particularly when organic matter is involved; this complicates the evaluation of their contribution to hysteresis. Experimental observations do not always reveal that measurements involve true hysteresis and permanent or semipermanent changes in the porous system.

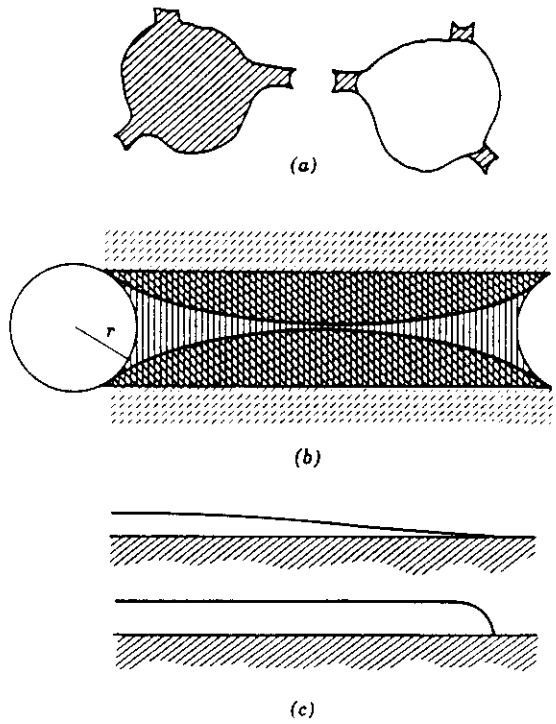

Figure 37.Diagrammatic representation of three forms of water content-matric potential hysteresis.

5. HOW TO EVALUATE THE FIELD WATER BALANCE

5.1 Introduction

The different soil water flow processes (e.g. infiltration, redistribution, drainage, evaporation and water uptake by plants) are strongly interdependent. To evaluate the field water cycle as a whole and the relative magnitudes of the various processes over a period of time it is necessary to consider the field water balance. The water balance of a field is an itemized statement of all gains, losses and changes of storage of water occurring in a given field within specified boundaries during a specified period of time. The task of monitoring and controlling the field water balance is vital to the efficient management of water and soil. Without knowledge of the water balance one cannot very well evaluate possible methods designed to minimize loss and to maximize gain and utilization of water which is so often the limiting factor of crop production.

5.2 Itemization of the water balance in the root zone

A water balance can be established for an entire watershed or for a small field. The latter will be discussed hereafter. Before the field water balance can be itemized the boundaries of the system have to be specified. From agricultural point of view it seems most pertinent to consider the whole crop's physical environment i.e. from the top of the canopy to the bottom of the root zone. To simplify the further discussion it is assumed herein that the system is stable and homogeneous (at least laterally). Such a hypothetical field is illustrated in figure 38. In its simplest form the water balance states that in a given volume of soil the difference between the amount of water added and the amount of water withdrawn during a certain period is equal to the change in water content during the same period. Gains of water in the field are generally due to the infiltration of rain or irrigation water. Occasionally there may be gains due to the accumulation of runoff from higher areas or due to upward flow from a shallow water table or from wet layers present at some depth. Losses of water include surface runoff from the field, deep percolation out of the root zone (drainage), evaporation from the soil surface and transpiration from the canopy. Possible changes in a given volume of soil due to subsurface lateral flow (q_l) whereby the inflow (q_{li}) different from the outflow (q_{lo}) may in general be regarded as negligible in comparison with the other components. This means that further on only vertical flow within the soil will be considered. How to measure the rate or magnitude of subsurface flow on hillslope plots has been discussed in detail by Atkinson (1978). The change in storage of water in the field can occur in the soil as well as in the plants. The change in plant water content can be assumed to be relatively unimportant. The total change in the amount of water stored in a zone between the surface and the bottom of the root zone within a given period of time Δt, must equal the difference between the sum of all gains and the sum of all losses.

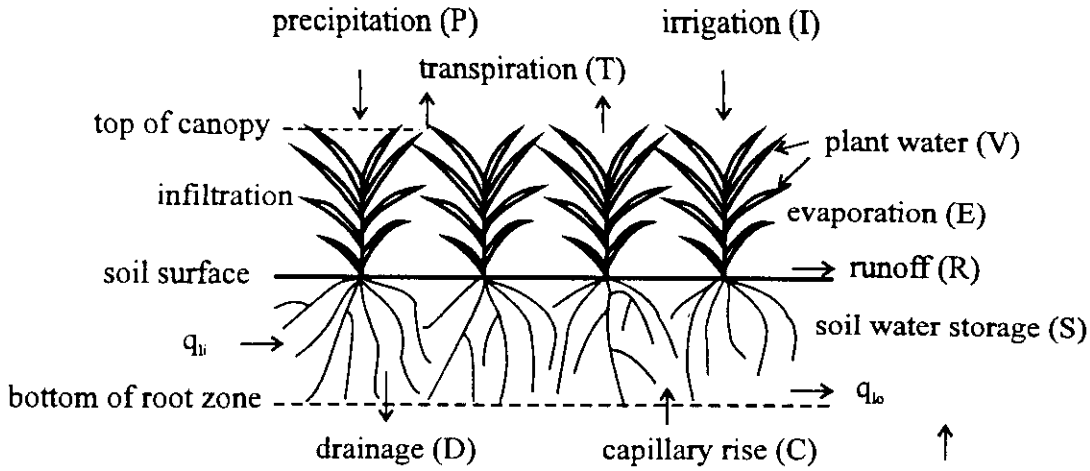

Figure 38. A schematic presentation of the different parameters involved in the field water balance.

Accordingly the water balance equation for the root zone can be represented as follows :

$$\underbrace{(P + I + C)}_{\text{gains}} - \underbrace{(R + D + E + T_r)}_{\text{losses}} = \underbrace{\Delta S}_{\text{changes in storage}} \qquad (22)$$

wherein
- P = the precipitation
- I = the irrigation water applied
- C = the upward flow into the root zone
- R = the surface runoff which can also be a gain (positive value)
- D = the downward drainage out of the root zone
- E = the direct evaporation from the soil surface
- ΔS = the change in soil water storage of the root zone during a given time period Δt

Upward capillary flow (C) and the downward drainage (D) can be included under the symbol D being negative if capillary rise occurs or positive when drainage is present and the equation (22) becomes :

$$\Delta S = P + I - R - D - E - T_r \qquad (23)$$

These quantities are expressed in terms of volume of water per unit area (equivalent depths of water in millimeters) during the period considered.

5.3 Time-period considerations

An important consideration in water balance studies is the period, or time interval, for which the balance is made. Too short a period might be impractical, while too long a period might be impractical, while too long a period might mask the occurrence of short-term critical stages. At such critical stages as flowering and fruit-set even temporary imbalance in crop-water status (e.g., under the influence of a sudden hot dry-spell) can have a lasting effect. Suppose, for instance, that seasonal precipitation is sufficient to balance the climatic evaporative demand is practically relentless, a precipitation event might come too late to save the plants. It therefore may not avail us to have a positive balance for the whole season, and we must ensure that the crop water balance is maintained positive continuously during the growing season.

5.4 Evaluation of the water balance

This water balance accounting system can be the basis for many irrigation scheduling methods certainly in areas where the water supply is scarce. The evapotranspiration of a crop (ET_{cr}) is often one of the most difficult components to measure directly. The most direct method for measuring the field water balance and consequently the evapotranspiration of a crop is by use of lysimeters. Although such devices, when equipped with weighing and drainage mechanisms allowed accurate measurements of the physical processes of the water balance, they are problematic in that they seldom provide a reliable representation of the real above-ground and soil environments of the field in which they are set. To obtain the ET_{cr} from the field water balance it requires that each other measurable item be evaluated independently and accurately (Hillel, 1980).

- It is relatively easy to measure with sufficient accuracy the amount of water added to the field by precipitation or irrigation though it is necessary to consider non uniformities in areal distribution.
- The amount of runoff in principle should be minimal in most agricultural fields (certainly in irrigation fields) so that it can sometimes be disregarded with respect to the major components of the water balance. However when runoff is appreciable it must be quantified.
- The measurement in soil water storage and thus its change (ΔS), which can be relatively large for short periods, can be made by sampling periodically or by using some specialized instruments viz. the neutron moisture gauge. The great advantage of the neutron moisture gauge over the traditional sampling method is that it measures wetness on the volume basis directly and that it samples a larger and hence more representative mass of soil while minimizing sampling errors and destructive augering (Greacen, 1981).
- A process very difficult to measure directly is the upward (capillary rise) or downward (drainage) flow through the bottom of the root zone. In the past the temptation was great to

omit the drainage component completely, based on the concept of "field capacity" which held that downward flow or drainage virtually ceased after two or three days.

It should be obvious that measurements of the root zone or subsoil water content by itself cannot give information about the rate and direction of the soil water movement. Even if the water content at a given depth remains constant one cannot conclude that the water is immobile since it might be moving steadily through that depth (figure 39).

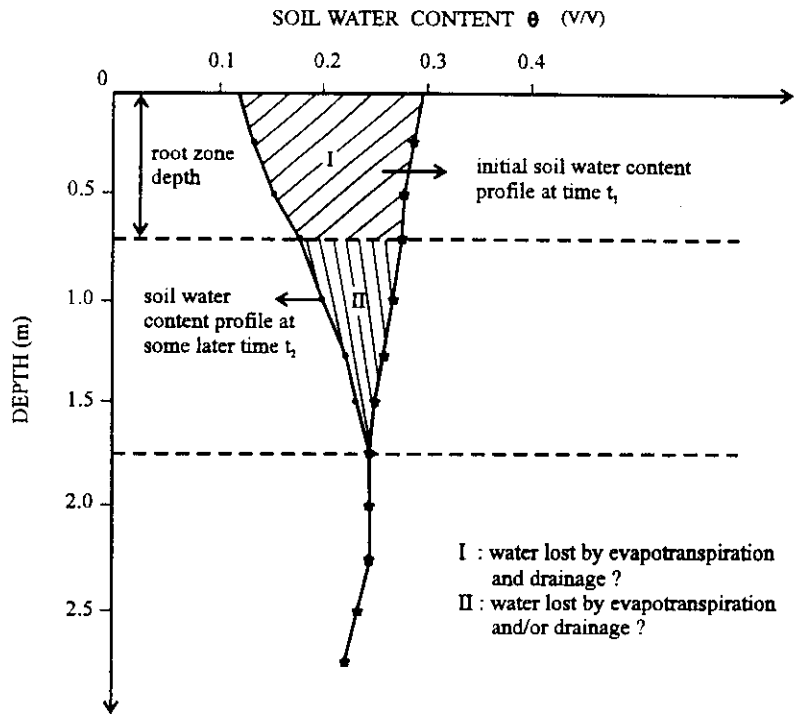

Figure 39. Soil water content profiles

This flow is not always negligible and often constitutes 20% or more of the field water balance even under a normal water regime (Hillel and Guron, 1970; and Reichardt *et al.*, 1974). It follows that rather than to be assumed negligible the drainage must in fact be measured and controlled if we are to increase the efficiency of water management. Some drainage is sometimes essential in irrigated agriculture, particularly in arid regions to prevent salinization in the root zone. Excessive drainage on the other hand, is also undesirable since it might leach nutrients out of the root zone. It means that movement of water below the root zone can be important in the field water balance and thus has to be measured and controlled. Tensiometric measurements can indicate the directions and magnitudes of the hydraulic potential gradients through the profile. To compute the drainage component at a certain depth z below the root zone, knowledge of the moisture content θ (v/v); the hydraulic

conductivity versus this moisture content (K-θ relation) and the hydraulic potential (head) gradient (dH/dz) at that depth z is required (see further). Consequently the evapotranspiration (of a crop) can be estimated from the field water balance if all other variables are known.

5.5 Soil water content profile - soil water storage

The soil water content profile can be established at different times e.g. by lowering a neutron probe at different depths and measuring the counts per minute at some reference depths. Using the calibration curve the soil water content profile as given in figure 40, can be established. In the case of a one-dimentional vertical water flow, where the soil water content profile is independent of the chosen vertical axis, the volume of water in a vertical soil column dV with a cross-section dσ and limited between the levels z_1 and z_2 (figure 40) equals:

$$\int_{z_1}^{z_2} \theta \, dV = d\sigma \int_{z_1}^{z_2} \theta \, dz \qquad (24)$$

or per unit area equation (24) becomes :

$$\int_{z_1}^{z_2} \theta \, dz = S\,(z_1, z_2) \qquad (25)$$

where "S" is called the soil water storage with dimension length allowing to compare it with precipitation or the amount of irrigation water.

The value of the cumulative storage between the soil surface and different depths is calculated by integrating the soil water content profile.

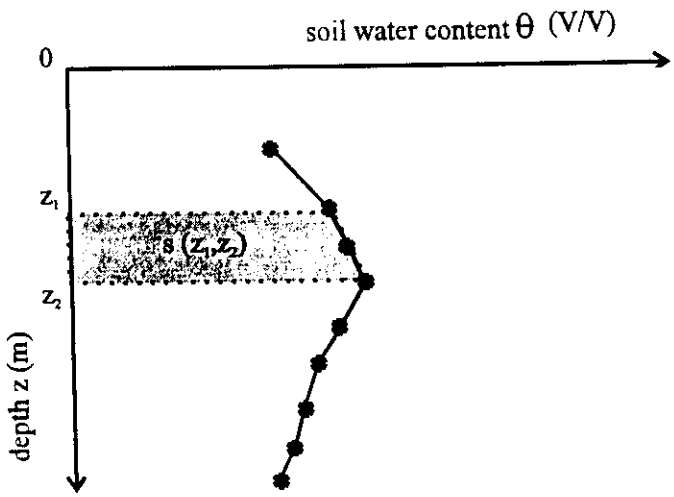

Figure 40. Soil water content profile

5.6 Hydraulic head profile

The basic flow equation describing the water movement in saturated soils and conceived by Darcy was extended to unsaturated flow. If we assume that the transfer occurs essentially in the vertical direction, Darcy's law is expressed as :

$$q = K(\theta)\frac{dH}{dz} \tag{26}$$

where
- q = the flux density which is the volume of water flowing through a unit
- K = the hydraulic conductivity being related to the soil water content
- dH = the difference in hydraulic potential (head)
- dz = the difference in distance over which the difference in hydraulic potential is measured
- dH/dz = the hydraulic potential (head) gradient or the driving force

$$H = h + z \tag{27}$$

where
- H = the hydraulic head
- h = the soil water pressure head
- z = the gravitational head

The negative sign in equation (26) indicates that the water flow is in the direction of decreasing potential. Therefore upward or downward flow in the profile will depend on the sign of the hydraulic gradient. The downward flux or drainage component at a depth z (q_z) can be estimated by measuring the hydraulic head gradient using tensiometers and the water content (e.g. by means of the neutron moisture meter) and using equation (26) knowing the K-θ relation of the soil at depth z (figure 41).

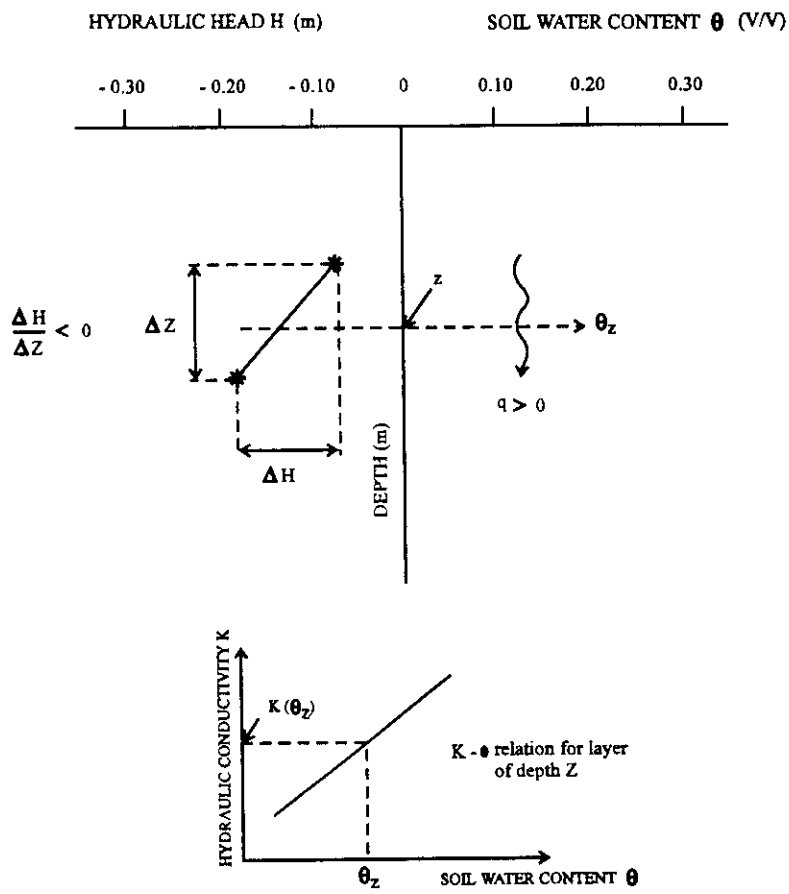

Figure 41. Determination of vertical flow within the soil profile.

When in a soil profile simultaneously a positive and negative hydraulic head gradient occur a zone or plane where dH/dz = 0 will be present between the zone of upward and downward flow, where according to equation (26) the flux q equals zero. That depth is often called the zero flux plane (z_o) (figure 42).

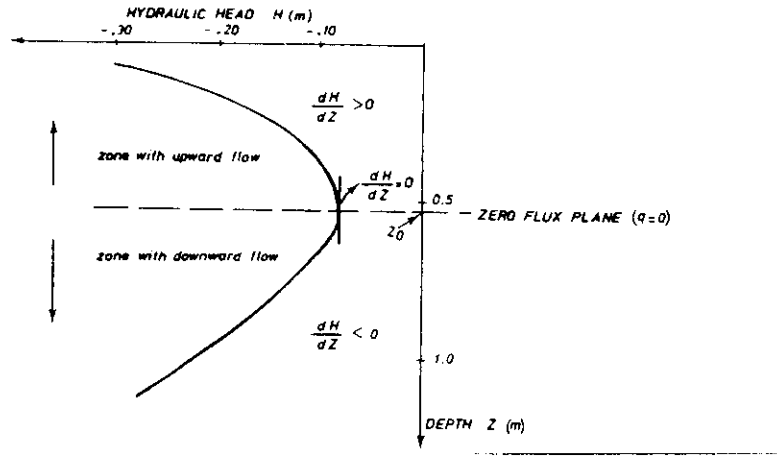

Figure 42. Hydraulic head profile with the presence of a zero flux plane.

5.7 Estimation of evaporation or evapotranspiration under different situations

The computation of the evaporation (E) or crop evapotranspiration (ET_{cr}) for a time period Δt, using the water balance equation, will be discussed for different situations and depending whether or not a zero flux plane is present in the profile.

5.7.1 Absence of a zero flux plane

Under such condition, either a continuous drainage or upward flow, takes place within the profile. The principle of calculating the fluxes and the E or ET_{cr} (for a bare or cropped soil respectively) will be identical if the depth z_r for which the soil water storages and fluxes are to be calculated, is taken below the rooting zone of the crop.

5.7.1.1 Downward flow

The hydraulic head gradient is negative throughtout the whole profile. The average flux q_{zr} at depth z_r, during the time interval Δt, is calculated using equation (26) and equals (figure 43) :

$$q_{z_r} = - K(\bar{\theta}) \frac{\overline{dH}}{dz} \qquad (28)$$

where $K(\bar{\theta})$ = the hydraulic conductivity corresponding to the mean soil water content $\bar{\theta}$ between two successive measurements at depth z_r.

$\frac{\overline{dH}}{dz}$ = the mean hydraulic head gradient during the time period $\Delta t = t_2 - t_1$ at depth z_r

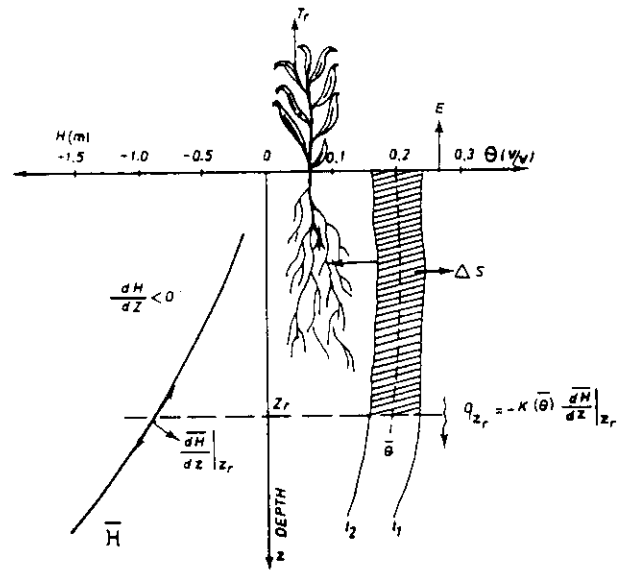

Figure 43. Soil water content profiles and mean hydraulic head profile during continuous downward flux.

The drainage component during the time period Δt equals :

$$q_{z_r} \cdot \Delta t$$

The soil water storage above the depth z_r is calculated according to equation (25) and is

$$S = \int_0^{z_r} \theta \, dz$$

consequently :

$$[\Delta S]_{z_r}^0 = S_{t_2} - S_{t_1}$$

The evaporation or crop evapotranspiration during the time period Δt is given by :

$$E \text{ or } ET_{cr} = P + I - [\Delta S]_{z_r}^{0} - q_{z_r} \Delta t - R \qquad (29)$$

5.7.1.2 Upward flow

The only difference with the situation of continuous downward flow or drainage is that the hydraulic head gradient is positive throughout the whole profile, resulting in a negative flux q_{zr}. Equation (29) is also to be used for calculation of E or ET_{cr} (figure 44).

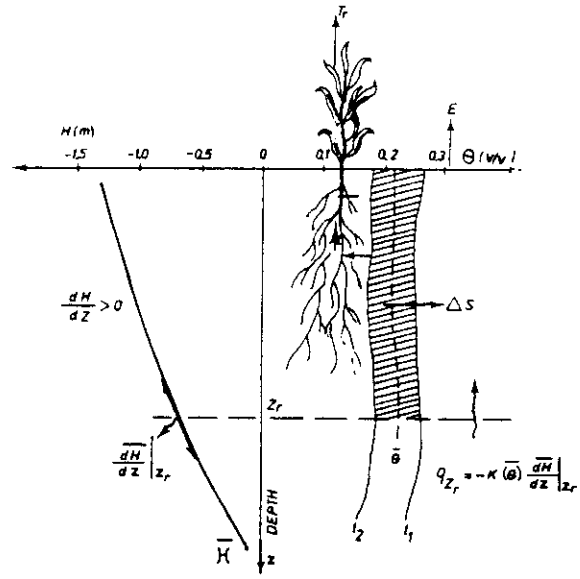

Figure 44. Soil water content profiles and mean hydraulic head profile during continuous upward flux.

5.7.2 Presence of a zero flux plane

The presence of a zero flux plane can be determined from the hydraulic head profile as shown in figure 42. The depth of the zero flux plane can change with time since equilibrium in the soil seldom occurs. The average depth of the zero flux plane ($\overline{z_0}$) during a period Δt (between t_1 and t_2) is calculated as follows :

$$\overline{z_0} = \frac{z_0(t_1) + z_0(t_2)}{2}$$

wherein : $z_0(t_1)$ = depth of the zero flux plane at time t_1
$z_0(t_2)$ = depth of the zero flux plane at time t_2

The calculation procedure is somewhat different for bare and cropped soil.

5.7.2.1 Bare soil

In a bare soil the change in water storage is calculated between the soil surface and the mean depth of the zero flux plane (figure 45). Since the flux at this depth is zero ($q_{\overline{z_0}} = 0$), the evaporation is given by :

$$E = P + I - [\Delta S]_{\overline{z_0}}^{0} - R$$

wherein

$$[\Delta S]_{\overline{z_0}}^{0} = \left(\int_0^{\overline{z_0}} \theta \, dz \right) t_2 - \left(\int_0^{\overline{z_0}} \theta \, dz \right) t_1$$

The drainage flux at a depth z_r below the average depth of the zero flux plane ($\overline{z_0}$) can be estimated in two ways :

a) by means of the zero flux plane, since the drainage will be equal to the change in storage between $\overline{z_0}$ and z_r during the time interval Δt or

$$q_{z_r} = \frac{[\Delta S]_{z_r}^{\overline{z_0}}}{\Delta t}$$

b) by means of Darcy's equation whereby :

$$q_{z_r} = - K(\theta) \left. \frac{\overline{dH}}{dz} \right|_{z_r}$$

The drainage component during the time interval will be :

$$q_{z_r} \cdot \Delta t$$

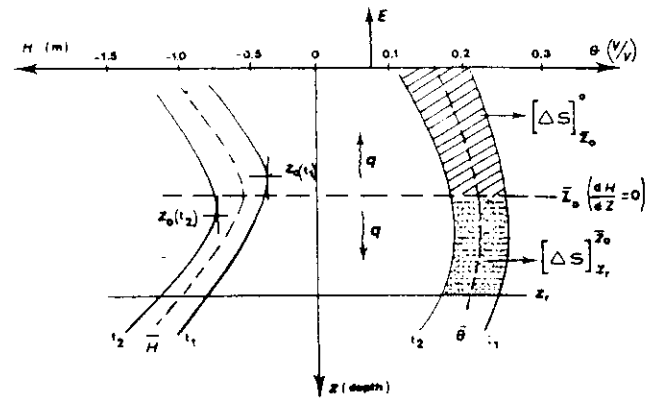

Figure 45. Soil water content and hydraulic head profiles in the presence of a zero flux plane under a bare soil (Vachaud et al., 1978).

5.7.2.2 Cropped soil

The calculation procedure for the evapotranspiration will depend on whether the zero flux plane is located above or below the rooting depth :

- if the rooting depth does not extend below the zero flux plane, the calculation procedure for ET_{cr} and the drainage component is similar as the one for a bare soil (figure 46).
- if the rooting depth is extended below the zero flux plane the evapotranspiration and the drainage component can only be calculated using Darcy's equation whereby the depth z_r is taken below the rooting depth (figure 47).

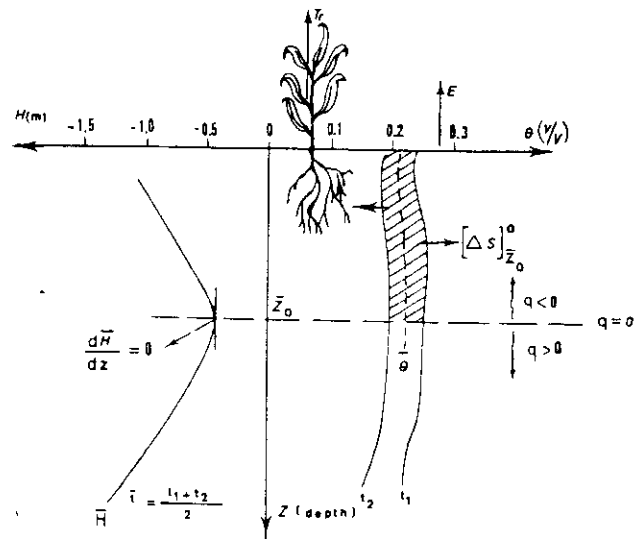

Figure 46. Diagram illustrating the calculation of crop evapotranspiration when the zero flux plane is located under the maximal root depth.

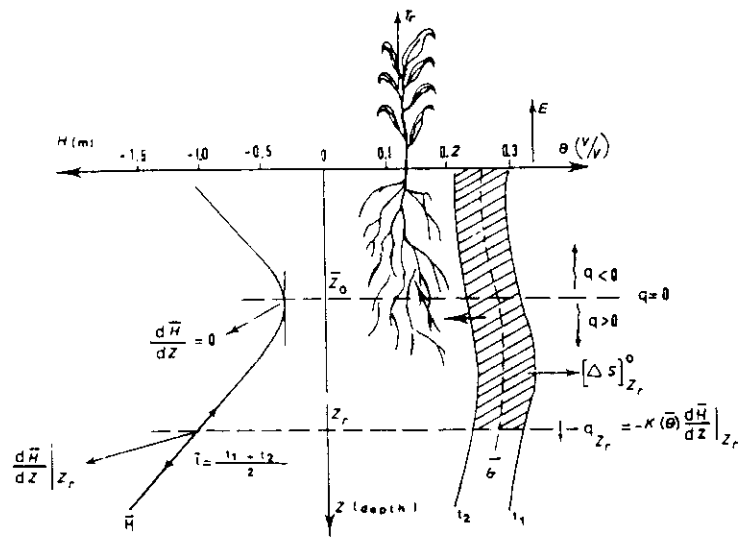

Figure 47. Diagram illustrating the calculation of the crop evapotranspiration when the zero flux plane is located within the root zone.

The drainage at depth z_r is given by :

$$q_{z_r} = - K(\theta) \left.\frac{\overline{dH}}{dz}\right|_{z_r}$$

and the evapotranspiration by :

$$ET_{cr} = P + I - [\Delta S]_{z_r}^{0} - q_{z_r} \Delta t - R$$

It is possible that more than one zero flux plane occurs in the soil profile, e.g. in case of successive wet and dry periods. In such a case one has to take the deepest zero flux plane into consideration for the calculation of ET_{cr} and q_{zr}.

5.8 Conclusions

From the previous discussion it appears that evapotranspiration and drainage can be obtained through adequate and regular field measurements. Such studies are not restricted to theoretical situations only but can be of practical importance in e.g. arid and semi-arid areas like the Sahel region where water availability is very often the principal factor limiting crop yield. The discussed water balance method is precise enough to examine :

- the effect of water deficiency on growth and crop yield,
- the efficiency of irrigation to meet the crop requirements essential to obtain good yields,
- the necessity of applying more irrigation water than needed in order to satisfy the leaching requirement for salt removal,
- agricultural operations - which are locally applicable - especially under dry-land conditions aiming at reducing the rate of evapotranspiration and increasing crop production.

5.9 References

Atkinson, T. 1978. Techniques for measuring subsurface flow on hillslopes. In *"Hillslope Hydrology"* edited by Kirkby.

Greacen, E. 1981. Soil Water Assessment by the Neutron Method. *Division of Soils. CSIRO*, Adelaide, Australia, pp 138.

Hillel, D. 1980. *Application of Soil Physics*. Academic Press, pp 385.

Hillel, D. and Guron, Y. 1970. The Use of Radiation Techniques in Water use Efficiency Studies. *Res. Rept. submitted to Int. At. Energy Agency*. The Hebrew University of Jeruzalem, Israel.

Reichardt, K., Libardi, P. and Dos Santos, J. 1974. An analysis of soil water movement in the field. II Water balance in a snap bean crop. *Boletin Cientifico BC-022*, Centro de Energia Nuclear na Agricultura, Brasil.

Vachaud, D., Dancette, C., Sanko, S. and Thony, J. 1978. Methodes de caractérisation hydrodynamique in sity d'un sol du Sénégal en vue de la détermination des termes du bilan hydrique. Ann. Agron. 29 : 1 - 36.

13 MODELS FOR DETERMINATION OF THE SOIL WATER CHARACTERISTIC CURVE AND THE UNSATURATED HYDRAULIC CONDUCTIVITY $K(\theta)$

13.1 Introduction

The soil moisture characteristic curve (or pF curve) can be determined based on a set of discrete measuring points determined in the laboratory or in the field (see Exercise 5 and 11 respectively). To represent the curve graphically, one can draw a best fitting curve by hand on mm paper or an analytical equation can be used to fit a curve through the set of measuring points. Because determination of the soil moisture characteristic curve in the lab or in the field is time consuming, models have been introduced to calculate the soil moisture characteristic curve based on readily available physical soil characteristics.

As regards the unsaturated hydraulic conductivity $K(\theta)$, it can be determined in the laboratory (e.g. crust method, Wind method) or in the field (e.g. internal-drainage method, see Exercise 11). Since this is also quite laborious, models have been developed that calculate $K(\theta)$ based on the saturated hydraulic conductivity K_s and the soil moisture characteristic curve, or on readily available physical soil characteristics.

13.2 Fitting pF curve to a discrete set of measuring points by modelling

13.2.1 The model of van Genuchten

13.2.1.1 Principle

There exists a non-linear relationship between the soil moisture content and de matric potential. To fit a curve through a discrete set of measuring points closed-form analytical equations can be used. One of the most widely used equations is that of van Genuchten (1978, 1980) :

$$\theta = \theta_r + (\theta_s - \theta_r) \cdot \left(\frac{1}{1 + (\alpha \cdot |h|)^n} \right)^m \qquad (1)$$

where θ = volumetric moisture content ($m^3 \cdot m^{-3}$),
θ_r = residual volumetric moisture content ($m^3 \cdot m^{-3}$),
θ_s = volumetric moisture content at saturation ($m^3 \cdot m^{-3}$),
h = matric potential (dimensionless, but expressed in cm H_2O),
α, n en m = parameters (dimensionless).

If, as proposed by van Genuchten,

$$m = 1 - \frac{1}{n} \quad \text{for } n > 1 \tag{2}$$

equation (2) contains 4 independent parameters (θ_r, θ_s, α and n), which have to be estimated for the observed soil-moisture retention data. This can be done by applying a non-linear least-squares analysis according to the Marquardt (1963) algorithm. This is an iterative method implying an initial estimate of the parameters.

The Marquardt algorithm can be performed by using mathematical software programmes such as Mathcad®. On the other hand most statistical software packages, as e.g. SPSS® contain the Marquardt algorithm. Graphical software such as SigmaPlot® also have the possibility to perform a non-linear regression. Finally, the RETC code, written in the programme language Fortran, can be used to determine the parameters of the van Genuchten model (van Genuchten et al., 1991; Yates et al., 1992).

13.2.1.2 Graphical interpretation and physical meaning of the parameters

As stated above the model of van Genuchten contains, after imposing the restriction $m = 1 - 1/n$, four independent parameters, namely θ_r, θ_s, α and n. The value for the **volumetric moisture content at saturation** θ_s is, in theory, equal to the porosity ε of the soil. It is the latter value that will be taken as initial estimate for θ_s.

From a practical point of view the **residual volumetric moisture content** θ_r can be defined as the pressure head at some large negative value, e.g. at the permanent wilting point (h = -15,495 cm H_2O or pF = 4.2). In some cases, however, significant decreases on h are likely to result in further desorption of water, especially on fine-textured soils. It seems that such further changes in θ are fairly unimportant for most practical field problems.

To obtain estimates of the remaining parameters α and n a characteristic point P on the curve has to be defined (see Figure 13.1). This point is located halfway between θ_r and θ_s. From equation (1) it follows that the **parameter** α is inversely proportional with the pressure head at P, h_P :

$$\alpha = \frac{1}{h_P} \cdot \left(2^{\frac{n}{n-1}} - 1 \right)^{\frac{1}{n}} \tag{3}$$

For n large enough, and hence m approaches 1, α is approximately equal to the inverse value of h_P. Most soils, however, have a m significant smaller than 1 ($n < 10$). The value for α then increases exponentially with decreasing m value.

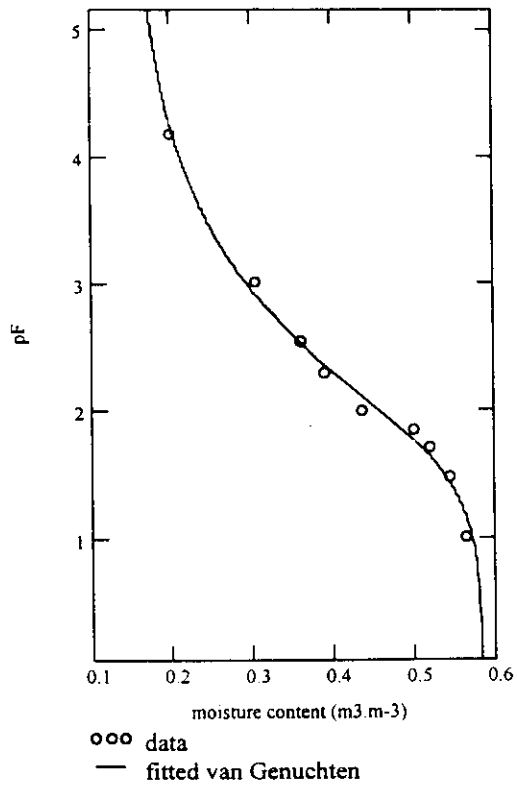

Figure 13.1 pF curve of a heavy sandy clay soil (Zeebrugge)

Finally, the **parameter** n can be obtained be differentiation of equation (1) ($d\theta dh^{-1}$) and by substituting equation (3). This gives a relation between $h \cdot d\theta dh^{-1}$ and n. Further calculating results in following equation for n :

$$n = \begin{cases} e^{(0,8 \cdot S_P)} & (0 < S_P \leq 1) \\ \left(\dfrac{0,5755}{S_P} + \dfrac{0,1}{S_P{}^2} + \dfrac{0,025}{S_P{}^3} \right)^{-1} & (S_P > 1) \end{cases} \tag{4}$$

where S_P = slope at point P.

The slope S_P is defined as :

$$S_P = \frac{1}{\theta_s - \theta_r} \cdot \left| \frac{d\theta}{d(\log h)} \right| \tag{5}$$

From equation (4) and (5) it is clear that as the ratio $d\theta d(\log h)^{-1}$ increases, and hence the flatter the curve at P, the value for n will increase.

13.2.2 Other models

13.2.2.1 The model of Brooks and Corey

The model of Brooks and Corey (1964) can be expressed as :

$$\theta = \theta_r + (\varepsilon - \theta_r) \cdot \left(\frac{h_b}{h}\right)^{\lambda} \tag{6}$$

where ε = porosity ($m^3 \cdot m^{-3}$),
h_b = bubbling pressure or air entry value (cm H_2O),
λ = pore size index (-).

The model of Brooks and Corey, and the model of Campbell (see *13.2.2.2*) do not permit a representation of the total soil moisture retention curve - they only represent that part of the curve for pressure heads lower than the air entry value -, whereas the model of van Genuchten does so. The model of van Genuchten does not account for the air entry value but does have an inflection point, allowing the van Genuchten model to perform better than the Brooks and Corey, and the Campbell model for many soils, particularly for data near saturation.

13.2.2.2 The model of Campbell

The model of Campbell (1974) can be represented by :

$$\theta = \varepsilon \cdot \left(\frac{H_b}{h}\right)^{\frac{1}{b}} \tag{7}$$

where H_b = bubbling pressure or air entry value (cm H_2O),
b = constant.

13.3 Methods to obtain the pF curve without laboratory determinations

13.3.1 Soil texture reference curves

The simplest method for estimating the $h(\theta)$ relationship is to use soil texture reference curves. These curves give the soil water characteristic curve for several soil textural classes (see Figure 13.2).

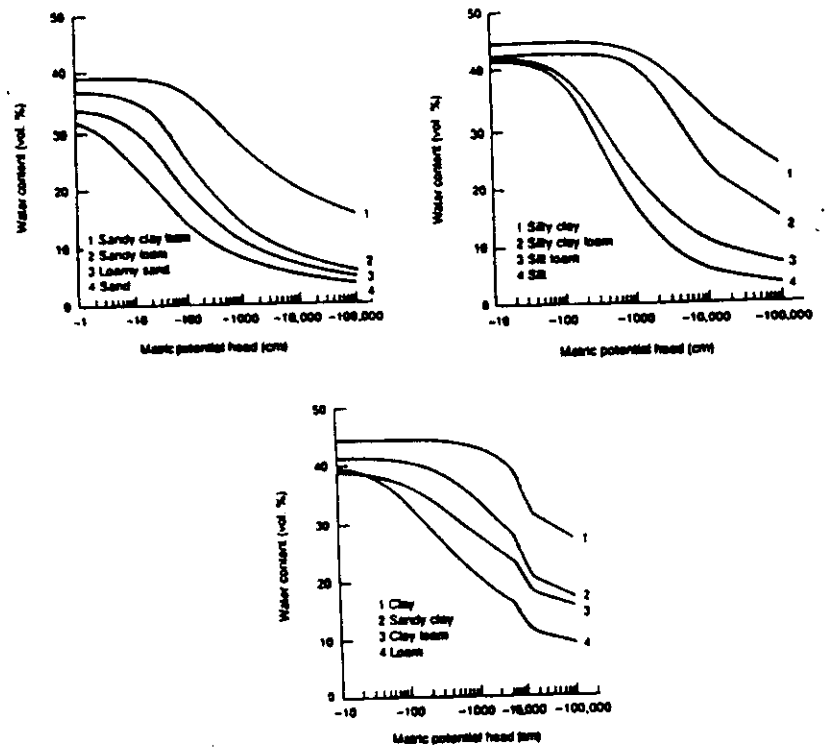

Figure 13.2 Soil water retention curves for USDA soil textures (Rawls et al., 1993)

13.3.2 Estimating soil water retention curves from soil physical characteristics

13.3.2.1 Introduction

The amount of water retained at high soil water potentials (> -10 kPa) depends primarily on the pore size distribution, and is thus strongly affected by soil structure, bulk density, and porosity. As the soil dries out (< -150 kPa), water adsorption becomes critical, and those soil properties that affect specific surface become important such as texture, organic matter content, and clay mineralogy. Most of the models that are developed to estimate the soil moisture characteristic curve from soil physical characteristics, the so called pedotransfer functions, make use of one or more of those characteristics.

Two approaches can be distinguished for estimating soil water retention characteristics from soil properties. The first approach estimates soil water retention *values* from soil physical properties using regression analysis. The second approach estimates *parameters* for water retention models (like van Genuchten, Brooks and Corey, and Campbell) from soil physical properties using regression analysis. An overview of both approaches is given in Rawls et al. (1991) and van Genuchten et al. (1992). More recently Kern (1995) evaluated six of the most cited models that use soil physical characteristics. These include the models of Gupta and Larson (1979), Rawls et al. (1982, 1983), De Jong et al. (1983), Cosby et al. (1984), Saxton et al. (1986) and Vereecken et al. (1989).

13.3.2.2 Estimation of specific points on the soil water retention curve

The most cited models to relate soil properties to the soil moisture held at specific matric potentials are those of Gupta and Larson (1979) and Rawls et al. (1982, 1983). To increase the accuracy of the regression equations using physical soil properties, Rawls et al. introduced the moisture content held at -1500 kPa (pF 4.2) or at both -33 kPa (pF 2.54) and -1500 kPa. Adding these variables, which require more costly and/or time-consuming laboratory procedures, increase the explained variation from 76% to 95%. The model of Rawls et al. can thus be written as :

$$\theta_x = a + b \cdot sand + c \cdot silt + d \cdot clay + e \cdot O.M. + f \cdot \rho_b + g \cdot \theta_{0,33\,bar} + h \cdot \theta_{15\,bar} \qquad (8)$$

where θ_x = predicted soil moisture content for a given suction x ($cm^{-3} \cdot cm^{-3}$),
$sand$ = percentage sand (%),
$silt$ = percentage silt (%),
$clay$ = percentage clay (%),
$O.M.$ = percentage organic matter (%),
ρ_b = bulk density ($g \cdot cm^{-3}$),
$\theta_{0,33\,bar}$ = moisture content at a matric potential of - 33 kPa ($cm^{-3} \cdot cm^{-3}$),
$\theta_{15\,bar}$ = moisture content at a matric potential of - 1500 kPa ($cm^{-3} \cdot cm^{-3}$),
a tot h = regression coefficients from tables.

Thus, in its simplest form the model of Rawls et al. exists of the first 6 terms of Equation (8). The values for regression coefficients differ depending on the chosen simplicity of the model (6, 7, or 8 terms) and the given matric potential. The tables of Rawls et al. include 12 different matric potentials, and hence a set of 12 discrete points can be determined. A best fitting curve can then be drawn through this set of points by modelling (e.g. van Genuchten).

The model of Gupta and Larson is similar with this difference that the intercept a is equal to zero (and hence the regression coefficients are different).

13.3.2.3 Estimation of soil water retention model parameters

With the increased interest on modelling, the need for a continuous function describing the soil water retention curve has become very important. Frequently water retention data is fitted to a water retention model (see **13.2**) and the model parameters subsequently related to physical soil properties using regression analysis.

One approach to relate the model parameters to soil properties is to develop average parameter values as a function of soil texture classes. Tables are available with values for the parameters of the different models. Clapp en Hornberger (1978), De Jong (1982) and Raws et al. (1982) calculated, for the different USDA textural classes, values for the models of Brooks and Corey, and Campbell. Vereecken et al. (1989) calculated the values for the parameters of the van Genuchten models for the seven textural classes of the Belgian textural triangle (see Table 13.1).

The second approach uses linear regression to relate the model parameters to soil physical properties. Examples of this approach are the pedotransfer functions of Bloemen (1977), Cosby et al. (1984) and Rawls and Brakensiek (1985) for the Brooks and Corey model. Using the correspondence between the model parameters given in **13.2**, i.e. $H_b = h_b$, $b = 1/\lambda$, $\alpha = h_b^{-1}$ and $n = \lambda + 1$, the same pedotransfer functions can be used with the Campbell and the van Genuchten model. Bloemen developed empirical expression relating the model parameters to a particle size distribution index and the median of particle size, whereas in Cosby et al. the parameters are function of percentage clay and sand. Rawls and Brakensiek included also porosity. Saxton et al. (1986) used the percentage clay and sand to calculate the parameters of a model that was derived from the model of Campbell. Widely used pedotransfer functions for the model of van Genuchten are those of Vereecken et al. (1989) which were developed based on the physical characteristics of 182 horizons of 40 different Belgian soils :

$$\theta_s = 0.81 - 0.283 \cdot \rho_b + 0.001 \cdot clay$$
$$\theta_r = 0.015 + 0.005 \cdot clay + 0.014 \cdot C$$
$$\ln(\alpha) = -2.486 + 0.025 \cdot sand - 0.351 \cdot C - 2.617 \cdot \rho_b - 0.023 \cdot clay$$
$$\ln(n) = 0.053 - 0.009 \cdot sand - 0.013 \cdot clay + 0.00015 \cdot sand^2$$

where C = carbon content (%).

De Jong et al. (1983) followed a similar approach but calculated the parameters from percentage organic matter, silt and clay. These parameters are then substituted in a model that expresses gravimetric moisture content as a function of matric potential by linear regression.

A third more recent approach introduced by Tyler and Wheatcraft (1990) uses fractal mathematics and scaled similarities to show that the empirical constant in the Arya and Paris (1981) model is equivalent to the fractal dimension of the tortuous fractal pore. This information can be used to predict soil water retention from measured particle size distributions.

13.4 Determination of the unsaturated hydraulic conductivity $K(\theta)$ by modelling

13.4.1 Introduction

To determine the unsaturated hydraulic conductivity $K(\theta)$, several approaches can be distinguished. The most common technique is to determine $K(\theta)$ from the pore-size distribution and the saturated hydraulic conductivity K_s. The pore-size distribution can be derived from the soil moisture characteristic curve. The K_s has to be determined in the laboratory (see Exercise 3) or in the field (see Exercise 4), or has to be calculated based on soil physical properties.

The $K(\theta)$ relationship can also be determined from readily available soil physical characteristics.

Table 13.1 Mean, minimum and maximum value for the parameters of the van Genuchten model for the seven textural classes according to the Belgian classification (N is the number of observations) with $m = 1$

Textural class	N	Mean	Minimum	Maximum
Heavy clay (U)	3			
θ_s		0.55	0.52	0.57
θ_r		0.27	0.25	0.29
$\alpha \cdot 10^{-3}$		1.60	0.60	2.40
n		0.66	0.57	0.71
Clay (E)	10			
θ_s		0.44	0.39	0.49
θ_r		0.16	0.00	0.30
$\alpha \cdot 10^{-3}$		2.00	2.00	7.77
n		0.63	0.30	0.96
Loam (A)	33			
θ_s		0.42	0.38	0.46
θ_r		0.11	0.04	0.14
$\alpha \cdot 10^{-3}$		1.56	0.40	4.20
n		0.80	0.42	1.44
Sandy loam (L)	55			
θ_s		0.41	0.36	0.48
θ_r		0.09	0.00	0.22
$\alpha \cdot 10^{-3}$		2.29	0.20	5.70
n		0.86	0.32	1.23
Light sandy loam (P)	10			
θ_s		0.37	0.35	0.42
θ_r		0.09	0.07	0.11
$\alpha \cdot 10^{-3}$		2.50	0.61	5.60
n		0.92	0.58	1.17
Loamy sand (S)	10			
θ_s		0.41	0.32	0.53
θ_r		0.09	0.07	0.14
$\alpha \cdot 10^{-3}$		7.42	3.41	20.61
n		1.21	0.76	1.27
Sand (Z)	62			
θ_s		0.39	0.30	0.54
θ_r		0.04	0.00	0.10
$\alpha \cdot 10^{-3}$		12.30	1.60	37.10
n		1.68	0.69	2.62

13.4.2 Estimating the unsaturated hydraulic conductivity $K(\theta)$ from water retention data

13.4.2.1 Introduction

A popular alternative to direct measurement of $K(\theta)$ (see Exercise 11) is the use of theoretical methods which predict $K(\theta)$ from more easily determined field or laboratory water retention data. Theoretical methods are usually based on statistical pore-size distribution models which assume water flow through cylindrical pores, and incorporate the equations of Darcy and Poiseuille. Three broad groups of models predicting the unsaturated hydraulic conductivity from measured water retention data can be identified, i.e., the models proposed by Childs and Collis-George (1950), Burdine (1953) and Mualem (1976).

13.4.2.2 Estimating K(θ) based on the model of Childs and Collis-George

The original equation by Childs and Collis-George (1950) has been later modified by Marshall (1958), Millington en Quirk (1959) and Jackson (1972). Jackson formulated the unsaturated hydraulic conductivity at moisture content θ_i ,$K(\theta_i)$, as :

$$K(\theta_i) = K_s \cdot \left(\frac{\varepsilon_i}{\varepsilon_1}\right)^p \cdot \frac{\sum_{j=i}^{m}\left((2\cdot j + 1 - \cdot 2\cdot i)\cdot h_j^{-2}\right)}{\sum_{j=1}^{m}\left((2\cdot j - 1)\cdot h_j^{-2}\right)} \qquad (9)$$

where K_s = saturated hydraulic conductivity ($m \cdot s^{-1}$),

ε_1 = amount of pores filled with water = θ_i ($cm^3 \cdot cm^{-3}$),

h_j = pressure head at midpoint of each θ increment $j = i$ (m),

i = number of moisture content class where $i = 1, 2, \ldots m$, and $i = 1$ at saturation and m = the total number of increments,

p = arbitrary constant assigned values of 0 to 4/3 by various workers (a value of unity was found to be satisfactory by Jackson) (-).

The saturated hydraulic conductivity K_s can be derived from field or laboratory measurements, or can be calculated based on statistical pore-size distribution models. Childs and Collis-George (1950) defined K_s as :

$$K_s = \frac{\gamma^2}{2\cdot\eta\cdot\rho_w\cdot g\cdot\tau}\cdot\Delta\theta\cdot\sum_{i=1}^{n} h_i^{-2} \qquad (10)$$

where γ = surface tension of water ($N \cdot m^{-1}$),

η = viscosity of water ($kg \cdot m^{-1} \cdot s^{-1}$),

ρ_w = density of water ($kg \cdot m^{-3}$),

g = gravitational acceleration ($m \cdot s^{-2}$),

τ = tortuosity ($m \cdot m^{-1}$),

$\Delta\theta$ = θ increment ($m^3 \cdot m^{-3}$),

n = number of different capillary size classes in the bundle of tubes making up the soil column,

h_i = pressure head at midpoint of each θ increment i (m).

Marshall (1958) and Millington and Quirk (1959) defined K_s as :

$$K_s = \frac{\gamma^2}{2 \cdot \eta \cdot \rho_w \cdot g} \cdot \frac{\varepsilon_1^p}{n^2} \cdot \sum_{j=1}^{m} \left((2 \cdot j - 1) \cdot h_j^{-2} \right) \tag{11}$$

13.4.2.3 Estimating K(θ) *based on the model of Burdine*

Burdine's (1953) model was later applied by Brooks and Corey (1964) to derive their classical function for the unsaturated hydraulic conductivity $K(\theta)$:

$$K(\theta) = \left(\frac{\theta - \theta_r}{\varepsilon - \theta_r} \right)^n \tag{12}$$

where $n = 3 + 2/\lambda$.

13.4.2.4 Estimating K(θ) *based on the model of Mualem*

Van Genuchten (1980) used the model of Mualem (1976) to derive his well-known equation for unsaturated hydraulic conductivity $K(\theta)$ or $K(h)$:

$$K(\theta) = K_s \cdot \left(\frac{\theta - \theta_r}{\theta_s - \theta_r} \right)^{\frac{1}{2}} \cdot \left(1 - \left(1 - \left(\frac{\theta - \theta_r}{\theta_s - \theta_r} \right)^{\frac{1}{m}} \right)^m \right)^2 \tag{13}$$

$$K(h) = K_s \cdot \frac{\left(1 - \left(\alpha \cdot |h|\right)^{n-1} \cdot \left(1 + \left(\alpha \cdot |h|\right)^{n}\right)^{-m}\right)^2}{\left(1 + \left(\alpha \cdot |h|\right)^{n}\right)^{\frac{m}{2}}} \qquad (14)$$

where α, n and m = parameters from the van Genuchten model.

13.4.3 Estimating the unsaturated hydraulic conductivity $K(\theta)$ from soil physical characteristics

13.4.3.1 Soil texture reference curves

As for the soil moisture retention curve, the K-θ relationship can be derived from soil texture reference curves (see Figure 13.3) The saturated hydraulic conductivity K_s can also be derived from soil texture reference curves (see Figure 13.4).

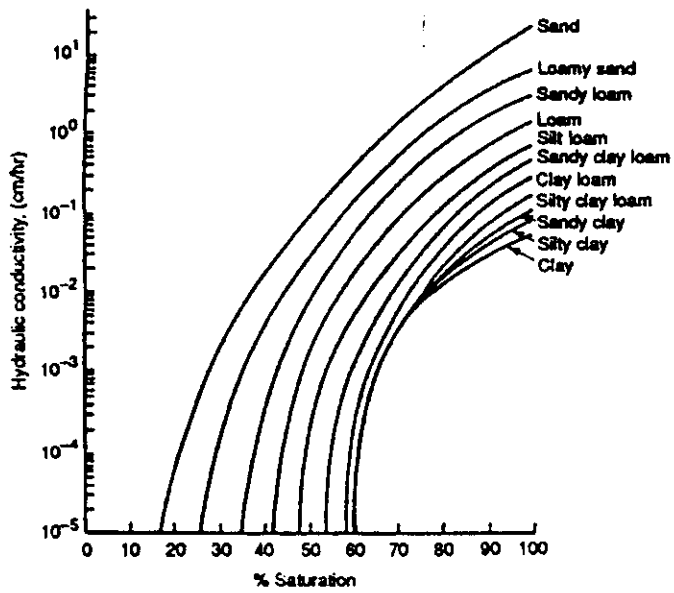

Figure 13.3 Hydraulic conductivity sorted by soil texture (Rawls et al., 1982)

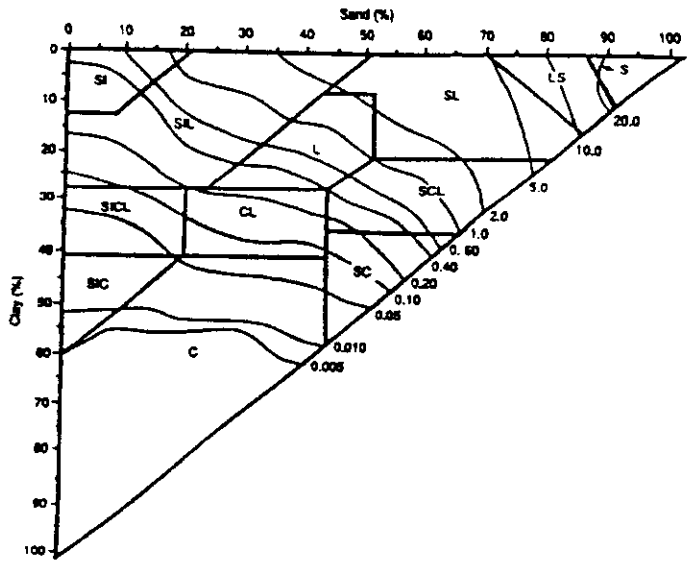

Figure 13.4 Saturated hydraulic conductivity K_s for USDA soil texture triangle (Rawls and Brakensiek, 1985)

13.4.3.2 Pedotransfer functions to estimate K(θ)

Very popular pedotransfer functions to determine K_s and $K(\theta)$ or $K(\psi)$ are those proposed by Campbell (1985) :

$$K_s = 4 \cdot 10^{-3} \cdot \left(\frac{13}{\rho_b}\right)^{1.3 \cdot B} \cdot e^{\left(-6.9 \cdot m_c - 3.7 \cdot m_s\right)} \cdot 3.53 \cdot 10^{-3} \tag{15}$$

$$K(\theta) = K_s \cdot \left(\frac{\theta}{\theta_s}\right)^m \tag{16}$$

$$K(\psi) = K_s \cdot \left(\frac{\psi_e}{\psi}\right)^n \tag{17}$$

where K_s = saturated hydraulic conductivity ($cm \cdot h^{-1}$),

m_c = clay mass fraction,

m_s = silt mass fraction,

$B = -2 \cdot \psi_{es} + 0.2 \cdot \sigma_g$

ψ_{es} = air entry potential ($J \cdot kg^{-1}$) for a standard bulk density of 1,300 $kg \cdot m^{-3}$,

$= -0.5 \cdot d_g^{-0.5}$,

d_g = geometric mean particle diameter,

$= e^{\sum m_i \cdot \ln d_i}$,

σ_g = geometric standard deviation,

$= e^{\sqrt{\sum m_i \cdot (\ln d_i)^2 - \left(\sum m_i \cdot \ln d_i\right)^2}}$,

m_i = mass fraction of textural class i,
d_i = arithmetic mean diameter of class i,
$m = 2 \cdot B + 3$,
$n = 2 + \frac{3}{B}$,
ψ_e = air entry potential ($J \cdot kg^{-1}$),
$= \psi_{es} \cdot \left(\frac{\rho_b}{1.3}\right)^{0.67 \cdot B}$.

13.5 References

Arya, L.M. and J.F. Paris (1981). A physicoemperical model to predict the soil moisture characteristic from particle-size distribution and bulk density data. Soil. Sci. Soc. Am. J., **45**, 1023-1030.

Bloemen, G.W. (1980). Calculation of capillary conductivity and capillary rise from grain size distribution. I. Real and theoretical values of the exponent in a formula of Brooks and Corey for the calculation of hydraulic conductivties. ICW Wageningen nota no. 952. II. Assessment of the values of the exponent in a formula of Brooks and Corey for the calculation of hydraulic condutivity from grain size distribution. ICW Wageningen nota no. 962. III. Air entry pressure and saturated conductivity calculated from grain size distribution and median grain size. ICW Wageningen nota no. 990. IV. Capillary rise in soil types and soil profiles. ICW Wageningen nota no. 1013.

Brooks, R.H. and A.T. Corey (1964). Hydraulic properties of porous media. Hydrology Paper 3, Colorado State University, Fort Collins, Colorado, USA.

Burdine, N.T. (1952). Relative permeability calculations for pore-size distribution data. Trans. AIME, **198**, 34-42.

Campbell, G.S. (1974). A simple method for determining unsaturated conductivity from moisture retention data. Soil Sci., **117**, 311-314.

Campbell, G.S. (1985). Soil physics with BASIC. Transport models for soil-plant systems. Developments in Soil Science 14. Dept. of Agronomy and Soils, Washington State University, Pullman, USA.

Childs, E.C. and N. Collis-George (1950). The permeability of porous materials. Proc. R. Soc. London Ser. A, **201**, 392-405.

Clapp, R.B. and G.M. Hornberger (1978). Empirical equations for some hydraulic properties. Water Resour. Res., **15**, 601-604.

Cosby, B.J., G.M. Hornberger, R.B. Clapp and T.R. Ginn (1984). A statistical exploration of soil moisture characteristics to the physical properties of soils. Water Resour. Res., **20**, 682-690.

De Jong, R. (1982). Assessment of empirical parameters that describe soil water characteristics. Can. Agric. Engin., **24**, 65-70.

De Jong, R., C.A. Campbell and W. Nicholaichuk (1983). Water retention equations and their relationship to soil organic matter and particle size distributions for disturbed samples. Can. J. Soil Sci., **63**, 291-302.

Gupta, S.C. and W.E. Larson (1979). Estimating soil water retention characteristics from particle size distribution, organic matter percent and bulk density. Water Resour. Res., **15**, 1633-1635.

Jackson, R.A. (1972). On the calculation of hydraulic conductivity. Soil Sci. Soc. Am. Proc., **36**, 380-383.

Kern, J.S. (1995). Evaluation of soil water retention models based on soil physical properties. Soil Sci. Soc. Am. J., **59**, 1134-1141.

Marquardt, D.W. (1963). An algorithm for least-squares estimation of non-linear parameters. J. Soc. Ind. Appl. Math., **11**, 431-441.

Marshall, T.J. (1958). A Relation between permeability and size distribution of pores. J. Soil Sci., **9**, 1-8.

Millington, R.J. and J.P. Quirk (1959). Permeability of porous media. Nature, **183**, 387-388.

Mualem, Y. (1976). A new model for predicting the hydraulic conductivity of unsatured porous media. Water Resour. Res., **12**, 513-522.

Rawls, W.J., D.L. Brakensiek and K.E. Saxton (1982). Estimation of soil water properties. Trans. ASAE, **25**, 1316-1328.

Rawls, W.J., D.L. Brakensiek and B.Soni (1983). Agricultural management effects on soil water processes, Part I. Soil water retention and Green and Ampt infiltration parameters. Trans. ASAE, **26**, 1747-1752.

Rawls, W.J. and D.L. Brakensiek (1985). Prediction of soil water properties for hydrological modeling. In : E.B. Jones en T.J. Wards (eds.). Watershed management in the eighties. Proc. of Symp. Sponsored by Comm. on Watershed Management, I & D Division, ASCE. ASCE Convention, Denver, Colorado, USA, April 30-May 1, 293-299.

Rawls, W.J., T.J. Gish and D.L. Brakensiek (1991). Estimating soil water retention from soil physical properties and characteristics. Adv. Soil Sci., **16**, 213-234.

Rawls, W.J., L.R. Ahuja, D.L. Brakensiek and A. Shirmohammadi (1993). Infiltration and soil water movement. In : D.R. Maidment (ed.). Handbook of hydrology. McGraw-Hill, Inc., USA.

Saxton, K.E., W.J. Rawls, J.S. Romberger and R.I. Papendick (1986). Estimating generalized soil-water characteristics from texture. Soil Sci. Soc. Am. J., **50**, 1031-1036.

Tyler, S.W. and S.W. Wheatcraft (1990). Fractal processes in soil water retention. Water Resour. Res., **26**, 1047-1054.

van Genuchten, M.Th. (1978). Calculating the unsaturated hydraulic conductivity with a new closed-form analytical model. Research Report 78-WR-08, Water Research Program, Dept. of Civil Engineering, Princeton University, Princeton, New Jersey, USA.

van Genuchten, M. Th. (1980). A closed-form equation for predicting the hydraulic conductivity of unsaturated soils. Soil Sci. Soc. Am. J., **44**, 892-898.

van Genuchten, M.TH., F.J. Leij and S.R. Yates (1991). The RETC code for quantifying the hydraulic functions of unsaturated soils. EPA/600/2-91/065, R.S. Kerr Environmental Research Laboratory, Office of Research and Development, U.S. Environmental Protection Agency, ADA, Oklahoma, USA.

van Genuchten, M.Th., F.J. Leij and L.J. Lund (1992). Indirect methods for estimating the hydraulic properties of unsaturated soils. Univ. of California, Riverside, USA.

Vereecken, H., J. Maes, J. Feyen and P. Darius (1989). Estimating the soil moisture retention characteristic from texture, bulk density and carbon content. Soil Sci., **148**, 389-403.

Yates, S.R., M.Th. van Genuchten, A.W. Warrick and F.J. Leij (1992). Analysis of measured, predicted, and estimated hydraulic conductivity using the RETC computer program. Soil Sci. Soc. Am. J., **56**, 347-354.